USGS
science for a changing world

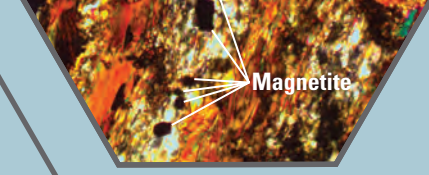

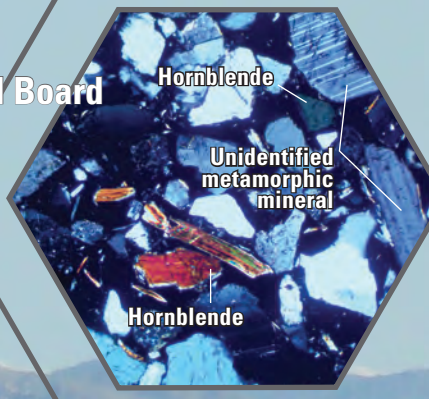

Prepared in cooperation with the Lahontan Regional Water Quality Control Board

Chromium in Minerals and Selected Aquifer Materials

Chapter C of

Natural and Anthropogenic (Human-Made) Hexavalent Chromium, Cr(VI), in Groundwater near a Mapped Plume, Hinkley, California

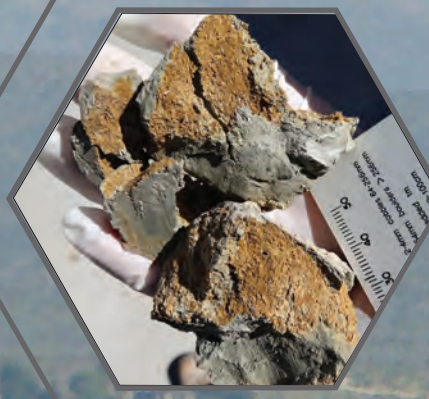

Professional Paper 1885-C

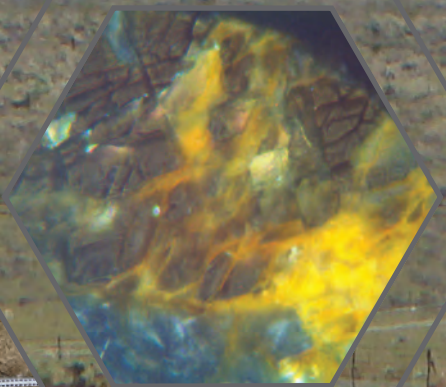

U.S. Department of the Interior
U.S. Geological Survey

Front cover

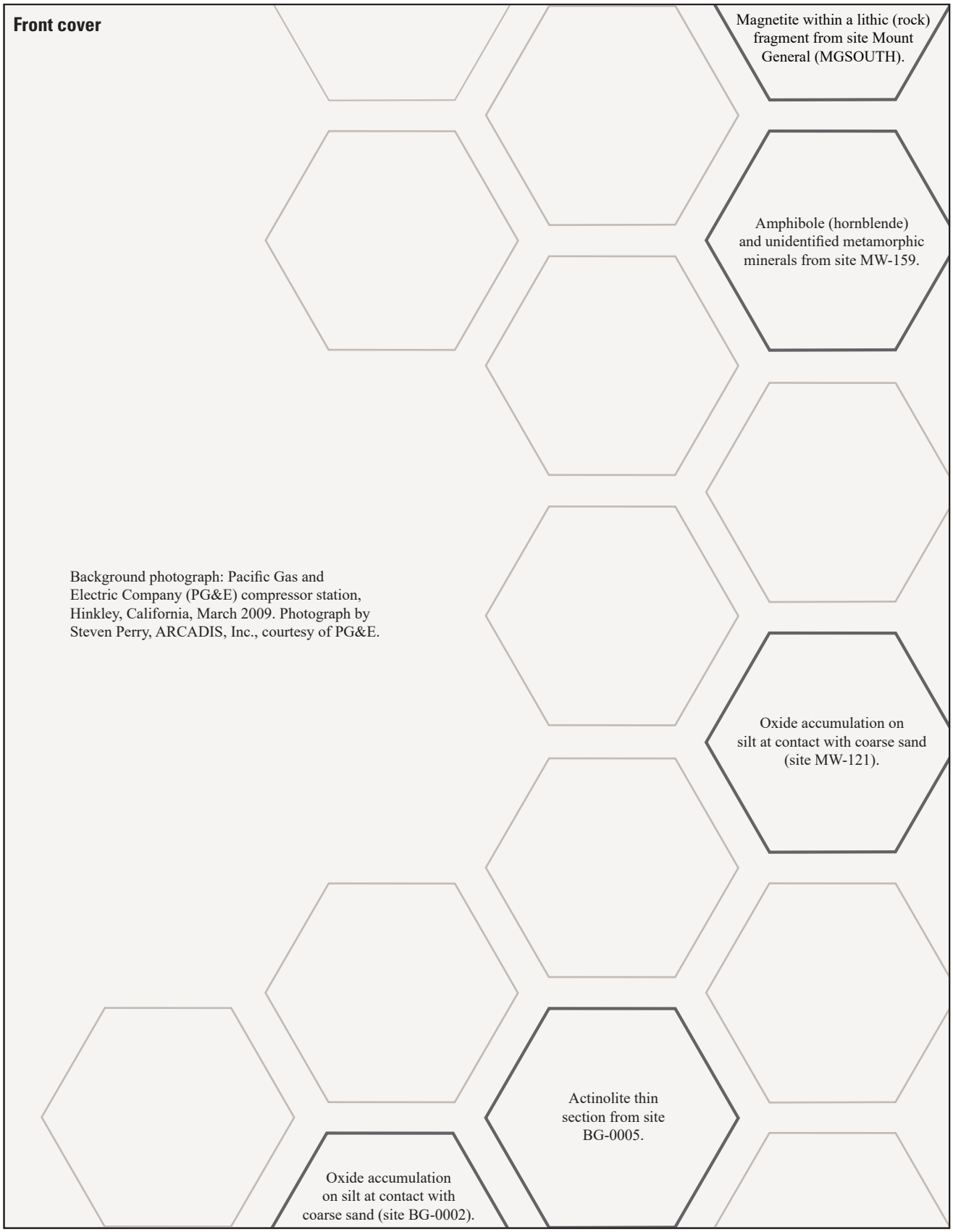

Magnetite within a lithic (rock) fragment from site Mount General (MGSOUTH).

Amphibole (hornblende) and unidentified metamorphic minerals from site MW-159.

Background photograph: Pacific Gas and Electric Company (PG&E) compressor station, Hinkley, California, March 2009. Photograph by Steven Perry, ARCADIS, Inc., courtesy of PG&E.

Oxide accumulation on silt at contact with coarse sand (site MW-121).

Actinolite thin section from site BG-0005.

Oxide accumulation on silt at contact with coarse sand (site BG-0002).

Chromium in Minerals and Selected Aquifer Materials

Chapter C of
Natural and Anthropogenic (Human-Made) Hexavalent Chromium, Cr(VI), in Groundwater near a Mapped Plume, Hinkley, California

By Krishangi D. Groover, John A. Izbicki, William Benzel, Jean Morrison, and Andrea L. Foster

Prepared in cooperation with the Lahontan Regional Water Quality Control Board

Professional Paper 1885-C

U.S. Department of the Interior
U.S. Geological Survey

U.S. Geological Survey, Reston, Virginia: 2023

Suggested citation:
Groover, K.D., Izbicki, J.A., Benzel, W., Morrison, J., and Foster, A.L., 2023, Chromium in minerals and selected aquifer materials, Chapter C of Natural and anthropogenic (human-made) hexavalent chromium, Cr(VI), in groundwater near a mapped plume, Hinkley, California: U.S. Geological Survey Professional Paper 1885-C, 49 p., https://doi.org/10.3133/pp1885C.

Associated data for this publication:
Foster, A.L., Wright, E.G., , Bobb, C., Choy, D., and Miller, L.G., 2023, Optical petrography, bulk chemistry, micro-scale mineralogy/chemistry, and bulk/micron-scale solid-phase speciation of natural and synthetic solid phases used in chromium sequestration and re-oxidation experiments with sand and sediment from Hinkley, CA: U.S. Geological Survey data release, https://doi.org/10.5066/P9ENBLGY.

Groover, K.D., and Izbicki, J.A., 2018, Field portable X-ray fluorescence and associated quality control data for the western Mojave Desert, San Bernardino County, California: U.S. Geological Survey data release, https://doi.org/10.5066/P9CU0EH3.

Morrison, J.M., Benzel, W.M., Holm-Denoma, C.S., and Bala, S., 2018, Grain size, mineralogic, and trace-element data from field samples near Hinkley, California: U.S. Geological Survey data release, https://doi.org/10.5066/P9HUPMG0.

ISSN 2330-7102 (online)

Acknowledgments

This study was developed by the U.S. Geological Survey (USGS) with input from a technical working group (TWG) composed of community members, the Lahontan Regional Water Quality Control Board (RWQCB), the Independent Review Panel Manager (Project Navigator, Ltd.), Pacific Gas and Electric Company (PG&E), and consultants for PG&E. The study was funded cooperatively under an agreement between the Lahontan RWQCB and the USGS. Funding for the study was provided by PG&E to the Lahontan RWQCB. Logistical support for field work, including access to wells, was provided by PG&E. The TWG met approximately quarterly during the study to provide input to the study, and the Hinkley community was updated annually on study progress.

The authors thank the many people involved in the design and implementation of this study including the staff of the Lahontan RWQCB, the staff of PG&E and their consultants, and the staff of Project Navigator, Ltd. The authors also acknowledge and thank the many involved community members who allowed access to their properties for sample collection, and who collectively donated thousands of hours on behalf of the local community in support of this project and for resolution of other issues related to anthropogenic hexavalent chromium, Cr(VI), within the Hinkley area.

Contents

Figures

Tables

Conversion Factors

U.S. customary units to International System of Units

Multiply	By	To obtain
	Length	
foot (ft)	0.3048	meter (m)
mile (mi)	1.609	kilometer (km)
	Mass	
pound, avoirdupois (lb)	0.4536	kilogram (kg)

International System of Units to U.S. customary units

Multiply	By	To obtain
	Length	
nanometer (nm)	0.00000003937	inch (in.)
micrometer (µm)	0.00003937	inch (in.)
millimeter (mm)	0.03937	inch (in.)
centimeter (cm)	0.3937	inch (in.)
	Volume	
liter (L)	33.81402	ounce, fluid (fl. oz)
	Mass	
microgram (µg)	0.00000003527	ounce, avoirdupois (oz)
milligram (mg)	0.00003527	ounce, avoirdupois (oz)
gram (g)	0.03527	ounce, avoirdupois (oz)
kilogram (kg)	2.205	pound avoirdupois (lb)
	Density	
gram per cubic centimeter (g/cm^3)	62.4220	pound per cubic foot (lb/ft^3)
	Energy	
Gigaelectron volt (GeV; 10^9electron volts)	3.93 x 10−26	pounds (lb)

Temperature in degrees Celsius (°C) may be converted to degrees Fahrenheit (°F) as follows:

$$°F = (1.8 \times °C) + 32.$$

Datum

Horizontal coordinate information is referenced to the North American Datum of 1983 (NAD 83).

Below land surface (bls) is the datum used to describe depth.

Supplemental Information

Concentrations of chemical constituents in water are given in either milligrams per liter (mg/L) or micrograms per liter (µg/L).

Concentrations of chemical constituents in rock or sediment are given in milligrams per kilogram (mg/kg).

An ampere is the amount of electrical current produced by the force of one volt acting through a resistance of one ohm. A milliampere is one-thousandth of an ampere and is a unit of measurement used for small electrical currents.

Redox, a combination of the words reduction and oxidation, refers to chemical processes in which one substance or molecule gains an electron (is reduced and its oxidation state is decreased) and another loses an electron (is oxidized and its oxidation state is increased). The processes of oxidation and reduction occur simultaneously and cannot occur independently.

Abbreviations

Al	aluminum
Ag	silver
Ba	barium
Cr(III)	trivalent chromium having an oxidation state of +3
Cr(VI)	hexavalent chromium having an oxidation state of +6
Cu	copper
EDS	energy dispersive X-ray spectroscopy
Fe	iron
Fe(II)	ferrous iron having an oxidation state of +2
Fe(III)	ferric iron having an oxidation state of +3
GGGSC	Geology, Geochemistry, Geophysics Science Center
GMEGSC	Geology, Minerals, Energy, and Geophysics Science Center
HCl	hydrochloric acid
$HClO_4$	perchloric acid
HF	hydrofluoric acid
HNO_3	nitric acid
ICP-MS	inductively coupled plasma-mass spectrometry
ICP42	multi-acid digestion used to prepare samples for ICP-MS analysis, the number refers to the number of elements determined on analysis of the digested solid material
ICP49	multi-acid digestion used to prepare samples for ICP-MS analysis, the number refers to the number of elements determined on analysis of the digested solid material
ICP-OES	inductively coupled plasma-optical emission spectroscopy
K	potassium
KCl	potassium chloride
LRL	laboratory reporting level
MCL	maximum contaminant level
Mn	manganese
Mn(II)	manganese oxide having an oxidation state of +2
Mn(III)	manganese oxide having an oxidation state of +3
Mn(II/III)	manganese oxide with some manganese having an oxidation state of +2 and some having an oxidation state of +3
Mn(III/IV)	manganese oxide with some manganese having an oxidation state of +3 and some having an oxidation state of +4
Mn(IV)	manganese oxide having an oxidation state of +4

N	normal
Na	sodium
Na_2O_2	sodium peroxide
NWQL	USGS National Water Quality Laboratory
O	oxygen
Pb	lead
PG&E	Pacific Gas and Electric Company
pXRF	portable (handheld) X-ray fluorescence
PZC	point of zero charge
Q4 2015	October–December 2015
R^2	coefficient of determination
SEM	scanning electron microscopy
Sr	strontium
SSA	summative-scale analysis
SSRL	Stanford Synchrotron Radiation Lightsource
USGS	U.S. Geological Survey
WDXRF	wavelength dispersive X-ray fluorescence
XANES	X-ray absorption near-edge structure
XRD	X-ray diffraction

Chromium in Minerals and Selected Aquifer Materials

By Krishangi D. Groover, John A. Izbicki, William Benzel, Jean Morrison, and Andrea L. Foster

Abstract

Between 1952 and 1964, hexavalent chromium, Cr(VI), was released into groundwater from a Pacific Gas and Electric Company (PG&E) compressor station in Hinkley, California, in the western Mojave Desert 80 miles northeast of Los Angeles, California. In 2015, the extent of anthropogenic Cr(VI) in groundwater in Hinkley and Water Valleys was uncertain, but some Cr(VI) in groundwater may be naturally occurring from rock and aquifer material.

To evaluate potential sources of natural Cr(VI), chromium and other selected trace-element concentrations were measured by inductively coupled plasma-mass spectrometry (ICP-MS), with multi-acid digestion, on 34 samples of surficial alluvium and core material from Hinkley and Water Valleys, California, and on 2 samples of alluvium from the mafic Sheep Creek fan to the southwest. Chromium concentrations in Hinkley and Water Valleys ranged from 2 to 110 milligrams per kilogram (mg/kg), with a median concentration of 14 mg/kg; concentrations were highest in weathered mafic hornblende diorite associated with Iron Mountain. High chromium concentrations also were present within fine-textured materials and visually abundant iron- and manganese-oxide coatings on the surfaces of mineral grains. For comparison, chromium concentrations as high as 170 mg/kg were measured in mafic alluvium from the Sheep Creek fan. In contrast, chromium concentrations were lowest in Mojave-type deposits (Mojave River stream and lake margin deposits), with a median of 6 mg/kg. Chromium concentrations measured by ICP-MS compared favorably with concentrations measured by portable (handheld) X-ray fluorescence (pXRF; chapter B), on the basis of least-squares regression results and a coefficient of determination (R^2) of 0.97.

Minerals in bulk samples and the heavy (dense) mineral fractions isolated from those samples were identified using optical techniques, X-ray diffraction (XRD), and scanning electron microscopy (SEM). Quartz and feldspar were the most abundant minerals, especially within recent and older Mojave River deposits. Chromium concentrations were as high as 1,250 mg/kg in the heavy-mineral fraction, with specific gravity greater than 3.32. Chromium was not commonly detected in the light-mineral fraction, with specific gravity less than 2.85. Most chromium within the heavy-mineral fraction was substituted within magnetite mineral grains less than 100 micrometers (μm) in diameter, and almost no chromite was present within the heavy-mineral fraction. Although magnetite is resistive to weathering, weathering of magnetite to hematite was identified (1) in Miocene materials underlying unconsolidated deposits in the western subarea of Hinkley Valley and (2) in alluvium within Water Valley that contains weathered minerals eroded from Miocene rock. Less-dense, more easily weathered chromium-containing amphiboles, such as actinolite in older Mojave River alluvium and hornblende in locally derived alluvium from Iron Mountain, were identified optically. Magnetite was not identified in weathered hornblende diorite and was less abundant in locally derived materials and in Miocene materials than in Mojave-type deposits. A comparison of ICP-MS data and sequential extraction data shows that approximately 90 percent of chromium in aquifer material within Hinkley and Water Valleys was not extractable and was interpreted to reside within unweathered mineral grains. Most extractable chromium was within the strong acid extractable fraction. Chromium within the weakly sorbed, and specifically sorbed extractable fractions in oxide accumulations within the regulatory Cr(VI) plume is potentially mobile into groundwater with changes in ionic strength or pH.

Although Hinkley and Water Valleys are regionally low in chromium, natural geologic sources of chromium may be present in aquifer materials penetrated by wells completed in (1) weathered hornblende diorite bedrock underlying the western subarea; (2) Miocene deposits underlying the western subarea and unconsolidated material in the northern subarea and Water Valley containing basalt or weathered minerals eroded from Miocene deposits; (3) unconsolidated material containing visually abundant iron- and manganese-oxide coatings on the surfaces of mineral grains that are present near the water table and near lithologic or geologic contacts; and (4) brown clay and mudflat/playa deposits in the northern subarea. Brown clay and mudflat/playa deposits in the eastern subarea near Mount General have a low-chromium, felsic mineralogy similar to Mojave River deposits and do not contain high concentrations of chromium; however, manganese(IV) oxides within these materials may facilitate oxidation of trivalent chromium, Cr(III), to Cr(VI).

In general, admixtures of geologic material eroded from various source terrains that were identified within Mojave-type deposits do not appear to greatly alter the elemental composition of the unconsolidated material composing aquifers in Hinkley and Water Valleys. Chemical and mineralogic data did not indicate high natural abundance, unusual mineralogy, or unusual sorptive properties for chromium on the surfaces of mineral grains within older Mojave River alluvium downgradient from the "western excavation site" in the western subarea.

C.1. Introduction

Between 1952 and 1964, hexavalent chromium, Cr(VI), was released into groundwater from a Pacific Gas and Electric Company (PG&E) compressor station in Hinkley, California, in the western Mojave Desert 80 miles (mi) northeast of Los Angeles, California. In 2015, the extent of anthropogenic Cr(VI) in groundwater in Hinkley and Water Valleys was uncertain, but some Cr(VI) in groundwater may be naturally occurring from rock and aquifer material. The U.S. Geological Survey (USGS) was requested by the Lahontan Regional Water Quality Control Board to complete an updated background study of Cr(VI) concentrations in Hinkley and Water Valleys.

Chromium concentrations in Hinkley and Water Valleys (fig. C.1), and much of the western Mojave Desert, are low (Smith and others, 2014; Groover and Izbicki, 2019) compared to the average bulk continental abundance in the Earth's crust of 185 milligrams per kilogram (mg/kg; Reimann and de Caritat, 1998). However, hornblende diorite that crops out on Iron Mountain along the western margin of Hinkley Valley (Dibblee, 1967; Boettcher and Walker, 1993) and basalt in Water Valley have chromium concentrations as high as 530 and 310 mg/kg, respectively (chapter B, table B.3). Additionally, older Mojave River deposits may contain chromium-bearing minerals, including actinolite, eroded from mafic rock in the San Gabriel Mountains 40 mi southwest of Hinkley (Ehlig, 1958; Evans, 1982; Izbicki and others, 2008; Groover and Izbicki, 2019). Chromium distribution within aquifer solids differs by particle size and mineral density, and chromium weathered from primary minerals is often sorbed to the surfaces of mineral grains prior to entering groundwater (fig. C.2). Chromium concentrations in groundwater are controlled by processes that are not solely related to chromium abundance in geologic material, including (1) distribution of chromium within aquifer solids owing to aquifer mineralogy and weathering rates of chromium-containing minerals, (2) accumulation of chromium on surface coatings, (3) oxidation of trivalent chromium, Cr(III), to the more soluble Cr(VI) by manganese (Mn) oxides, and (4) desorption of Cr(VI) from surface coatings into groundwater under appropriate aqueous geochemical conditions in alkaline oxic groundwater (fig. C.2; Izbicki and others, 2008; Ščančar and Milačič, 2014).

Chromium in rocks within the Earth's crust is most commonly present as chromite ($Fe^{II}Cr^{III}_2O_4$). Chromite is typically found in mafic to ultramafic rocks (Reimann and de Caritat, 1998; Nesse, 2000) and is highly resistant to weathering (Oze and others, 2007; Morrison and others, 2009). Chromium also may substitute for ferric iron, Fe(III), within the structure of magnetite ($Fe^{II}Fe^{III}_2O_4$; Deer and others, 1992; Reimann and de Caritat, 1998). Magnetite is present in a wider variety of rocks than chromite, including granitic rock (Nesse, 2000), and also is resistant to weathering (White and others, 1994; Reimann and de Caritat, 1998; Lumpkin, 2001). Although less common than chromite or magnetite, chromium also may be substituted within other minerals, including amphiboles, garnets, pyroxenes, olivine, and micas. Chromium substituted within these minerals may be more likely to weather and become available to groundwater than chromium within chromite or magnetite.

Chromium in rocks and minerals is present as Cr(III), which has low solubility in groundwater at the pH and redox conditions within Hinkley and Water Valleys (Rai and Zachara, 1984; Ball and Nordstrom, 1998; Izbicki and others, 2015a). After weathering from mineral grains, chromium must oxidize to Cr(VI) before entering most groundwater (fig. C.2). Under natural conditions, chromium oxidation typically occurs in the presence of Mn oxides (Schroeder and Lee, 1975; Oze and others, 2007). Chromium may accumulate on the surfaces of mineral grains, sorbed as Cr(III) or Cr(VI), in a variety of different forms, each having different potential mobility into groundwater (Chao and Sanzolone, 1989; Wenzel and others, 2001; Groover and Izbicki, 2019).

C.1.1. Site Description and Notable Mineral Occurrences

Hinkley and Water Valleys are in the western Mojave Desert, 80 mi northeast of Los Angeles, California. Unconsolidated deposits that compose aquifers within Hinkley and Water Valleys include alluvium from older and recent Mojave River stream, lake-margin, local alluvial fan, lake (lacustrine), mudflat/playa, and groundwater-discharge deposits (chapter A, table A.1; Miller and others, 2018, 2020). For the purposes of this professional paper, Mojave River stream and lake-margin deposits sourced from the Mojave River are collectively referred to as "Mojave-type" deposits. On the basis of subsurface geologic conditions, Hinkley Valley has been divided into eastern, western, and northern subareas, with Water Valley to the north of Hinkley Gap (fig. C.1).

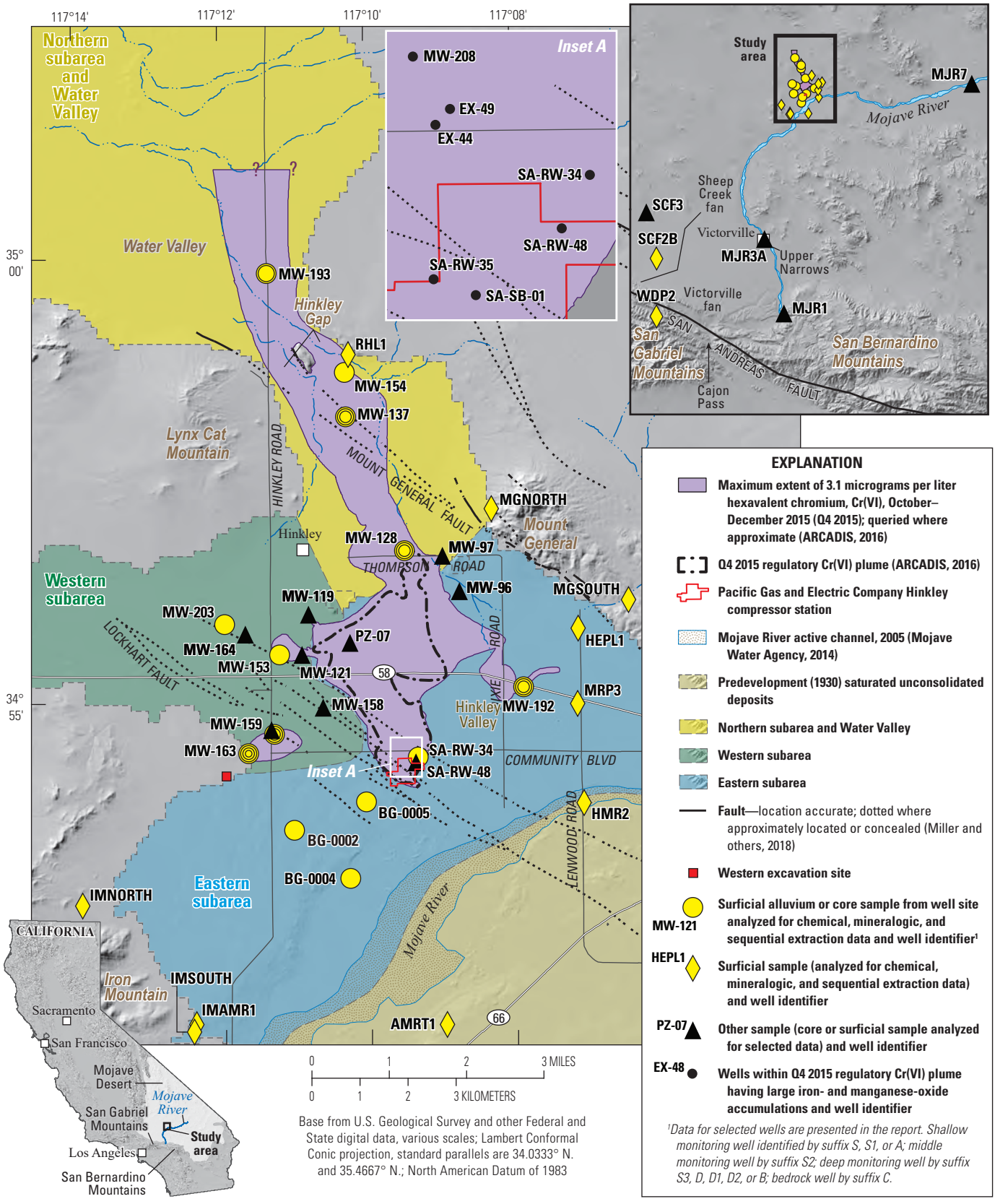

Figure C.1. Location of surficial alluvium and core material samples analyzed for mineralogic composition and chemistry, Hinkley and Water Valleys, western Mojave Desert, California. Well data are from U.S. Geological Survey (2021).

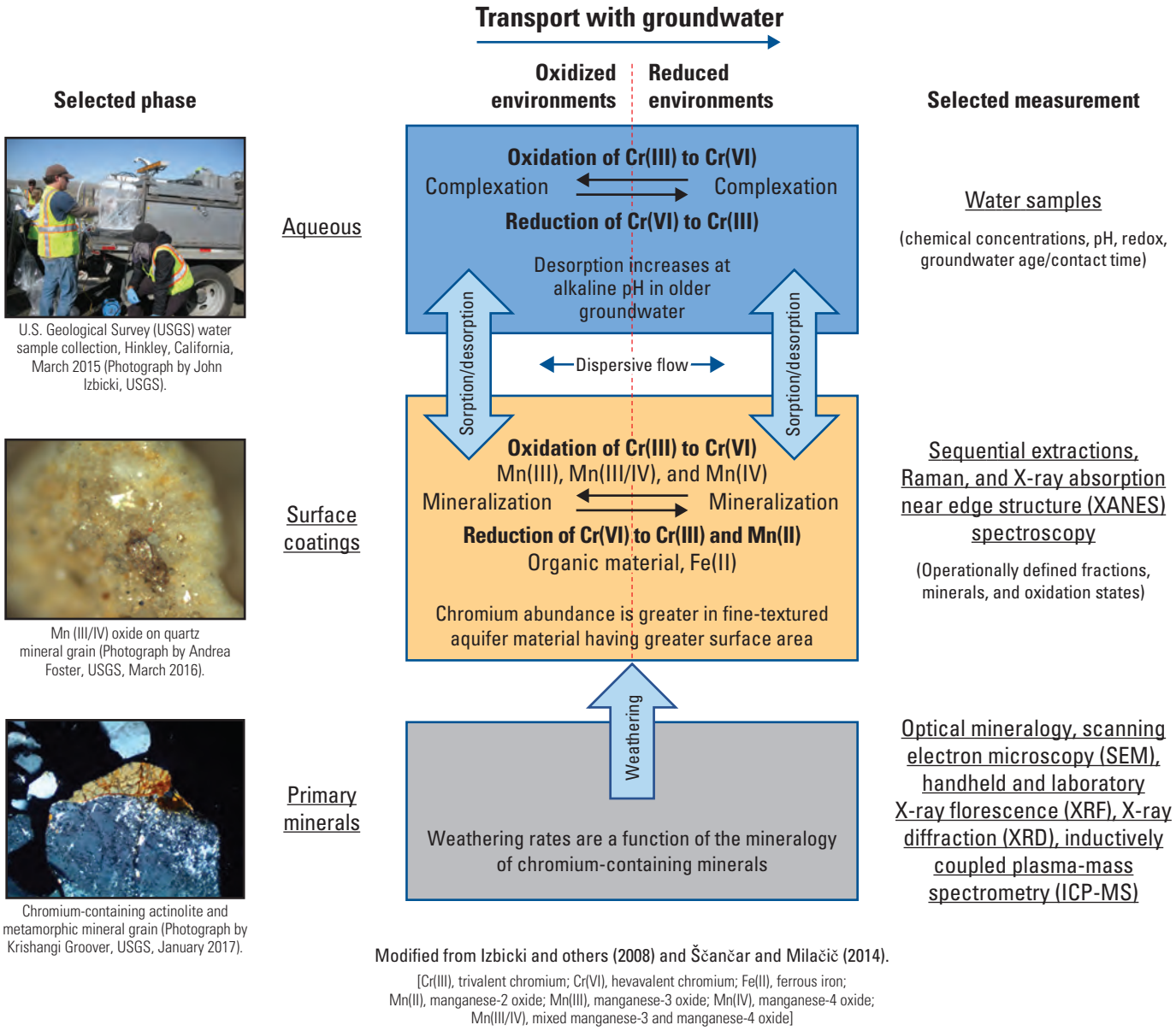

Figure C.2. Conceptual model of processes controlling mineral weathering and dissolution to groundwater in the presence of oxide coatings on mineral grains.

Mojave-type deposits are generally coarse textured and felsic in composition, with abundant quartz, plagioclase, microcline (potassium feldspar), mica, and minor quartzite pebbles (Cox and others, 2003; Cyr and others, 2015). Minor to trace hornblende, heavy (dense) minerals, and lithic clasts picked up by the river on its course from the San Bernardino Mountains south of Victorville also are present within Mojave-type deposits (fig. C.1). Due to movement along the San Andreas Fault over geologic time (fig. C.1), older Mojave River deposits (chapter A, fig. A.5) contain mafic chromium-containing minerals, such as actinolite, sourced from the San Gabriel Mountains 40 mi southwest of Hinkley Valley (Izbicki and others, 2008; Groover and Izbicki, 2019). More recent Mojave River deposits contain fewer of these mafic minerals.

Locally derived alluvium is composed of material eroded from local mountains surrounding Hinkley and Water Valleys (chapter B, fig. B.3). Iron Mountain, along the western margin of Hinkley Valley, contributes clasts of hornblende diorite, marble, gneiss, and quartzite (Dibblee, 1967; Boettcher and Walker, 1993; U.S. Geological Survey, 2005). Shallow intrusive (hypabyssal) basalt dikes within marble near the northern part of Iron Mountain contain coarse phenocrysts of clinopyroxene and pyrite. Gneissic rocks also crop out on Mount General on the east side of Hinkley Valley, along with dacite/rhyolite rocks that are highly mineralized in places (Dibblee, 1967; Fletcher and Martin, 1998; U.S. Geological Survey, 2005). Rocks in Mount General contain minor amounts of magnetite (Dibblee, 1967) and trace amounts of barite, galena, malachite, and chrysocolla (Housley and Reynolds, 2002). In the past, mines in Mount General extracted lead (Pb), silver (Ag), barium (Ba), and copper (Cu; Bezore and Shumway, 1994; U.S. Geological Survey, 2005). Dendritic manganese oxides coating some outcrops in Mount General were observed during field sample collection as part of this study. Desert varnish, composed of clay minerals in addition to iron and manganese oxides (primarily hematite and birnessite, respectively; Potter and Rossman, 1979), coats most of the local rock outcrops surrounding Hinkley Valley.

Fine-textured mudflat/playa deposits are present at the surface in the eastern subarea near alluvium eroded from Mount General and at depth within the eastern subarea. Mudflat/playa and lacustrine deposits (Stantec, 2013; Garcia and others, 2014) also are present in the northern subarea. Most of the unconsolidated material composing aquifers of interest in Hinkley Valley are unconsolidated older Mojave River alluvium and lake-margin deposits sourced from the Mojave River (Miller and others, 2018). In many areas, these Mojave-type deposits are underlain by fine-textured lacustrine and groundwater-discharge deposits (Miller and others, 2018, 2020), with locally derived alluvium and weathered bedrock overlying unweathered rock (CH2M Hill, 2013). Water Valley contains locally derived alluvium overlain by Mojave-type near-shore lake deposits. Much of the Mojave-type deposits in Water Valley, the northern subarea, and the western subarea of Hinkley Valley downgradient from the Lockhart fault (fig. C.1) are currently unsaturated as a result of declining water levels from agricultural pumping (Stamos and others, 2001). Under 2015 conditions, saturated Mojave-type deposits are only a thin veneer overlying local alluvium, fine-textured lacustrine or mudflat/playa deposits, weathered bedrock, or groundwater-discharge deposits (Miller and others, 2018, 2020).

Hexavalent chromium was released into groundwater from the PG&E Hinkley compressor station between 1952 and 1962. In October–December 2015 (Q4 2015), the regulatory Cr(VI) plume extended 3 mi downgradient from the release point within the Hinkley compressor station (fig. C.2; ARCADIS, 2016). However, the actual extent of the Cr(VI) release was uncertain, and Cr(VI) concentrations in water from wells greater than the interim regulatory Cr(VI) background of 3.1 micrograms per liter (µg/L) were present in water from wells as far downgradient as Water Valley, more than 8 mi from the Hinkley compressor station (ARCADIS, 2016). Remediation of Cr(VI) released from the Hinkley compressor station began in 1992, and in 2010, site cleanup was projected to require 10 to 95 years (Haley and Aldrich, Inc., 2010; Pacific Gas and Electric Company, 2011). In addition to releases from the Hinkley compressor station, Cr(VI) may have been released from other locations in the valley, including the “western excavation site” in the western subarea (Lahontan Regional Water Quality Control Board, 2014).

Monitoring well sites installed by PG&E for regulatory purposes are commonly identified by the prefix MW (fig. C.1), with sites numbered sequentially in the order they were drilled (ARCADIS, 2016). Shallow wells at a site, commonly screened across or just below the water table, are identified with the suffix S or S1; older monitoring wells are identified with the suffix A. Deeper wells are identified with the suffix D, D1, or D2, or with S2 or S3 if a hydrologically important clay layer is not present between the wells; older monitoring wells are identified with the suffix B (ARCADIS, 2016). The suffix R was added if the well was a replacement for a well that was destroyed (ARCADIS, 2016). Wells installed by PG&E as part of the USGS Cr(VI) background study are identified with the prefix BG; these sites are numbered sequentially in the order they were permitted, and wells are identified from shallowest to deepest with the suffix A, B, or C. Although drilling and well-construction methods changed over time in response to site conditions and regulatory requirements, most monitoring wells were drilled using auger rigs. Core material, archived by PG&E, is available for most wells installed after 2011 from near the water table to below the depth of the deepest well. Core material collected during drilling at a site is identified by the site number and depth interval the material was collected from; if adjacent to the screened interval of the well, the core material also may be identified by the well identification.

C.1.2. Purpose and Scope

The purpose of this chapter is to provide information on the mineralogy and potential mobility of natural chromium into groundwater in Hinkley and Water Valleys. Scope of the work included (1) chemical analyses of selected samples of surficial alluvium and core material, including analyses by particle-size and density fractions; (2) mineral identification within surficial alluvium and core material; and (3) analyses of chromium within operationally defined sorption sites on alluvium and core material. Chemical, mineral, and surface sorption data are presented for selected sites to evaluate potential chromium mobility into groundwater at those sites. Chemical analyses of surficial alluvium and core material by inductively coupled plasma-mass spectrometry (ICP-MS) presented within this chapter are generally considered to be higher quality (more accurate and precise) than the analyses by portable (handheld) X-ray fluorescence (pXRF) presented in chapter B within this professional paper. Inductively coupled plasma-mass spectrometry data are intended to support the data and interpretations presented in chapter B within this professional paper.

C.2. Methods

Thirty-six samples of surficial alluvium and core material (fig. C.1) were selected for detailed chemical and mineralogical analyses on the basis of pXRF data (chapter B) and field lithologic descriptions (table C.1). Thirty-four samples were collected from Hinkley or Water Valleys. Two samples, included for comparison purposes, were from alluvium composing the Sheep Creek fan eroded from mafic rock in the San Gabriel Mountains southwest of the study area. Samples from Hinkley and Water Valleys included surficial alluvium eroded from identifiable source terrains, including the Mojave River, Iron Mountain, Mount General, and mudflat/playa deposits. Samples of surficial alluvium represent selected endmembers eroded from known geologic materials that have not been extensively altered by soil forming processes. Core material was obtained from material collected during monitoring well installation that was archived by PG&E. Core material included recent and older Mojave River deposits (ranging in texture from clayey sand to coarse-textured sand), lake-margin deposits, lacustrine deposits, mudflat/playa deposits, and weathered hornblende diorite bedrock.

Between 5 and 7 pounds (2.3 to 3.2 kg) of material were collected for analyses. Samples were described by physical attributes, including color and texture. Color was described using numerical designations according to Munsell soil color charts (Munsell Color, 1975, 1994). Texture was described on the basis of visual and tactile features using methods developed by Folk (1954) and descriptions following the National Research Council classification (Lane, 1947). Provenance of core materials was described by Miller and others (2018, 2020). Descriptions are available in Groover and Izbicki (2018). Samples were homogenized using the "rolling method" (U.S. Department of Agriculture, 1996; U.S. Environmental Protection Agency, 2007), disaggregated, and sieved at the USGS San Diego office laboratory prior to shipment to the USGS Geology, Geochemistry, Geophysics Science Center (GGGSC) minerals laboratory in Denver, Colorado. A small subsample, about 200 grams (g), was retained at the USGS San Diego office and processed for sequential extraction analyses. Selected material from this subsample was sieved to less than 1-millimeter (mm) diameter and sent to a contract lab to produce standard 30-µm-thick petrographic thin sections for optical analysis at the USGS San Diego office. For the purposes of this professional paper, unsieved materials and materials sieved to less than 2-mm diameter, without further processing into particle-size or density fractions, are referred to as bulk samples.

After arrival at the GGGSC minerals laboratory, samples were further homogenized and disaggregated, sieved to a particle size less than 2 mm, and separated into seven different particle-size fractions using a sonic sifter. The dry-sieve method requires complete manual disaggregation of samples, which can be difficult to achieve in samples that have a high clay content. The 53- to 500-µm particle-size fraction, separated using the sonic sifter, was further processed using a Wilfley table to obtain material with a specific gravity greater than 2.86 (Strong and Driscoll, 2016). Specific gravity is unitless and is the ratio of the density of a material to the density of a standard, usually pure water with a density of 1 gram per cubic centimeter at 20 °C. The material was placed into a column filled with methylene iodide, which has a specific gravity of 3.32 (Strong and Driscoll, 2016). The fraction of the material that settled to the bottom of the column, minerals having specific gravity greater than 3.32, was cleaned with acetone and weighed prior to further analyses. The light-mineral fraction, having specific gravity less than 2.86, was saved for analyses by pXRF. Most materials within the light-heavy-mineral fraction, having specific gravity between 2.86 and 3.32, were inadvertently discarded, although 11 samples were retained for analyzes by pXRF.

Table C.1. Samples of surficial alluvium and core material processed for detailed chemical and mineralogical analyses, Hinkley and Water Valleys, California.

[Number of samples=36. Detailed chemical, mineralogic, and size distribution analyses, along with heavy mineral identification and analyses using field-portable X-ray fluorescence (pXRF) by the U.S. Geological Survey (USGS) Geology, Geochemistry, Geophysics Science Center (GGGSC), Denver, Colorado are in Morrison and others (2018, https://doi.org/10.5066/P9HUPMG0). Sequential extraction data for the sites below are available in appendix C.1, table C.1.1 or the National Water Information System (NWIS) web (https://waterdata.usgs.gov/nwis) and may be looked up using the USGS site identification (ID) column. Depositional environment from Miller and others (2020)]

Site identifier	Sample depth (feet)	USGS site number	Field description	Depositional environment
			Surficial alluvium	
AMRT1	0	345121117085601	Coarse sand	Older Mojave River
HEPL1	0	345548117070701	Sandy silt with minor clay and granules	Mudflat/playa
HMR2	0	345350117070301	Coarse sand	Recent Mojave River
IMAMR1	0	345122117122201	Fine sand and silt	Older Mojave River
IMNORTH	0	345243117135501	Sand with minor silt and granules to medium pebbles	Local fan (metamorphic), Iron Mountain
IMSOUTH	0	345117117122401	Sand with minor silt and granules to medium pebbles	Local fan (mafic), Iron Mountain
MGNORTH	0	345643117080001	Sand with minor silt and granules to medium pebbles	Local fan (volcanic), Mount General
MGSOUTH	0	345447117044701	Sand with minor silt and granules to medium pebbles	Local fan (metamorphic), Mount General
MRP3	0	345457117070701	Silty sand	Mudflat/playa
RHL1	0	345854117101401	Clayey sandy silt, shells	Lacustrine deposits
WDP2	0	342033117371301	Silty sandy gravel	Pelona Schist (mafic)
SCF2B	0	342923117371001	Silty gravelly sand	Pelona Schist (mafic)
			Core material	
BG-0004	57–61	345300117101501	Coarse sand	Recent Mojave River
BG-0005	106–109	345352117100201	Coarse sand	Older Mojave River
MW-128	88–92	345642117092901	Clayey sand	Recent Mojave River
MW-128	117–122	345642117092901	Coarse sand	Recent Mojave River
MW-128	166–173	345642117092901	Fine sand/silt	Lake margin (older Mojave River)
MW-137	88–91	345812117101601	Coarse sand	Lake margin (recent Mojave River)
MW-137	130–136	345812117101601	Brown clay	Mudflat/playa
MW-137	158–161.5	345812117101601	Fine sand/silt	Lake margin
MW-159	93–100	345438117111901	Coarse sand	Older Mojave River
MW-159	115–120	345438117111901	Fine sand/silt	Older Mojave River
MW-159	122–126.5	345438117111901	Reduced silt/clay, diatoms	Lake deposits
MW-163	90–96	345425117113801	Coarse sand	Older Mojave River/lake margin
MW-163	106.2–110	345425117113801	Fine sand/silt, minor clay	Lake deposits
MW-163	113.5–118	345425117113801	Reduced silt/clay, diatoms	Lake deposits
MW-163	123–128	345425117113801	Weathered bedrock, gneiss	Local fan
MW-153	100.5–108.5	345531117111201	Weathered bedrock, gneiss/mafic tonalite	Local fan, mafic tonalite
MW-154	72–77	345842117101702	Blue lake	Mudflat/playa
MW-192	60–62, 70–72	345509117075201	Clayey sand	Recent Mojave River
MW-192	62–67	345509117075201	Coarse sand	Recent Mojave River
MW-192	117–122	345509117075201	Fine sand/silt	Lacustrine deposits
MW-193	76–81.5	345955117112004	Silty/clayey sand	Local fan
MW-193	135–141	345955117112002	Sandy clayey silt	Local fan
MW-203	108–115	345552117115702	Local, silty/clayey	Local fan
SA-RW-34	90–97	345422117091901	Fine to coarse sand	Older Mojave River and lake margin

C.2.1. Chemical Analyses

Bulk samples (less than 2-mm diameter grain size) were digested and analyzed for major, minor, and selected trace-element concentrations using ICP-MS, inductively coupled plasma-optical emission spectroscopy (ICP-OES) and wavelength dispersive X-ray fluorescence (WDXRF; Taggart, 2002; Morrison and others, 2018) by a laboratory contracted by the GGGSC. For simplicity, ICP-MS and ICP-OES are collectively referred to as ICP-MS within this paper. Digestions were done by using three methods optimized for different ranges of elemental concentrations: (1) lithium metaborate fusion with dissolution by dilute nitric acid (HNO_3), (2) sodium peroxide (Na_2O_2) fusion with dissolution by dilute nitric acid, and (3) multi-acid digestion using hydrochloric (HCl), nitric, perchloric ($HClO_4$), and hydrofluoric (HF) acid at low temperature. Laboratory reporting limits (LRL) for chromium using the three digestions are 100, 10, and 1 mg/kg, respectively, and the multi-acid digestion data (Methods ICP42 and ICP49; Morrison and others, 2018) are most commonly presented within this professional paper. Laboratory reporting levels for the other elements and data from the three digestions are provided in Morrison and others (2018).

All materials within the particle-size and heavy-mineral fractions were analyzed by pXRF at the GGGSC minerals laboratory (Morrison and others, 2018). The ThermoFisher Niton pXRF instrument used by the GGGSC minerals laboratory (Morrison and others, 2018) differed from the Olympus DP-4000 Delta Premium pXRF instrument used in the field (chapter B). Although both instruments were operated in similar modes, the GGGSC minerals laboratory data for chromium were not optimized for high concentrations.

Four of the seven particle-size fractions for each of the 13 selected samples also were analyzed using ICP-MS. Sample digestion techniques for ICP-MS analyses were optimized for low (less than one percent by mass) and high (up to 10 percent by mass) concentration ranges. The optimized concentration was selected from the various digest results on the basis of the median pXRF survey data on bulk samples measured by Groover and Izbicki (2018). Portable (handheld) X-ray fluorescence data also were collected on bulk samples, seven particle-size fractions, and heavy-mineral fractions at the GGGSC minerals laboratory. Calculations of the contribution of chromium from different fractions of each sample were done using the percent of each size or density fraction multiplied by the chromium concentration in each fraction. Chemical data and associated quality-assurance data from all digests for bulk and particle-size fractions analyzed by the GGGSC minerals laboratory are reported by Morrison and others (2018).

C.2.2. Mineralogic Analyses

Optical identification and quantification of minerals was done on petrographic thin sections of sieved samples (less than 1-mm diameter). Thin sections, prepared at a contract laboratory, were vacuum impregnated with epoxy, cut to 30-µm thickness, and stained to highlight the presence of potassium feldspar. Mineral point counts were done on a 0.01-mm spaced grid to obtain a minimum of 300 counts or until the standard deviation of mineral proportions was stable. Fine-textured samples and local fan material were not point counted; instead, mineral proportions for these samples were estimated using comparisons to a visual percentage chart. Mineral point counts were time-consuming, and only selected samples were evaluated in this manner, whereas minerals proportions within thin sections were estimated optically for a much larger number of samples.

Selected particle-size fractions and the heavy-mineral fraction isolated from bulk samples were pulverized and scanned using X-ray diffraction (XRD) to identify minerals at the GGGSC minerals laboratory. X-ray diffraction has a reporting limit of approximately 3 percent by weight in bulk samples. Minerals were identified using the computer program Jade 9 Pro (KSA Analytical Systems, Aubrey, Texas) and grouped using cluster analyses on the basis of the intensity of the 2-theta refraction angle using the computer program HighScore (Degen and others, 2014). Clay fractions from selected samples were treated using ethylene glycol and sequentially scanned to determine the clay-mineral composition (Morrison and others, 2018). Some samples, selected on the basis of chemical data, were hand sorted under a binocular microscope, and individual mineral grains within these samples were mounted and made into polished thin sections for investigation by scanning electron microscopy (SEM). The elemental composition of the minerals of interest was obtained using energy dispersive X-ray spectroscopy (EDS) interfaced with the SEM, and minerals were identified on the basis of the EDS data. The detection limit for chromium measured by EDS, 100 mg/kg, was higher than the chemical and pXRF methods used in this study; consequently, it was not always possible to identify chromium-containing minerals in samples known to contain chromium using SEM/EDS. Data collected on samples analyzed by the GGGSC minerals laboratory are available in Morrison and others (2018).

Raman spectra were collected under ambient conditions using a ThermoDXR microRaman (μRaman) spectrometer at the USGS Geology, Minerals, Energy, and Geophysics Science Center (GMEGSC) in Menlo Park, California. Spectra were collected using the 532-nanometer (nm) laser with 100x or 50x objective lenses, which provide laser spot sizes of 1 and 2 micrometer (μm), respectively. Spectra were background subtracted, and a commercialized version of the 2013-era RUFF database (https://rruff.info/) of over 3,000 mineral Raman spectra was used with Omnic 9.2 software (ThermoScientific) to rank and display the highest-quality matches in the database to the unknown spectrum. Optical images were collected from samples via a digital camera system on the ThermoDXR with calibrated x, y dimensions.

Synchrotron-based X-ray absorption near-edge structure (XANES) spectroscopy was used to determine the solid phase speciation of Mn, characterizing both its general coordination chemistry and oxidation state in aquifer materials. Synchrotron data were collected by USGS personnel at the Stanford Synchrotron Radiation Lightsource (SSRL) in Menlo Park, Calif., which operated at ring energy of 3 gigaelectron-volts (GeV) and near-constant current of 500 milliamperes (mA) maintained by "top-off" reinjection every 10 minutes. Samples were mounted perpendicularly to the X-ray beam, in "spacers" made of rigid material (aluminum or plastic). Additional information on Raman and X-ray absorption spectroscopy procedures is provided in chapter I within this professional paper.

C.2.3. Sequential Extraction Analyses

Sequential extractions were done on sieved material (less than 1-mm diameter) from 34 samples of surficial alluvium and core material collected in Hinkley and Water Valleys and from two samples of mafic alluvium from the Sheep Creek fan eroded from the San Gabriel Mountains. Sequential extractions were done using progressively stronger extractants following a procedure modified from Chao and Sanzolone (1989) and Wenzel and others (2001) to determine the concentrations of arsenic, chromium, uranium, and vanadium on operationally defined sorption sites on the surfaces of mineral grains (table C.2). The modified procedure is described by Izbicki and others (2015b) and Groover and Izbicki (2018). Concentrations of aluminum, iron, and manganese, which form oxide coatings on mineral grains, also were analyzed in the extracts.

Table C.2. Summary of the sequential extraction procedure from mineral grains. Modified from Chao and Sanzolone (1989) and Wenzel and others (2001).

[Modified from Chao and Sanzolone (1989); Wenzel and others (2001); **Abbreviations:** Al, aluminum; Fe, iron; Mn, manganese; KCl, potassium chloride; $(NH_4)H_2PO_4$, ammonium dihydrogen phosphate; $(NH_4)_2C_2O_4 \cdot H_2O$, ammonium oxalate; $C_6H_8O_6$, ascorbic acid; HNO_3, nitric acid; M, molar; N, normal; ˚C, degrees Celsius]

Extraction solution	Operationally defined surface-sorption sites	Reaction time
0.05M KCl	Weakly sorbed	4 hours
0.05M $(NH_4)H_2PO_4$	Specifically sorbed	16 hours
0.2M $(NH_4)_2C_2O_4 \cdot H_2O$	Amorphous Al, Fe, and Mn hydroxides	4 hours in the dark
0.2M $(NH_4)_2C_2O_4 \cdot H_2O$ + 0.1M $C_6H_8O_6$	Well-crystallized Al, Fe, and Mn hydroxides	30 minutes at 96 ˚C
4N HNO_3	Strong acid extractable	16 hours

Sample extracts prepared at the USGS San Diego office laboratory were preserved and shipped to the USGS National Water Quality Laboratory (NWQL) in Denver, Colorado, for analysis by ICP-MS (Garbarino and others, 2006). At the NWQL, sample extracts were diluted prior to analysis to prevent damage to the ICP-MS instruments during analyses. Dilution resulted in laboratory reporting levels for chromium in extracts that ranged from 9 to 150 μg/L, and chromium concentrations that were below detection in most sample extracts. Samples were reanalyzed for chromium by graphite furnace atomic absorption spectrometry using U.S. Environmental Protection Agency (EPA) Method 7010 (U.S. Environmental Protection Agency, 2007) without dilution prior to analysis, at the USGS trace element laboratory in Boulder, Colorado, to obtain a lower reporting level of 0.02 μg/L. Extract concentrations were multiplied by 0.005 to adjust for the extraction ratio (one-part sample to five-parts extraction solution) and convert results from μg/L to equivalent mg/kg. Chemical concentrations in extract solutions are available in appendix C.1 within this professional paper.

In addition to samples listed in table C.1, samples from within the Cr(VI) plume containing visually abundant oxides (six samples from SA-RW-48) and no visible oxides (one sample from MW-208) were sequentially extracted (table C.3). These data were compared with sequential-extraction data for visually abundant oxides outside the margin of the mapped Cr(VI) regulatory plume.

Table C.3. Selected samples from October–December 2015 (Q4 2015) of regulatory hexavalent chromium, Cr(VI), plume downgradient from the Pacific Gas and Electric Company (PG&E) Hinkley compressor station and selected samples outside the mapped plume having visually abundant oxides that were processed for sequential extractions, Hinkley, California.

[Number of samples=9. Colors in the field description column were obtained using a Munsell Color (1975) chart (designations for hue, value, and chroma) on wet samples, unless otherwise indicated. Sequential extraction data for the sites below are available on National Water Information system (NWIS) web (U.S. Geological Survey, 2021) and may be looked up using the U.S. Geological Survey (USGS) site identification (ID) column]

Site identifier	Sample depth (feet)	USGS site number	Field description	Depositional environment
			Within plume	
SA-RW-48	111	345418117092301	Sand, brown (10YR 4/3)	Plume material; oxidized
SA-RW-48	115	345418117092301	Sand, light yellowish brown (2.5YR 6/4)	Plume material; oxidized
SA-RW-48	117	345418117092301	Silty sand, yellowish brown (10YR 5/4)	Plume material; oxidized
SA-RW-48	119	345418117092301	Silty sand, pale brown (10YR 6/3)	Plume material; oxidized
SA-RW-48	125	345418117092301	Silty sand, reddish brown (5YR 5/3)	Plume material; oxidized
SA-RW-48	125.5	345418117092301	Silty sand, strong brown (7.5YR 5/6)	Plume material; oxidized
MW-208	104	345433117093901	Sand, light yellowish brown (2.5YR 6/4)	Plume material; oxidized
			Outside plume	
MW-121	112.4	345529117105801	Silty sand, brownish yellow (10YR 6/8)	Oxide (lithologic contact)
BG-0004	64	345300117101501	Sand, yellowish brown (10YR 5/4)	Oxide (water table feature)

Elements of interest were extracted sequentially from the surfaces of mineral grains in the following order. First, the weakly sorbed extraction removed water soluble elements. Second, the specifically sorbed extraction removed elements sorbed by pH dependent anion exchange. The amorphous, well-crystallized, and strong acid extractions were more aggressive than the weakly sorbed and specifically sorbed extractions (table C.2) and included dissolution of secondary materials coprecipitated on the surfaces of mineral grains. Primary mineral grains (with the exception of carbonate minerals) were assumed to not be digested by the sequential extraction procedures used as part of this study. Total extractable concentrations were calculated as the sum of the weakly sorbed, specifically sorbed, and strong-acid extractable fractions (table C.2). Other extraction procedures, often specific for individual elements or for operational fractions sorbed or coprecipitated on the surfaces of mineral grains that are not used in this professional paper, are described in the literature (Stover and others, 1976; Keon and others, 2001; Neaman and others, 2004).

C.2.4. Statistical Methods

Most statistics in this chapter were calculated using the computer program Statistical Analysis System (SAS; SAS Institute, Cary, North Carolina). Comparison of least-squares regression slopes and intercepts to values of 1 and 0, respectively, were made on the basis of the t-statistic (Neter and Wasserman, 1974). Comparison of median values were done on the basis of the median test (Neter and Wasserman, 1974). Results of the statistical tests presented within the chapter were considered statistically significant at a significance criterion (significance level) of α=0.05, unless otherwise stated. Probability values (p-values) for individual tests are not provided. Cluster analysis used to group X-ray diffraction data were done using the computer program HighScore (Degen and others, 2014).

C.3. Results of Chemical, Mineralogic, and Sequential Extraction Analyses

Results are presented for chemical, mineralogic, and sequential extraction data. Chemical results include a comparison of ICP-MS and pXRF data (chapter B) and presentation of trace-element data within selected particle-size and mineral-density fractions. Portable (handheld) X-ray fluorescence and texture data (Groover and Izbicki, 2018) are less expensive and easier to collect than ICP-MS and particle-size data (Morrison and others, 2018) and were measured more frequently and on more materials. Portable (handheld) X-ray fluorescence and texture survey data support interpretations presented previously (chapter B) that were not expected to be interpreted independently without additional higher quality data. Mineralogy results include optical, X-ray diffraction, and SEM data. These data also are expensive and difficult to analyze and are provided for selected samples having ICP-MS and particle-size data (Morrison and others, 2018). Sequential extraction results are presented to define the availability of surface exchange sites and potentially mobile fractions of selected trace elements on mineral grains in different geologic settings.

C.3.1. Chromium and Trace-Element Composition of Surficial Alluvium and Core Material

Analyses of chromium and selected trace-element composition of surficial alluvium and core material include a comparison of ICP-MS and pXRF data to determine the accuracy of pXRF data presented in chapter B within this professional paper. Chromium and selected trace-element concentrations within various particle-size fraction and mineral-density fractions also are presented.

C.3.1.1. Comparison of Inductively Coupled Plasma-Mass Spectrometry (ICP-MS) and Portable (Handheld) X-Ray Fluorescence (pXRF) Data

Chromium was most commonly detected using multi-acid digestion with concentrations in samples from Hinkley and Water Valleys ranging from 2 to 110 mg/kg (fig. C.3). Chromium and vanadium concentrations in Hinkley and Water Valleys were less than the average bulk continental abundances, while arsenic and uranium concentrations were greater than the average bulk continental abundances reported by Reimann and de Caritat (1998; fig. C.3). Chromium concentrations were higher in material eroded from or weathered from hornblende diorite associated with Iron Mountain along the western margin of Hinkley Valley. For comparison, chromium concentrations as high as 170 mg/kg were measured in mafic alluvium from the Sheep Creek fan that had eroded from the Pelona Schist in the San Gabriel Mountains southwest of the study area (fig. C.3).

Chemical concentration data for selected elements in alluvium and core material analyzed by ICP-MS (Morrison and others, 2018) were compared to pXRF concentration data for splits from the same material discussed in chapter B within this professional paper. Comparisons of ICP-MS and pXRF data for chromium, nickel, and rubidium had least-squares regression slopes and intercepts not significantly different from 1 and 0, respectively; coefficient of determination (R^2) values for these comparisons were 0.97, 0.77, and 0.93, respectively (fig. C.4; table C.4). Copper and manganese also had least-squares regression slopes and intercepts statistically similar to 1 and 0, but lower R^2 values of 0.40 and 0.69, respectively (fig. C.4; table C.4). Portable (handheld) X-ray fluorescence data for vanadium were about 300 mg/kg greater than ICP-MS data, and pXRF vanadium concentrations were adjusted by subtracting 300 mg/kg from the measured value.

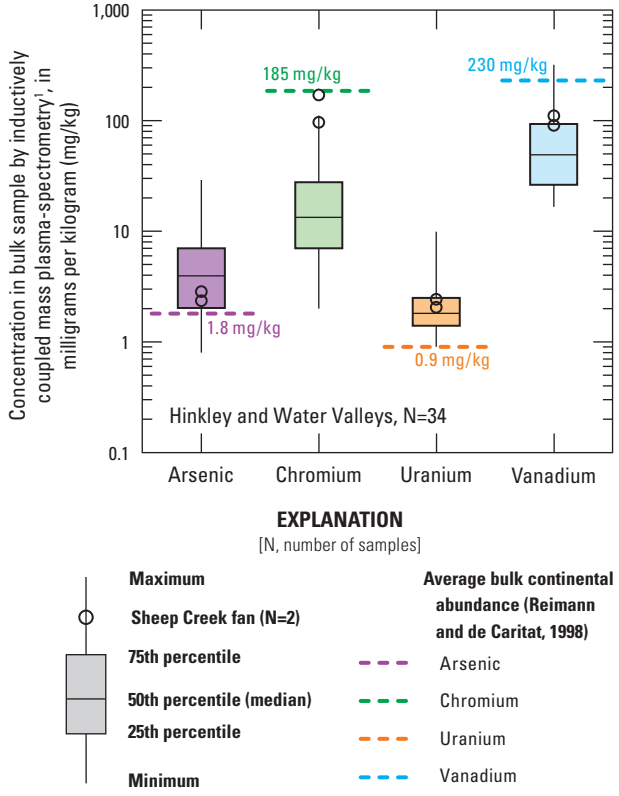

[1]Elemental concentration data measured by inductively coupled plasma-mass spectrometry (ICP-MS) with multi-acid digestion (Methods ICP42 or ICP49; Morrison and others, 2018).

Figure C.3. Arsenic, chromium, uranium, and vanadium concentrations in surficial alluvium and core material in Hinkley and Water Valleys, western Mojave Desert, California.

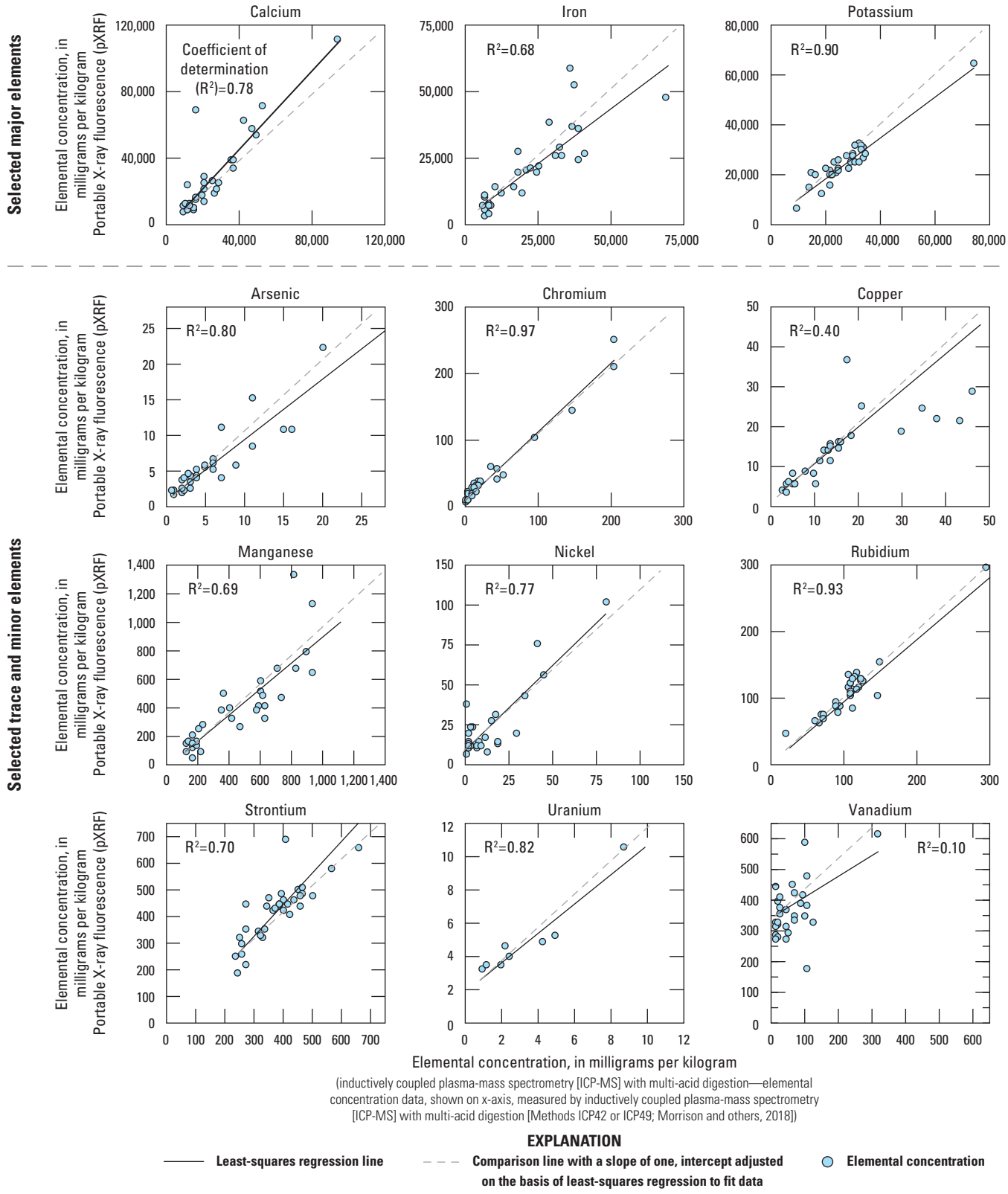

Figure C.4. Least-squares regression comparisons of selected elemental concentrations in surficial alluvium and core material measured using inductively coupled plasma-mass spectrometry with four-acid digestion (Methods ICP42 or ICP49; Morrison and others, 2018) and portable (handheld) X-ray fluorescence data (pXRF; Groover and Izbicki, 2018), Hinkley and Water Valleys, western Mojave Desert, California, 2015 to 2018.

Table C.4. Least-squares regression comparisons of slope, fit, and intercept for selected elemental concentrations in surficial alluvium and core material measured using portable (handheld) X-ray fluorescence (pXRF) and inductively coupled plasma-mass spectrometry (ICP-MS), Hinkley and Water Valleys, California, 2015 to 2018.

[Number of samples=36; inductively coupled plasma-mass spectrometry (Methods ICP42 or ICP49; Morrison and others, 2018) was the independent variable, and portable X-ray fluorescence (pXRF) was the dependent variable. Bold font indicates elements with slopes within ±10 percent of 1 between the 2 methods. R^2 is the coefficient of determination. Slope is in units of (milligrams per kilogram)/(milligrams per kilogram). R^2 is unitless. Mean standard error and intercept are in milligrams per kilogram]

Element	Slope	R^2 value	Mean standard error	Intercept
Arsenic (As)	0.84	0.80	0.591	1.01
Calcium (Ca)	1.2	0.78	3,980	−2,508
Chromium (Cr)	**1.0**	0.97	2.26	8.89
Copper (Cu)	**0.92**	0.40	4.49	1.69
Iron (Fe)	0.81	0.68	2,941	2,896
Lead (Pb)	0.51	0.66	2.33	2.75
Manganese (Mn)	**0.90**	0.69	63.8	−14.2
Molybdenum (Mo)	0.22	0.13	0.180	2.06
Nickel (Ni)	**1.1**	0.77	3.38	10.6
Potassium (K)	0.82	0.90	1,560	1,833
Rubidium (Rb)	**1.1**	0.93	6.45	−10.6
Strontium (Sr)	1.3	0.70	66.9	−76.2
Tin (Sn)	1.3	0.057	1.97	14.8
Titanium (Ti)	0.67	0.63	294	714
Uranium (U)	0.84	0.82	0.393	2.18
Vanadium (V)	0.69	0.087	40.5	338
Zinc (Zn)	0.75	0.75	5.20	3.80
Zirconium (Zr)	1.6	0.88	19.6	−59.7

Portable (handheld) X-ray fluorescence data also were analyzed at the GGGSC minerals laboratory on particle-size fractions and the density fractions isolated from bulk samples (Morrison and others, 2018). Least-squares regression comparison of chromium ICP-MS multi-acid digestion with GGGSC pXRF concentrations showed a slope of 1.15 and an R^2 of 0.94 (fig. C.5). When the three high values, from MW-153, WDP2 (Sheep Creek fan), and SCF2B (Sheep Creek fan), ranging from 137 to 226 mg/kg, were replaced with chromium concentrations analyzed by sodium peroxide fusion, the slope of the regression line decreased to 1.02 with an R^2 of 0.93 (fig. C.5). The results indicate that the pXRF data collected on selected particle-size fractions and mineral density fractions, which are not optimized for chromium concentrations at the GGGSC, may overestimate chromium concentration in particle-size and mineral-density fractions.

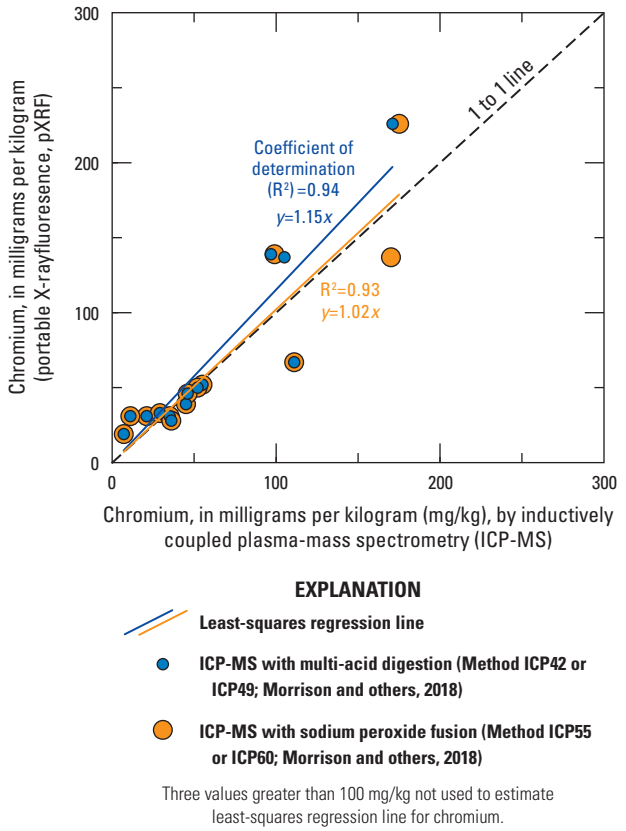

Figure C.5. Least-squares regression comparison for chromium concentrations in surficial alluvium and core material measured using inductively coupled plasma-mass spectrometry (ICP-MS) and portable (handheld) X-ray fluorescence (pXRF) data from the U.S. Geological Survey, Geology, Geochemistry, Geophysics Science Center (GGGSC), Hinkley and Water Valleys, western Mojave Desert, California, 2015 to 2018.

The results also demonstrate the importance of selecting the appropriate sample digestion technique for higher concentration samples.

C.3.1.2. Distribution of Chromium and Selected Trace Elements by Particle-Size Fraction

Median chromium and other selected trace elements are lower in coarser particle-size fractions and higher in finer particle-size fractions (fig. C.6). In general, median concentrations increase monotonically with decreasing particle size. Pair-wise comparison of "very coarse to medium sand" fractions and "very fine sand to silt and clay" fractions show statistically significant differences in median chromium concentrations. Observed differences in chromium concentration based on particle size are consistent with increases in chromium concentrations in fine-textured material measured by pXRF (chapter B, fig. B.8). Similar differences for other elements, except iron and manganese in locally derived alluvium, also were statistically significant.

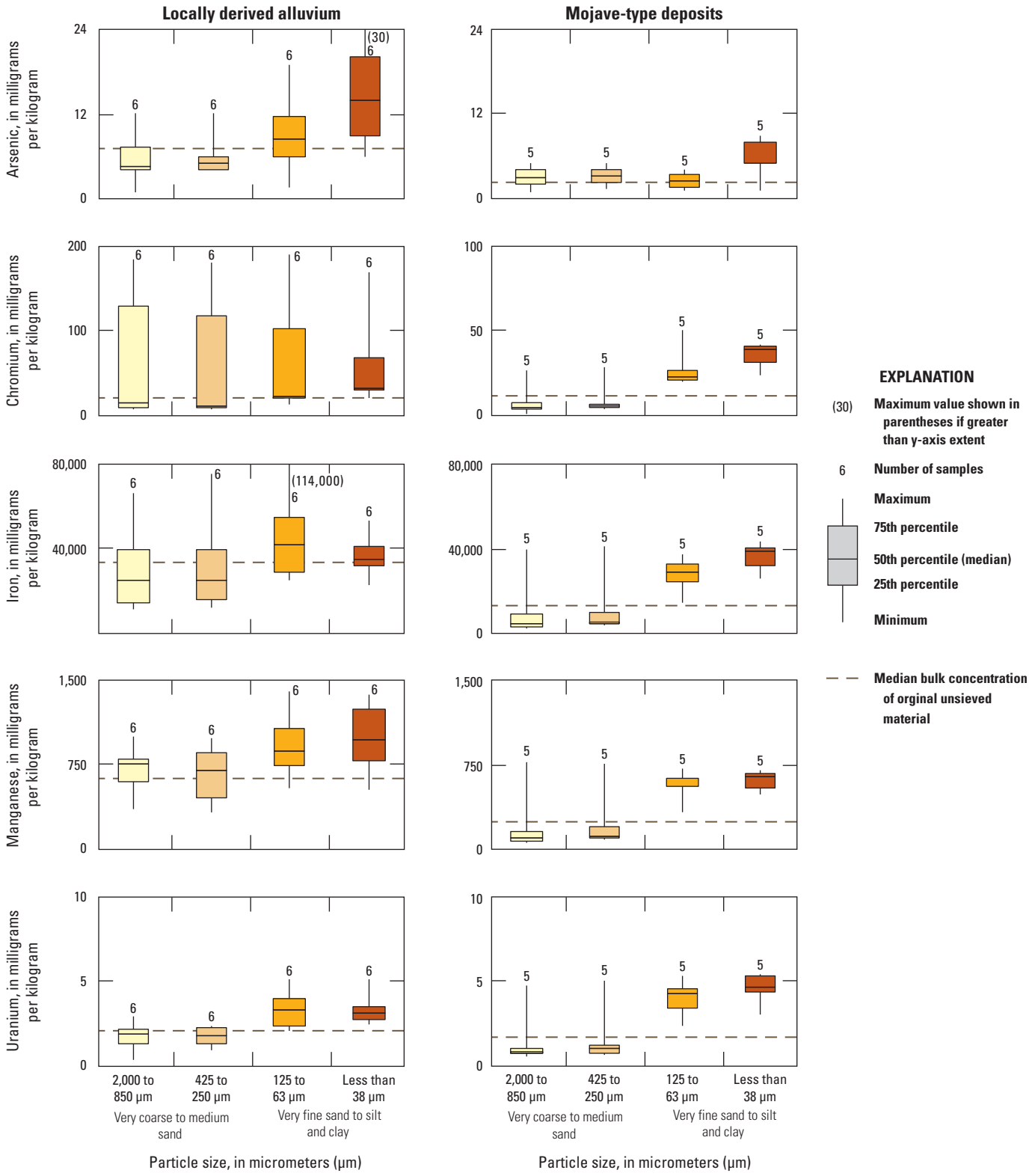

Figure C.6. Selected trace-element concentrations in different particle-size fractions from surficial alluvium and core material in Mojave-type deposits and locally derived alluvium, Hinkley and Water Valleys, western Mojave Desert, California. Data are from Morrison and others (2018).

Chromium and other elemental concentrations are tightly grouped (relatively small interquartile range) for various particle-size fractions in Mojave-type deposits (fig. C.6). This is consistent with sorting and disintegration of lithic fragments into component mineral grains during transport from source rock in the San Bernardino Mountains by the Mojave River. In contrast, the wider range in elemental concentrations in coarser-size fractions within locally derived alluvium (fig. C.6) may result from less sorting and less disintegration of lithic fragments during the shorter transport of alluvium eroded from local source areas. This contrast is largest for chromium. Chromium concentrations representing the upper-quartile range (upper 75th percentile) decreases with particle size (fig. C.6), presumably as a result of less sorting and less disintegration of lithic fragments in the coarser particle-size fractions within locally derived alluvium compared to Mojave-type deposits.

C.3.1.3. Distribution of Chromium and Selected Trace Elements by Mineral Density

Heavy minerals, having specific gravity greater than 3.32, include common chromium-containing minerals, such as spinels. Chromite and magnetite within the spinel mineral group have specific gravity of 4.5 to 4.8 and 5.2, respectively. Most samples had less than 1 percent heavy minerals by weight. One surficial sample of older Mojave River alluvium, AMRT1 (fig. C.1), contained 2.9 percent heavy minerals by weight. The heavy-mineral fraction of this sample may have increased as a result of winnowing of less-dense minerals from the material by wind. Almost no heavy minerals were isolated from samples of core material from mudflat/playa deposits penetrated by well MW-154S1 or weathered hornblende diorite penetrated by well MW-153S (fig. C.1).

Arsenic, chromium, vanadium, and uranium concentrations measured by pXRF were commonly an order of magnitude, or more, greater in the heavy-mineral fraction than in bulk samples (fig. C.7). Median arsenic concentrations in heavy minerals increased with decreasing particle size, whereas median chromium, vanadium, and uranium concentrations decreased with finer texture (smaller particle size), although these differences were not statistically significant.

The highest arsenic concentration within the heavy-mineral fraction, 1,130 mg/kg, was in the coarse-textured fraction within a sample of lacustrine deposits from site MW-159 (fig. C.2) at 120 to 126 feet (ft) below land surface (ft bls). Although generally fine textured, this sample contained visible masses of secondary pyrite mineral grains. Accretion of fine-textured mineral grains into larger grains cemented together by secondary pyrite within the sample may have resulted in higher concentrations within the coarse-textured fraction. The highest chromium concentration within the heavy-mineral fraction, 1,250 mg/kg, was in surficial alluvium eroded from the northern part of Iron Mountain (IMNORTH; fig. C.1). This high chromium concentration may result from material eroded from mafic dikes (hypabyssal basalt) that intrude marble host rock in this area. These dikes are not areally extensive, are not mapped as a separate unit (Dibblee, 1967; Jennings and others, 2010), and are likely not a major source of chromium to Hinkley Valley (chapter B). Six of the eight samples having more than 50 percent of their chromium within the heavy-mineral fraction were Mojave-type materials (Morrison and others, 2018). Uranium concentrations within heavy-mineral fraction from Mojave-type deposits were as high as 140 mg/kg, with a median concentration of 69 mg/kg (fig. C.7). Although uranium is high in some rock and minerals that crop out on Mount General (chapter B, fig. B.14*C*), concentrations within the heavy-mineral fraction of surficial alluvium eroded from Mount General did not exceed 50 mg/kg. Heavy uranium-containing minerals in Mojave-type deposits eroded from the San Bernardino Mountains were transported and deposited in Hinkley Valley by the Mojave River and appear to be an important source of uranium in Hinkley and Water Valleys.

The light-heavy-mineral fraction, having specific gravity between 2.85 and 3.32, was measured on 11 samples (Morrison and others, 2018). The light-heavy-mineral fraction includes chromium-containing amphiboles such as actinolite and hornblende, and it generally composed about 2 percent of the total sample by weight. Light-heavy-minerals were abundant in samples from the mafic Sheep Creek fan (SCF2B) and weathered hornblende diorite bedrock (MW-153), where they composed 11 and 6 percent of the sample by weight, respectively. The light-heavy-mineral fraction also was abundant in older Mojave River alluvium (BG-0004 and BG-0005), where it composed 8 and 5 percent of the sample by weight, respectively. Chromium concentrations in the light-heavy-mineral fraction ranged from 80 to 210 mg/kg. Although higher than concentrations in the bulk sample, chromium concentrations in the light-heavy-mineral fraction were not as high as chromium concentrations in the heavy-mineral fraction. Arsenic and uranium concentrations measured by pXRF in the light-heavy-mineral fraction were typically less than the reporting limits for these elements, while vanadium concentrations were similar to concentrations in the bulk sample.

With few exceptions, possibly attributable to incomplete weathering of heavy minerals within less dense silicate lithic fragments, chromium was either not detected or detected at low concentrations within the light-mineral fraction (specific gravity less than 2.85; Morrison and others, 2018). These results indicate limited substitution of chromium within clay minerals.

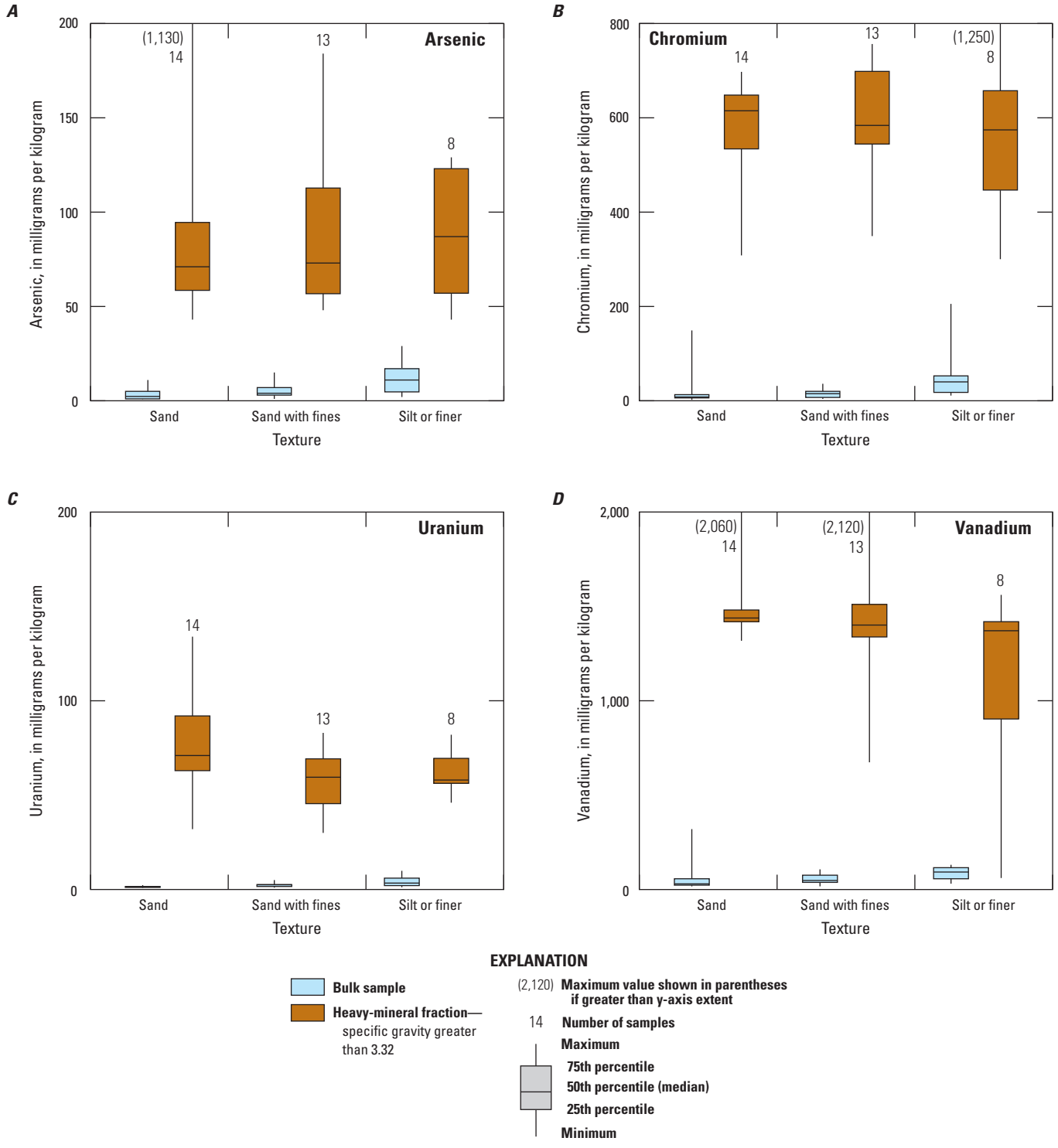

Elemental data measured by portable (handheld) X-ray fluorescence (pXRF) at U.S.Geological Survey Geology, Geochemistry, and Geophysics minerals laboratory (Morrison and others, 2018).

Figure C.7. Concentrations of *A*, arsenic, *B*, chromium, *C*, uranium, and *D*, vanadium in the heavy-mineral (specific gravity greater than 3.32) fraction and bulk samples for selected textures within surficial alluvium and core material, Hinkley and Water Valleys, western Mojave Desert, California.

C.3.2. Mineralogy of Surficial Alluvium and Core Material

Mineral-density data indicate that chromium-containing minerals, such as spinels (including magnetite and chromite) and amphiboles (including actinolite and hornblende), may be present within surficial alluvium and aquifer materials in the study area. These materials were examined optically with XRD, and SEM with EDS were used to identify specific chromium-containing minerals. Some of these minerals, such as actinolite or hornblende, may weather readily and potentially release chromium at a relatively rapid rate, whereas other minerals, such as chromite or magnetite, are more resistant to weathering and likely release chromium at slower rates.

C.3.2.1. Optical Mineralogy

Quartz and feldspar (plagioclase feldspar plus microcline) composed more than 80 percent of the minerals identified optically within Mojave-type deposits, including recent and older Mojave River and lake-margin deposits (fig. C.8). The mineral composition of recent Mojave River deposits is tightly grouped on a ternary diagram (fig. C.8), and recent Mojave River deposits contain less than 10 percent accessory minerals or lithic fragments. Older Mojave River deposits have a greater proportion of accessory minerals, including mica, amphibole (including actinolite and hornblende), clay, apatite, sphene, and opaque minerals (including magnetite; table C.5) with proportionately less quartz and feldspar compared to recent Mojave-type deposits (fig. C.8). Local fan deposits were not fully characterized because of the time required to determine quantitative mineral point counts. However, on the basis of mineral proportions, quartz and feldspar are less abundant in locally derived alluvial fan deposits eroded from Iron Mountain and Mount General, and locally derived alluvium eroded from these sources has a higher proportion of lithic fragments and accessory minerals compared to Mojave-type deposits (fig. C.8). Mudflat/playa deposits (MRP3) near the edge of the playa draining Mount General within the eastern subarea appear similar to material collected at the mountain front (MGSOUTH) on the ternary diagram because of their higher clay content (fig. C.8). In contrast, mudflat/playa deposits from MW-154S1 containing minor manganese oxides, trace microfossils (ostracods), and a large amount of clay have a ternary mineral composition that appears dissimilar to Mojave-type or local source terrains (fig. C.8).

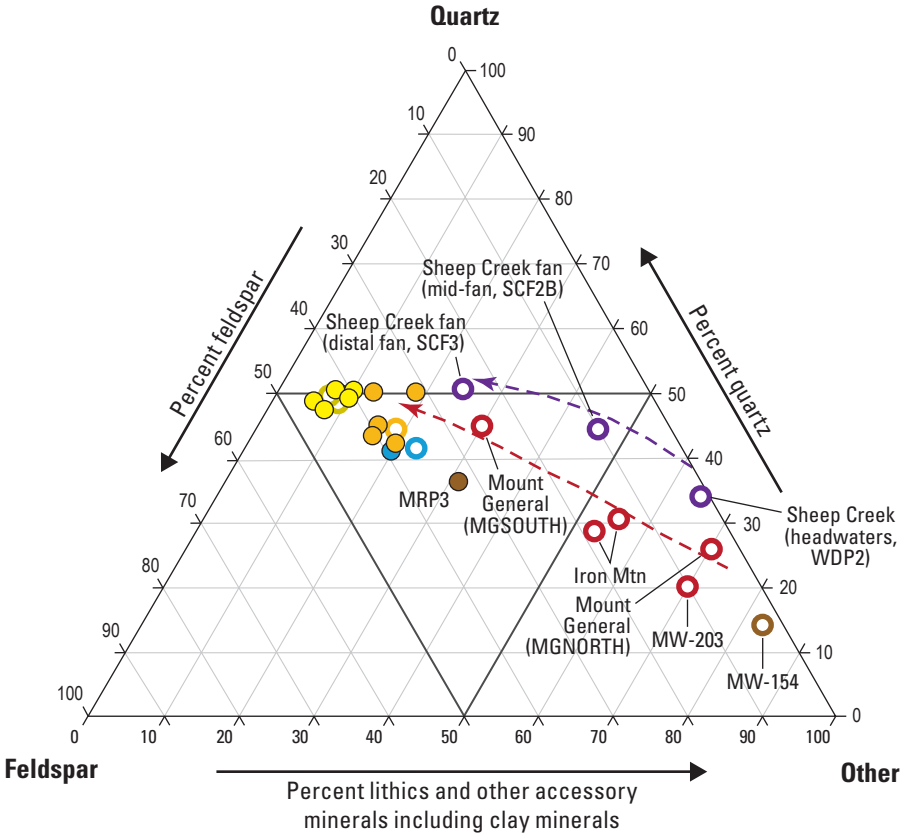

Figure C.8. Percent quartz, feldspar (plagioclase feldspar plus microcline or potassium feldspar), and accessory minerals from thin section analysis, Hinkley and Water Valleys, western Mojave Desert, California. Data are from Groover and Izbicki (2018).

Table C.5. Minerals identified in surficial alluvium and core material, Hinkley and Water Valleys, and the Sheep Creek fan, western Mojave Desert, California. Data are from Groover and Izbicki (2018).

[Minerals listed in order of abundance in each category (major, minor, trace). Major minerals are present at greater than 15 percent abundance, minor minerals are present between 5 and 15 percent, and trace minerals compose less than 5 percent of the sample. Italicized font indicates minerals typically present at less than 0.5 percent in the sample. **Abbreviations:** ft, foot; bls, below land surface]

Depositional provenance	Bulk minerals	Samples
Recent Mojave River	Major: quartz, microcline (potassium feldspar) Minor: plagioclase Trace: lithic (rock fragments), mica, hornblende, opaque minerals (including magnetite); *epidote,actinolite, apatite, biotite, sphene*	BG-0004 (57–61 ft bls), HMR2
Older Mojave River	Major: quartz, microcline (potassium feldspar) Minor: plagioclase, lithic (rock) fragments Trace: mica, hornblende, opaque minerals (including magnetite), clay, actinolite, pyroxene; *epidote,apatite, sphene, zircon, biotite, chlorite, olivine, zircon*	BG-0005 (106–109 ft bls), MW-159 (93–100 ft bls), MW-159 (115–120 ft bls), MW-128 (117–122 ft bls), MW-192 (60–62, and 70–72 ft bls), MW-192 (62–67 ft bls), MW-137 (88–91 ft bls), AMRT1, IMAMR1
Lake margin	Major: quartz, microcline (potassium feldspar) Minor: plagioclase, lithic (rock) fragments Trace: lithic (rock fragments), mica, clay, hornblende, opaque minerals; *pyroxene, epidote, actinolite, apatite, chlorite, biotite, sphene, manganese oxides (unidentified)*	MW-128 (88–92 ft bls), MW-128 (166–173 ft bls), MW-137 (158–161.5 ft bls), MW-163 (90–96 ft bls), SA-RW-34 (90–97 ft bls)
Lake	Major: clay, quartz, microcline (potassium feldspar), plagioclase Minor: mica Trace: lithic (rock fragments), hornblende, opaque minerals, pyroxene, actinolite; *microfossils (diatoms), apatite, epidote, zircon*	MW-159 (122–126.5 ft bls), MW-163 (106.2–110 ft bls), MW-163 (113.5–118 ft bls), MW-192 (117–122 ft bls), RHL1
Mudflat	Major: clay, quartz, microcline (potassium feldspar), mica Minor: plagioclase, calcite Trace: lithic (rock fragments), hornblende, opaque minerals; *olivine, actinolite, pyroxene (orthopyroxene), microfossils (ostracodes); manganese oxide stains*	MW-137 (130–136 ft bls), MW-154S1 (72–77 ft bls), HEPL1, MRP3
Local fan, weathered bedrock	Major: quartz, plagioclase, microcline Minor: lithic (rock) fragments (limestone, volcanics) Trace: amphibole (hornblende), calcite, epidote, magnetite, mica, olivine, serpentine, pyroxene, sphene	MW-193S1 (76–81.5 ft bls), MW-193S3 (135–141 ft bls), MW-203D (108–115 ft bls), MW-163 (123–128 ft bls), MW-153 (100.5–108 ft bls), IMNORTH, IMSOUTH, MGNORTH, MGSOUTH
Other (Sheep Creek fan, eroded from Pelona Schist)	Major: quartz, plagioclase Minor: mica, amphibole (hornblende) Trace: actinolite, sphene	WDP2, SCF2B

In contrast to Hinkley and Water Valleys, where mineral proportions are related to different geologic source terrains, the Sheep Creek fan, eroded from mafic rock in the San Gabriel Mountains, has a single source area. Mineral proportions within the Sheep Creek fan differed according to physical sorting of material during deposition and subsequent weathering. Alluvium from the headwaters of the Sheep Creek fan through the distal portions of the fan plot to the right and above samples of local alluvium from Hinkley Valley, with higher proportions of quartz and lower proportions of feldspar than older and recent Mojave River deposits. Accessory minerals such as amphiboles (including actinolite) are present as minor minerals in the upgradient portion of the fan (WDP2), whereas chromium-bearing mica (fuchsite) present in rocks that compose the greenschist facies of the Pelona Schist presumably weathered completely and was not identified. Farther down the fan, samples contain progressively less of the easily weathered amphiboles (including actinolite), and the fan becomes dominated by quartz, feldspar, and mica. With increasing distance from the mountain front, the Sheep Creek fan resembles the ternary mineral composition of older Mojave River alluvium within Hinkley Valley (fig. C.8), which contains mafic material eroded from the San Gabriel Mountains in the geologic past (chapter A).

Optical examination of older Mojave River alluvium and lake-margin deposits in core material showed trace actinolite associated with the mafic Sheep Creek fan (fig. C.9*A*). Where present, actinolite mineral grains are generally fractured and appear weathered. Chromium concentrations in actinolite measured using pXRF as part of this study (chapter B) ranged from 920 to 4,000 mg/kg (Groover and Izbicki, 2018). Actinolite would be present within the light-heavy-mineral fraction that composed as much as 11 percent of older Mojave River material. Where measured, chromium concentrations within the light-heavy-mineral fraction ranged from 3 to 210 mg/kg (Morrison and others, 2018). Actinolite was not observed optically in alluvium from recent Mojave River deposits, although actinolite was observed in local fan deposits at MW-193 (76–81 ft bls) within Water Valley, indicating that these materials contain some older Mojave River alluvium. Optical examination of older Mojave River alluvium also shows graphite-stained feldspars eroded from Pelona Schist within the San Gabriel Mountains (fig. C.9*A*). Older Mojave River alluvium from sites MW-159 and MW-163 (in the western subarea downgradient from the western excavation site) contained trace amounts of unidentified opaque metamorphic minerals (fig. C.9*B*), possibly associated with metavolcanics that crop out on the southern end of Iron Mountain, that were not observed elsewhere in the valley. These materials do not contain high chromium concentrations (chapter B, table B.3).

Magnetite, although absent in samples from sites MW-153 and MW-154, was identified optically in a wide range of samples throughout Hinkley and Water Valleys, including recent and older Mojave River alluvium and local fan deposits. Magnetite has a specific gravity of about 5.2 and is within the heavy-mineral fraction. Chromium concentrations within the heavy-mineral fraction are an order of magnitude greater than bulk material. In some cases, magnetite has not completely weathered from the surrounding silicate lithic fragment (fig. C.9*B*). Chromium-containing magnetite encased within less-dense silicates may not have been properly sorted by density and could contribute chromium to the light-heavy-mineral fraction (specific gravity 2.85 to 3.32) or the light-mineral fraction (specific gravity less than 2.85).

Although magnetite is resistant to weathering, magnetite from site MW-193 (76–81 ft bls) shows minor oxidation (red rind) around the edges of the grain (fig. C.9*B*), indicating partial weathering to hematite. Oxide coatings and weathering rinds are common on mineral grains and range from thin rinds (fig. C.9*C*) to thick coatings (fig. C.9*D*). Iron oxides also occur as small particles within fine-textured clay-mineral masses from mudflat/playa deposits in MW-154 (72–77 ft bls). These particles may have originated as magnetite disseminated throughout the mudflat/playa material during deposition, which was later oxidized to hematite (potentially releasing chromium). Magnetite is notably absent in core material from MW-154.

Manganese oxides in MW-154 form dendritic structures known as “dragon’s breath,” and in some samples, manganese nodules are visible without a microscope (fig. C.9*C*). Manganese nodules commonly form in calcite-rich materials subject to intermittent wetting and drying (Dixon and Weed, 1989), conditions common in mudflat/playa deposits.

Some feldspars within local alluvium in Water Valley, partly eroded from Miocene deposits east of the study area, are highly weathered with weathering rinds, etching, and pitting (fig. C.9*D*). These features are consistent with the greater age of these materials compared to most other materials in Hinkley or Water Valleys.

C.3.2.2. X-Ray Diffraction

X-ray diffraction analysis of bulk samples was used to confirm optical data and to identify minerals in samples that could not be identified optically. As with the results of optical analyses, quartz and plagioclase (within the feldspar mineral group) were the most common minerals identified by XRD analysis (fig. C.10). These minerals were present in almost all samples, although quartz and plagioclase feldspar were present at only trace to minor amounts in some clay-rich materials (discussed in the following paragraph). Amphiboles were present at minor to trace levels in almost all samples, with the exception of material from MW-203D, which had no identifiable amphiboles (table C.6). Chromium-containing actinolite and hornblende are within the amphibole mineral group but were not identified separately by XRD (fig. C.10).

Cluster analysis was used to characterize XRD results (fig. C.10). Minerals within bulk samples clustered in six groups from generally higher to lower chromium concentrations (fig. C.11). Higher chromium concentrations were measured in samples from the Sheep Creek fan (mafic alluvium) and three clay-rich mineral clusters, including (1) clay-1 minerals associated with weathered rock from Iron Mountain, (2) clay-2 minerals associated with lacustrine deposits in the western subarea and mudflat/playa deposits in the northern subarea, and (3) clay-3 minerals eroded from granitic source material. Lower chromium concentrations were measured in samples within the felsic mineral cluster having a locally derived alluvium or a Mojave River depositional history. This group included core material from MW-137 (158 to 161 ft bls) that had a high abundance of heavy minerals presumably sourced from the Mojave River. One sample (MW-192; 117 to 122 ft bls), with a strong mineral influence consistent with Mojave-type deposits containing admixtures from Mount General, clustered by itself (fig. C.10).

Mineralogy and chromium concentrations of mafic alluvium from the Sheep Creek fan were measured for comparison and contrast with samples from Hinkley and Water Valleys. Abundant mica and amphibole minerals characterized samples WDP2 and SCF2B from the Sheep Creek fan. These samples have chromium concentrations as high as 170 mg/kg and do not cluster with samples from Hinkley and Water Valleys (fig. C.11). Results are consistent with their mafic source area and chromium-containing amphiboles identified optically within the samples.

A Actinolite in older Mojave-type deposits

(Photographs by Krishangi Groover, U.S. Geological Survey; ft bls, feet below land surface)

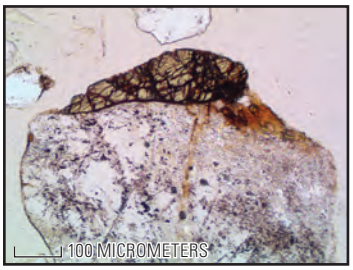

Actinolite on feldspar mineral grain from site BG-0005 (106 to 109 ft bls), plain polarized light. Note black graphite staining on feldspar mineral grain eroded from Pelona Schist.

Actinolite from site MW-163 (90 to 96 ft bls), plain polarized light.

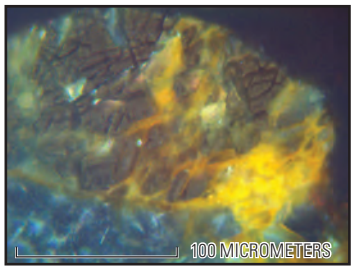

Actinolite from site BG-0005 (106 to 109 ft bls), reflected light.

B Magnetite and other minerals

(Photographs by Krishangi Groover, U.S. Geological Survey; ft bls, feet below land surface)

Amphibole (hornblende) and unidentified metamorphic minerals from site MW-159 (93 to 100 ft bls), cross-polarized light.

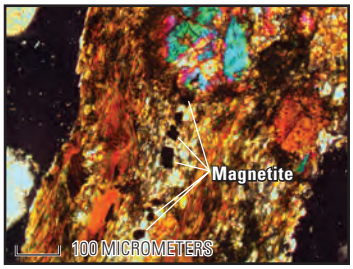

Magnetite within a lithic (rock) fragment from site Mount General (MGSOUTH), cross-polarized light.

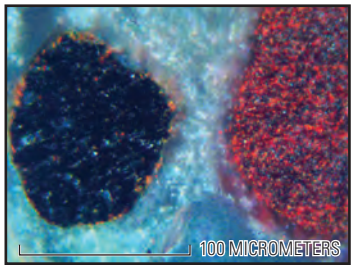

Magnetite with surface oxidation to hematite, and weathering rinds, within heavy mineral fraction from site MW-193 (76 to 81.5 ft bls), reflected light.

C Oxide coatings

(Photographs by Krishangi Groover, U.S. Geological Survey; ft bls, feet below land surface)

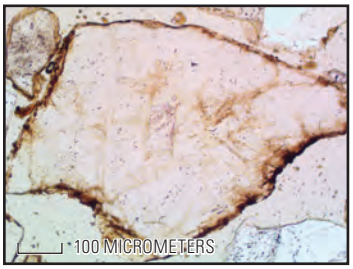

Oxide coatings and weathering rinds on feldspar mineral grain from site BG-0004 (64 ft bls), plain polarized light.

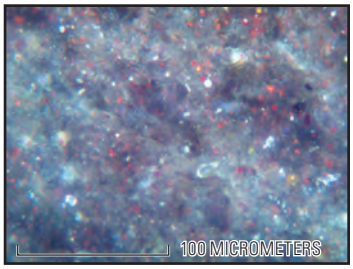

Iron oxide, hematite (red spots), in mudflat/playa deposites from site MW-154 (72 to 77 ft bls), reflected light.

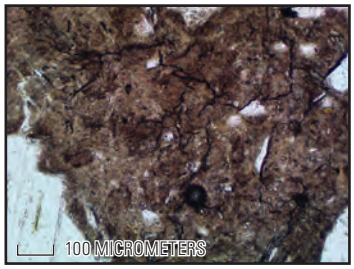

Manganese oxides (dark lines and spots) from site MW-154 (72 to 77 ft bls), plain polarized light.

D Weathered minerals

(Photographs by Krishangi Groover, U.S. Geological Survey; ft bls, feet below land surface)

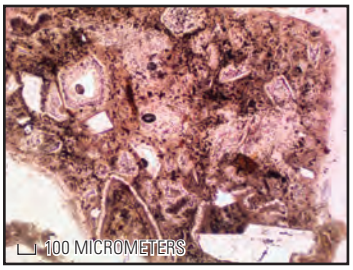

Weathering rinds on mineral grains from site MW-193 (76 to 81.5 ft bls), plain polarized light.

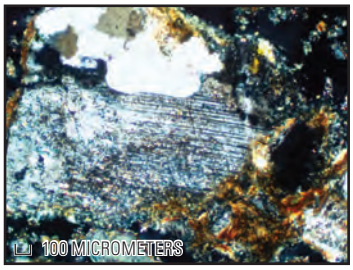

Weathered feldspar from site MW-193 (135 to 141 ft bls), cross-polarized light.

Weathered mineral grains and oxide coatings in Miocene-age deposits from site MW-203 (108 to 115 ft bls), plain polarized light.

Figure C.9. Selected minerals in thin section, including *A*, actinolite in Mojave-type alluvium, *B*, magnetite and opaque minerals in locally derived alluvium, *C*, oxide coatings, and *D*, weathered minerals from local alluvium, Hinkley and Water Valleys, western Mojave Desert, California. (Photographs by Krishangi Groover, U.S. Geological Survey, January 2017).

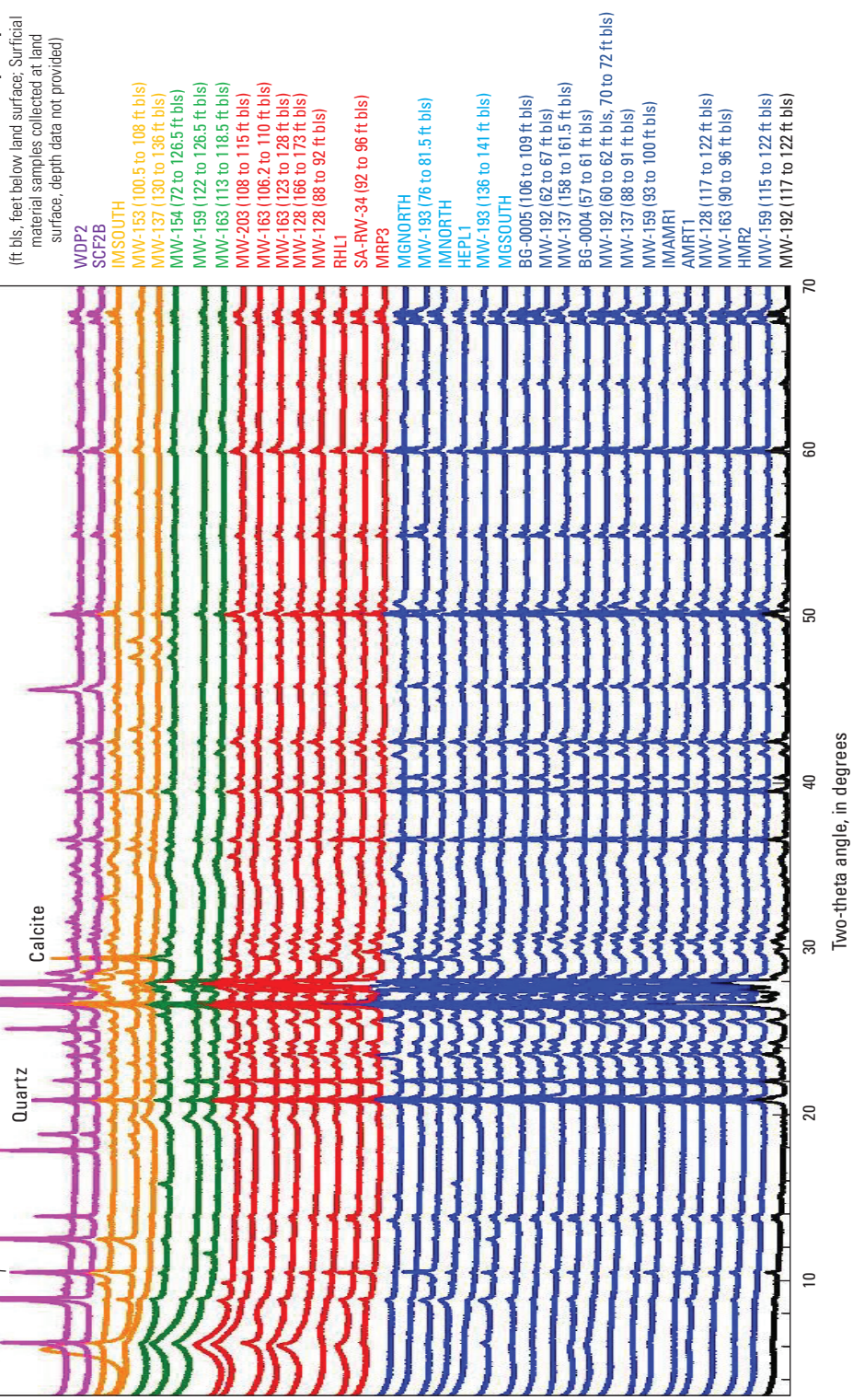

Figure C.10. X-ray diffraction (XRD) scans for selected samples of surficial alluvium and core material from wells, grouped by mineralogy, Hinkley and Water Valleys, western Mojave Desert, California. Data are from Morrison and others (2018).

Table C.6. Minerals identified by X-ray diffraction (XRD) in alluvium and core material, Hinkley and Water Valleys, and the Sheep Creek fan, western Mojave Desert, California.

[Data from Morrison and others (2018). Minerals listed in order of abundance in each category (major, minor, trace). Major minerals are present at greater than 15 percent abundance, minor minerals are present between 5 and 15 percent, and trace minerals compose less than 5 percent of the sample. **Abbreviation:** ', foot below land surface]

Depositional provenance	Bulk sample	Heavy mineral fraction	Samples
Recent Mojave	Major: plagioclase, microcline (potassium feldspar), quartz	Major: sphene (titanite), pyroxene, hematite, epidote	BG-0004 (57'–61'); HMR2
	Minor:	Minor: ilmenite	
	Trace: amphibole, mica, chlorite, magnetite	Trace:	
Older Mojave	Major: quartz, plagioclase, microcline (potassium feldspar)	Major: sphene (titanite), hematite	BG-0005 (106'–109'); MW-159 (93'–100'); MW-159 (115'–120'); MW-128 (117'–122'): MW-192 (60'–62', 70'–72'); MW-192 (62'–67'); MW-137 (88'–91'); AMRT1; IMAMR1
	Minor: mica	Minor: magnetite, epidote, amphibole, ilmenite	
	Trace: amphibole, magnetite, calcite, chlorite, clay (undifferentiated), rutile, sphene (titanite)	Trace: pyroxene, rutile, zircon	
Lake margin	Major: quartz, plagioclase, microcline (potassium feldspar)	Major: sphene (titanite), epidote	MW-128 (88'–92'); MW-128 (166'–173'); MW-137 (158'–161.5'); MW-163 (90'–96'); SA-RW-34 (90'–97')
	Minor: clay (undifferentiated), amphibole, mica	Minor: hematite, amphibole, magnetite	
	Trace: calcite, chlorite, pyroxene, tourmaline, magnetite	Trace: ilmenite, pyroxene, zircon	
Lacustrine (lake)	Major: mica, plagioclase, quartz	Major: sphene (titanite), hematite	MW-159 (122'–126.5'); MW-163 (106.2'–110'); MW-163 (113.5'–118'); MW-192 (117'–122'); RHL1
	Minor: microcline (potassium feldspar), clay (undifferentiated), chlorite, calcite	Minor: ilmenite, pyroxene, magnetite, pyrite, rutile	
	Trace: amphibole, gypsum	Trace: amphibole, epidote, zircon	
Mudflat/playa	Major: plagioclase, quartz, mica, microcline (potassium feldspar)	Major: sphene (titanite), hematite, epidote, magnetite	MW-137 (130'–136'); MW-154 S1 (72'–77'); HEPL1; MRP3
	Minor: clay (undifferentiated), calcite, chlorite	Minor: pyroxene, amphibole	
	Trace: amphibole, analcime, andalusite, magnetite	Trace: ilmenite, microcline (potassium feldspar)	
Local fan, weathered bedrock	Major: plagioclase, quartz, microcline (potassium feldspar)	Major: hematite, sphene (titanite)	MW-193 S1 (76'–81.5'); MW-193 S3 (135'–141'); MW-203 D (108'–115'); MW-163 (123'–128'); MW-153 (100.5'–108'); IMNORTH; IMSOUTH; MGNORTH; MGSOUTH
	Minor: amphibole, chlorite, mica	Minor: amphibole, ilmenite, magnetite	
	Trace: calcite, clay (undifferentiated), magnetite, pyroxene, heulandite	Trace: barite, epidote, pyroxene	
Other (Sheep Creek fan eroded from mafic Pelona Schist)	Major: chlorite, mica, plagioclase, quartz	Major: epidote, sphene (titanite), garnet, hematite	WDP2; SCF2B
	Minor: amphibole	Minor: amphibole, pyroxene, rutile	
	Trace: calcite, clay	Trace: ilmenite	

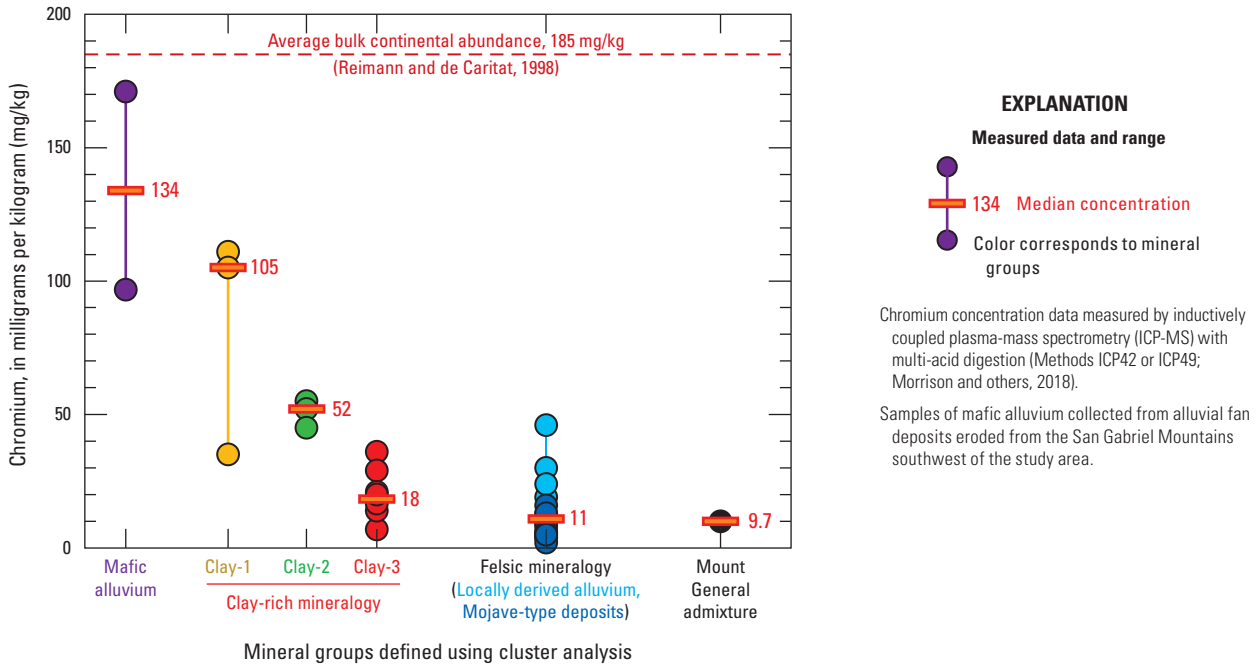

Figure C.11. Chromium concentrations in selected samples of surficial alluvium and core material, grouped by mineralogy, Hinkley and Water Valleys, and the Sheep Creek fan, western Mojave Desert, California. Data are from Morrison and others (2018).

Clay minerals, including chlorite group minerals and expandable smectite, characterized samples within the clay-1, clay-2, and clay-3 mineral clusters (fig. C.10). Chlorite group minerals, including clinochlore and chamosite, were not identified separately by XRD and are collectively referred to as chlorite for the purposes of this professional paper. Consistent with their generally fine texture (chapter B, fig. B.8), chromium concentrations in clay mineral groups ranged from less than 10 to 110 mg/kg, with median concentrations of 105, 52, and 18 mg/kg, respectively (fig. C.11).

The clay-1 cluster included coarse-textured surficial alluvium eroded from Iron Mountain (IMSOUTH) and weathered hornblende diorite bedrock from MW-153 (102 to 106 ft bls), with chromium concentrations of 110 and 105 mg/kg, respectively (fig. C.11). Mudflat/playa deposits from MW-137 (130 to 136 ft bls) in the northern subarea also cluster within the clay-1 mineral group, although chromium concentrations in this sample were only 35 mg/kg. Mudflat/playa deposits likely cluster within the clay-1 mineral group because of chlorite (eroded or weathered) from mafic rock associated with Iron Mountain.

The clay-2 cluster was composed of lacustrine deposits from MW-159 (122 to 126.5 ft bls) and MW-163 (113.5 to 116 ft bls), and mudflat/playa deposits from MW-154 (72 to 77 ft bls), with chromium concentrations ranging from 45 to 55 mg/kg. Quartz was identified by XRD in only minor amounts within the clay-2 cluster. Lacustrine deposits from MW-159 and MW-163 that underlie older Mojave River alluvium were reduced and largely contain locally derived material. Material from MW-154 differs from most other mudflat/playa deposits sampled in Hinkley Valley, in that the material was partly reduced (green color) with trace microfossils and had some characteristics similar to lacustrine deposits. Analcime, possibly eroded from nearby basalt, was present in minor amounts in core material from MW-154. Similar to the clay-1 cluster, mineralogy in the clay-2 cluster was dominated by chlorite, with expandable clay minerals (such as smectite) present at minor to trace amounts. Although chromium can substitute within chlorite (Dixon and Weed, 1989), chromium concentrations in the light-mineral fraction within the clay-1 and clay-2 cluster did not exceed 50 mg/kg, consistent with limited substitution of chromium within clay minerals.

Quartz and plagioclase were present with clay minerals within the clay-3 cluster. These minerals reflect a granitic source that may originate from local source materials or from the Mojave River. Although generally fine-textured, clay-3 samples are generally coarser than clay-1 or clay-2 samples, often containing sand and gravel (or granitic rock fragments in MW-203). Chromium concentrations in the clay-3 group ranged from less than 10 to 36 mg/kg with a median concentration of 18 mg/kg.

Most samples (19 of 36) were characterized by felsic mineralogy predominated by quartz and plagioclase with an absence of clay minerals (fig. C.10). Felsic materials are composed of Mojave-type deposits (including Mojave River stream and lake-margin deposits) and locally derived alluvium. Samples of locally derived surficial alluvium from Iron Mountain (IMNORTH), Mount General (MGNORTH and MGSOUTH), as well as core material from Water Valley (MW-193 both depths), cluster together within the upper portion of the felsic mineral group and were not sufficiently distinct to cluster separately from Mojave-type deposits (fig. C.10). Chromium concentrations in felsic samples ranged from 2 to 46 mg/kg, with a median concentration of 11 mg/kg. Chromium concentrations were higher in locally derived alluvium with a median concentration of 22 mg/kg (not shown on fig. C.11) and lower in Mojave River stream and lake-margin deposits with a median concentration of 6 mg/kg (not shown on fig. C.11). The highest chromium concentrations within the felsic mineral group were in surficial alluvium eroded from hornblende diorite that crops out on Iron Mountain (IMNORTH).

Lacustrine deposits from MW-192 (117 to 122 ft bls) cluster within their own group but were not distinctly different from samples having a felsic mineralogy. Presumably this sample differs on the basis of accessory minerals, possibly eroded from nearby Mount General, that are present in the XRD scan but are not specifically identified (fig. C.10). Mudflat/playa material from HEPL1 in the eastern subarea near Mount General within the felsic mineral group, also contained metamorphic accessory minerals, such as andalusite, likely eroded from nearby Mount General. Chromium concentrations within this sample were low, 9.7 mg/kg (fig. C.11).

X-ray diffraction also was used to determine the mineralogy of the heavy-mineral fraction, but cluster analysis was not done with these data. Common minerals identified by XRD in the heavy-mineral fraction include hematite, ilmenite, magnetite, and titanite (table C.6; Morrison and others, 2018). Epidote was present at minor to major abundances in the heavy-mineral fraction from most Mojave-type, lacustrine, and mudflat/playa samples. Amphibole was common in older Mojave River deposits, but generally was not present in the heavy-mineral fraction from recent Mojave River alluvium. Weathered hornblende diorite bedrock at MW-153 does not contain magnetite in either the bulk or heavy-mineral fractions.

C.3.2.3. Scanning Electron Microscopy

Heavy-mineral grains isolated from surficial alluvium and core materials were examined using SEM with EDS. Energy dispersive X-ray spectroscopy was used to determine the elemental composition of mineral grains to assist with mineral identification and to identify chromium substitution within mineral grains. The detection limit for chromium by EDS is between 100 and 200 mg/kg and higher than the reporting limits for pXRF or ICP-MS data. Consequently, it was not always possible to identify chromium substituted within minerals by EDS, and most magnetite did not contain detectable chromium by EDS. Despite this limitation, chromium substitution for Fe(III) within magnetite mineral grains was identified (figs. C.12*A*, *B*) and ranged from trace substitutions near the reporting level to near complete substitution of Cr(III) for Fe(III) in magnetite ($Fe^{II}Fe^{III}_2O_4$) that approached the composition of chromite ($Fe^{II}Cr^{III}_2O_4$; fig. C.12*B*). Although a high level of chromium substitution within some magnetite mineral grains was identified, chromite was not identified in residual minerals remaining after four-acid digestion of selected samples (Morrison and others, 2009). Most chromium-containing magnetite grains showed no evidence of weathering on the SEM, although optical examination of magnetite in locally derived alluvium from MW-193 (76 to 81.5 ft bls; fig. C.9*B*) partly eroded from Miocene deposits showed evidence of oxidation of magnetite to hematite. Similarly, MW-154 (72 to 77 ft bls) in mudflat/playa deposits containing Miocene material shows almost complete oxidation of magnetite to hematite (fig. C.9*C*). Where chromium-containing magnetite mineral grains were identified within Mojave-type materials, they were commonly smaller than 100 µm and would contribute chromium to the smaller particle-size fractions (figs. C.12*B,C*). Larger chromium-containing magnetite mineral grains were present within locally derived alluvium (fig. C.12*A*), possibly contributing to the unusual distribution of chromium by particle size in locally derived alluvium (fig. C.6).

A wide range of minerals not readily identified optically or below the reporting level for XRD were identified in the heavy-mineral fraction by SEM (fig. C.12*C*). Chromium-containing minerals, such as actinolite, hornblende, and chlorite, having specific gravities less than 3.32, were not present in the heavy-mineral fraction; chromium substitution within heavy minerals, other than magnetite, was not observed by SEM with EDS (Morrison and others, 2018). The phosphate mineral group monazite, present within the heavy-mineral fraction (fig. C.12*C*), is an important ore for thorium. Along with uranium, decay of thorium may contribute to high gross alpha activities in water from wells in Hinkley and Water Valleys. In addition to the iron and manganese coatings discussed previously, abundant aluminum-oxide coatings were present on the surfaces of some heavy-mineral grains (fig. C.12*D*).

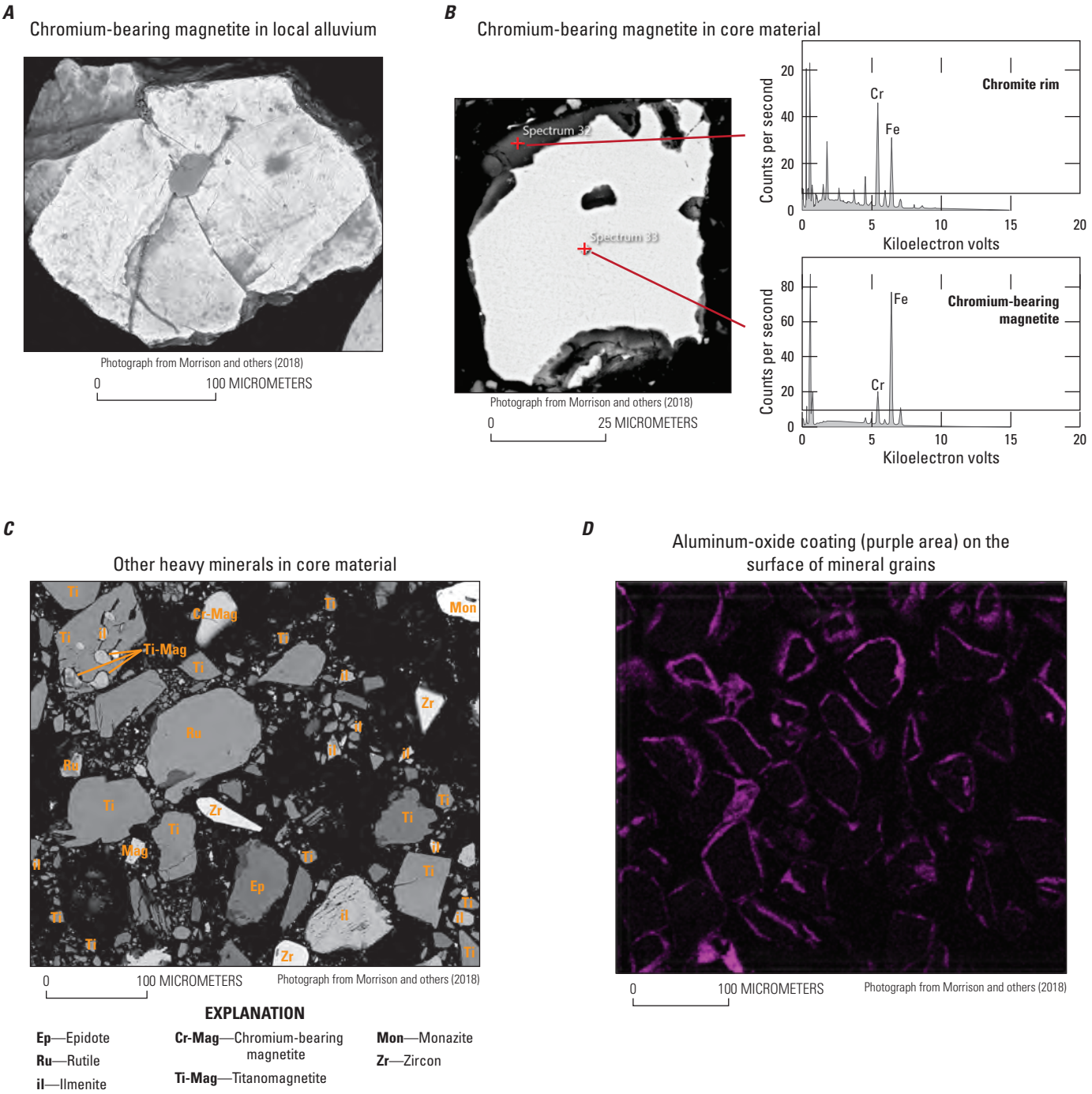

Figure C.12. Scanning electron photomicrographs of *A*, chromium-bearing magnetite in local alluvium, *B*, chromium-bearing magnetite in Mojave-type core material with elemental composition by X-ray energy dispersive spectroscopy (EDS), *C*, other heavy minerals in core material, and *D*, aluminum-oxide coatings on the surfaces of mineral grains, Hinkley and Water Valleys, western Mojave Desert, California. Data are from Morrison and others (2018).

C.3.3. Coatings on the Surfaces of Mineral Grains

Iron-, manganese-, and aluminum-oxide coatings are ubiquitous on the surfaces of mineral grains that compose aquifers. These oxide coatings serve as sorption sites for chromium and other trace elements. Trace elements extractable from these oxide coatings are potentially mobile and may enter groundwater under the proper aqueous geochemical conditions (fig. C.2). In contrast, elements contained within primary mineral grains are less mobile and must weather from minerals before they can enter groundwater (Izbicki and others, 2008; Ščančar and Milačič, 2014; Morrison and others, 2015).

At the microscale, optical examination of mineral grains indicates that oxide coatings may be more abundant near surface imperfections (cracks) and at boundaries between minerals in rock fragments and in weathered Miocene materials. In some cases, oxide accumulations appear to be associated with weathering of less resistant minerals, such as actinolite present in older Mojave River deposits (fig. C.9*A*). Optical examination shows oxide coatings can be as much as 20 µm thick on some grains, although generally they are less than 5 µm thick to indistinguishable.

At the macroscale, visual examination of core material shows layers up to 3 ft thick with visually abundant iron- and manganese-oxide coatings on the surfaces of mineral grains near the water-table interface, near redox boundaries associated with lithologic and other geologic contacts, and within other geologic materials including mudflat/playa deposits (figs. C.13*A*, *B*, *C*). These oxide coatings have trace-element concentrations greater than the surrounding host material, with chromium and arsenic concentrations as high as 120 and 300 mg/kg, respectively (chapter B).

In addition to iron, manganese, and aluminum oxides, carbonate minerals were present in the matrix surrounding mineral grains in groundwater-discharge deposits in Hinkley and Water Valleys (fig. C.13*D*). Chromium concentrations within these materials were low. Uranium, which strongly complexes with carbonate in groundwater-discharge deposits, can be as high as 19 mg/kg (Groover and Izbicki, 2018).

For the purposes of this professional paper, selected trace elements (including arsenic, chromium, vanadium, and uranium) were extracted from the surfaces of mineral grains using progressively stronger extraction solutions (Chao and Sanzolone, 1989; Wenzel and others, 2001). Concentrations within each extract represent operationally defined fractions associated with surface-sorption sites on the surfaces of mineral grains (table C.2). The most mobile fraction is the weakly sorbed fraction, followed by the specifically sorbed fraction. The pH-dependent sorption/desorption reactions commonly involve the specifically sorbed fraction. The most refractory (least-mobile) materials are associated with the well-crystallized and strong-acid extractable fractions. Both the well-crystallized (Wenzel and others, 2001) and the strong-acid extractable fractions (Chao and Sanzolone, 1989) are intended to characterize similar crystalline hydroxides on the surfaces of mineral grains. In general, chromium and other trace-element concentrations were higher in the strong-acid extractable fraction than in the well-crystallized extractable fraction, and the strong-acid extractable data are discussed in this professional paper. Total extractable concentrations were calculated as the sum of the weakly sorbed, specifically sorbed, and strong-acid extractable fractions (table C.2).

C.3.3.1. Abundance of Aluminum, Iron, and Manganese Sorption Sites

Aluminum, iron, and manganese form oxides and other coatings on the surfaces of mineral grains that act as substrates for sorption of trace elements. Aluminum, iron, and manganese within the strong-acid extractable fraction were used to evaluate the potential abundance of sorption sites. Sorption of trace elements to various oxides and other coatings is pH dependent, related to the anion exchange capacity, and to the point of zero charge (PZC) of the sorbent, which differs for various oxides and mineral configurations. The anion exchange capacity varies with the active surface area exposed on the surfaces of mineral grains but was approximated by mass of aluminum (Al), iron (Fe), and manganese (Mn) oxides in the strong acid extractable fraction for the purposes of this professional paper. In general, the PZC for Mn oxides is less than Fe oxides and less than Al oxides. Trace elements sorbed to iron and manganese oxides (or incorporated within secondary minerals) also may be mobilized by changing redox conditions as a consequence of reductive dissolution of iron- and manganese-oxide surface coatings. Additionally, manganese-3 (Mn-III) and manganese-4 (Mn-IV) oxides may oxidize Cr(III) to Cr(VI) under the proper redox conditions (Schroeder and Lee, 1975).

A

Oxides near the water table

Water table oxide accumulation near the Mojave River at BG-0004
(46 to 47 feet below land surface)

Photograph by Krishangi Groover, U.S. Geological Survey, October 2016

Water table oxide accumulation at MW-158
(95 to 101 feet below land surface)

Photograph by Krishangi Groover, U.S. Geological Survey, March 2016

B

Oxides near lithologic contacts

Oxide accumulation on silt at contact with coarse sand, MW-121
(112.4 feet below land surface)

Photograph by Krishangi Groover, U.S. Geological Survey, March 2016

Oxide accumulation on silt at contact with coarse sand, BG-0002
(132.5 to 135.5 feet below land surface)

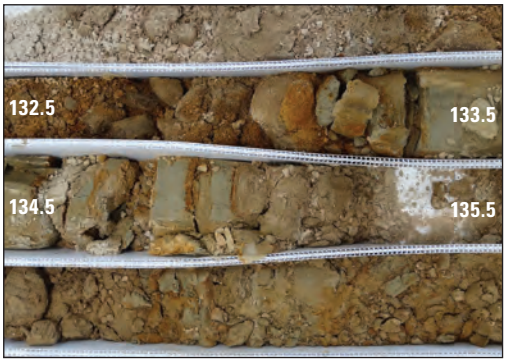

Photograph by Krishangi Groover, U.S. Geological Survey, October 2016

C

Manganese oxides

Manganese-oxide nodules in mudflat/playa deposits,
MW-137 (130 to 136 feet below land surface)

Photograph by Krishangi Groover, U.S. Geological Survey, March 2016

D

Groundwater discharge

Groundwater discharge deposits overlying bedrock, MW-153
(94 to 108.5 feet below land surface)

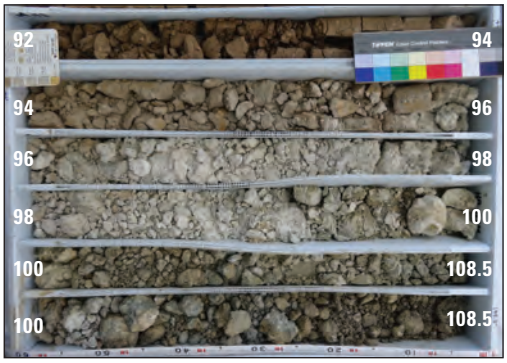

Photograph by Krishangi Groover, U.S. Geological Survey, March 2015

Poor sample recovery from 100 to 108.5 feet below land surface.
Recovered material shown.

Figure C.13. Visually abundant iron- and manganese-oxide coatings in core material *A*, near the water table, *B*, near lithologic contacts, *C*, within mudflat/playa deposits, and *D*, groundwater-discharge deposits, Hinkley and Water Valleys, western Mojave Desert, California.

Total aluminum, iron, and manganese concentrations on the surfaces of mineral grains were estimated from the strong-acid extractions from bulk samples. Extractable aluminum and iron concentrations were about an order of magnitude lower than total concentrations, while extractable manganese concentrations were about one-third lower than total manganese concentrations. Extractable aluminum and iron were approximately equal and about two orders of magnitude more abundant than manganese on a per weight basis (fig. C.14); however, aluminum oxides would be about twice as abundant as iron oxides on a molar basis. Compared to aluminum and iron, a greater fraction of manganese is extractable and presumably has weathered more extensively from primary mineral grains (fig. C.14*B*). Aluminum, iron, and manganese concentrations in the strong-acid extractable fraction are greater in finer-textured material—consistent with the greater surface area of those materials providing more sorption sites for chromium and other trace elements. The highest extractable aluminum and iron concentrations were within the clay-2 mineral cluster (fig. C.10) from clay-texture lacustrine deposits from MW-159 (112 to 126.5 ft bls) and weathered gneiss from MW-163 (113 to 118.5 ft bls) that underlie older Mojave River deposits downgradient from the western excavation site (Lahontan Regional Water Quality Control Board, 2014). The highest extractable manganese concentrations were from MW-193 (136 to 141 ft bls) in Water Valley within the local felsic mineral cluster (fig. C.10). Although extractable aluminum, iron, and manganese concentrations vary with texture, fine-textured felsic Mojave-type deposits commonly had lower extractable aluminum, iron, and manganese concentrations (indicating fewer surface sorption sites) than similar-texture material from other depositional provenances.

C.3.3.2. Chromium and Other Trace Elements Extractable from Sorption Sites

Total chromium concentrations in mineral grains from multi-acid digestion (Methods ICP42 or ICP49; Morrison and others, 2018) were lower than the average bulk continental abundance of 185 mg/kg (Reimann and de Caritat, 1998), although some materials had chromium concentrations that exceeded the threshold of 85 mg/kg (chapter B, fig. B.11) for the summative-scale analyses (SSA) presented within this professional paper (chapter H). Most extractable chromium was in the strong-acid extractable fraction (fig. C.15). Chromium within the amorphous fraction was about an order of magnitude less abundant, and chromium within the specifically sorbed and weakly sorbed fractions were about two orders of magnitude less abundant than chromium within the strong-acid extractable fraction (fig. C.15).

The median chromium concentration extractable from mineral grains was 9 percent of the total chromium concentration within the sample (fig. C.16*A*). The data indicate that, typically, more than 90 percent of chromium remains within unweathered mineral grains and is relatively unavailable to groundwater. Median extractable percentages of chromium varied with texture and ranged from 5 percent in sand and gravel to 11 percent in silt and finer-textured material (figs. C.16*B*, *C*, *D*). The highest extractable percentage of chromium, 34 percent, was in clay-textured mudflat/playa core material from site MW-192 in the eastern subarea between 60 to 62 and 70 to 72 ft bls. However, this material was felsic (fig. C.10), with a chromium concentration of only 11 mg/kg, and the total extractable chromium concentration was 3.7 mg/kg.

Miocene materials from site MW-203 in the western subarea (between 108 and 115 ft bls) and local alluvium containing Miocene materials from site MW-193 in Water Valley (between 76 and 81.5 ft bls) had 27 percent extractable chromium, which was consistent with weathering of Miocene materials. The chromium concentrations in core materials analyzed at these sites were 11 and 15 mg/kg, respectively, and the total extractable chromium concentrations were 3 and 4 mg/kg, respectively. However, pXRF data (Groover and Izbicki, 2018) show chromium concentrations in Miocene core material adjacent to the screened interval of well MW-203D are as high as 347 mg/kg, and extractable chromium concentrations in Miocene materials penetrated by well MW-203D could be as high as 94 mg/kg. Similarly, pXRF data (Groover and Izbicki, 2018) show chromium concentrations in core material adjacent to the screened interval of well MW-193S3 are as high as 31 mg/kg, and extractable chromium concentrations in materials penetrated by well MW-193S3 could be as high as 8.4 mg/kg.

The extractable percentage of chromium from weathered hornblende diorite in core material adjacent to the screened interval of well MW-153S between 108 and 115 ft bls was only 14 percent. However, chromium concentrations in core material adjacent to the screened interval of well MW-153S were 105 mg/kg, and the total extractable chromium concentration was 14.7 mg/kg.

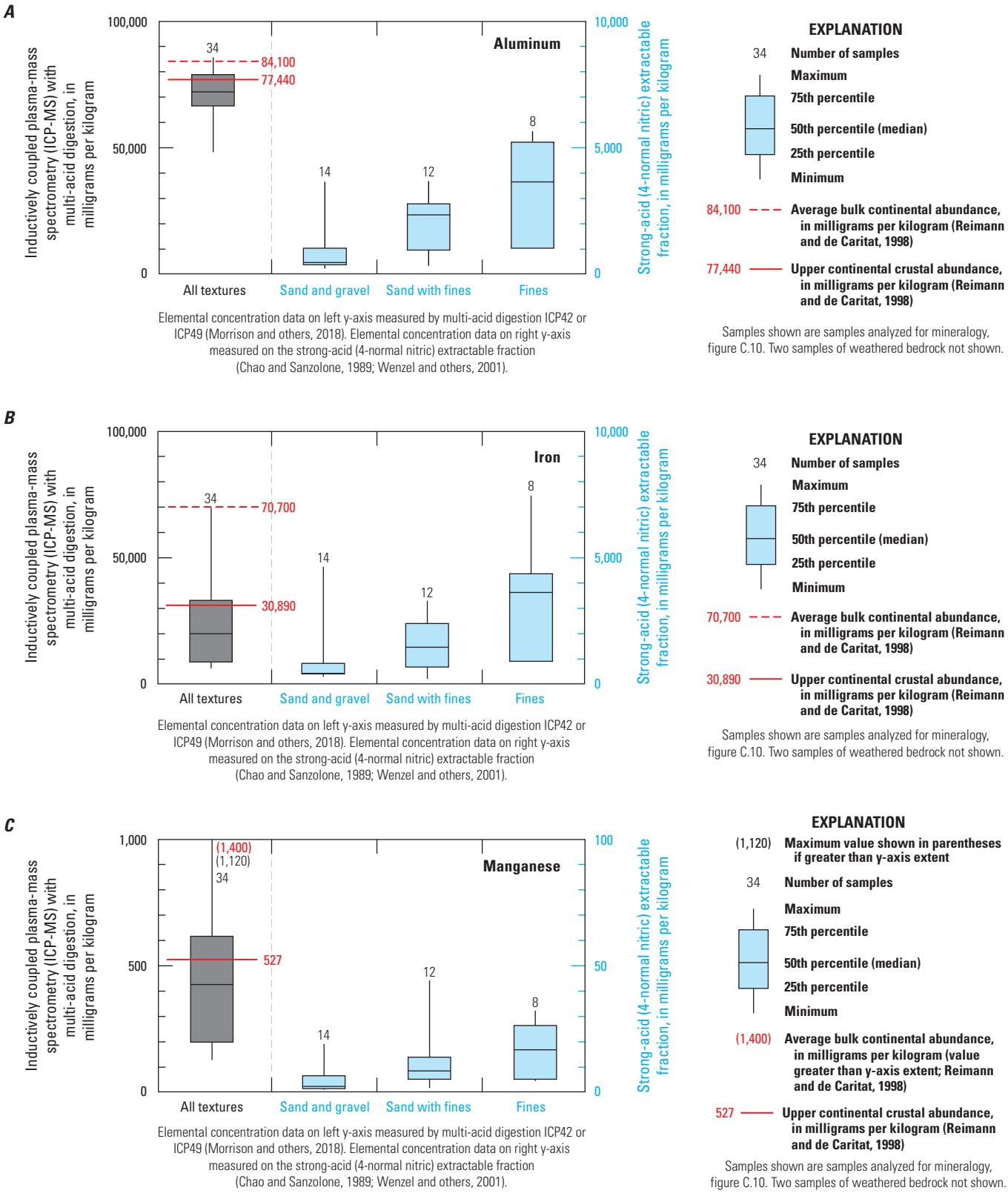

Figure C.14. Concentrations of *A*, aluminum, *B*, iron, and *C*, manganese in multi-acid digestions and in the strong-acid extractable fraction by texture from selected surficial alluvium and core material in Hinkley and Water Valleys, western Mojave Desert, California. Data are from U.S. Geological Survey (2021).

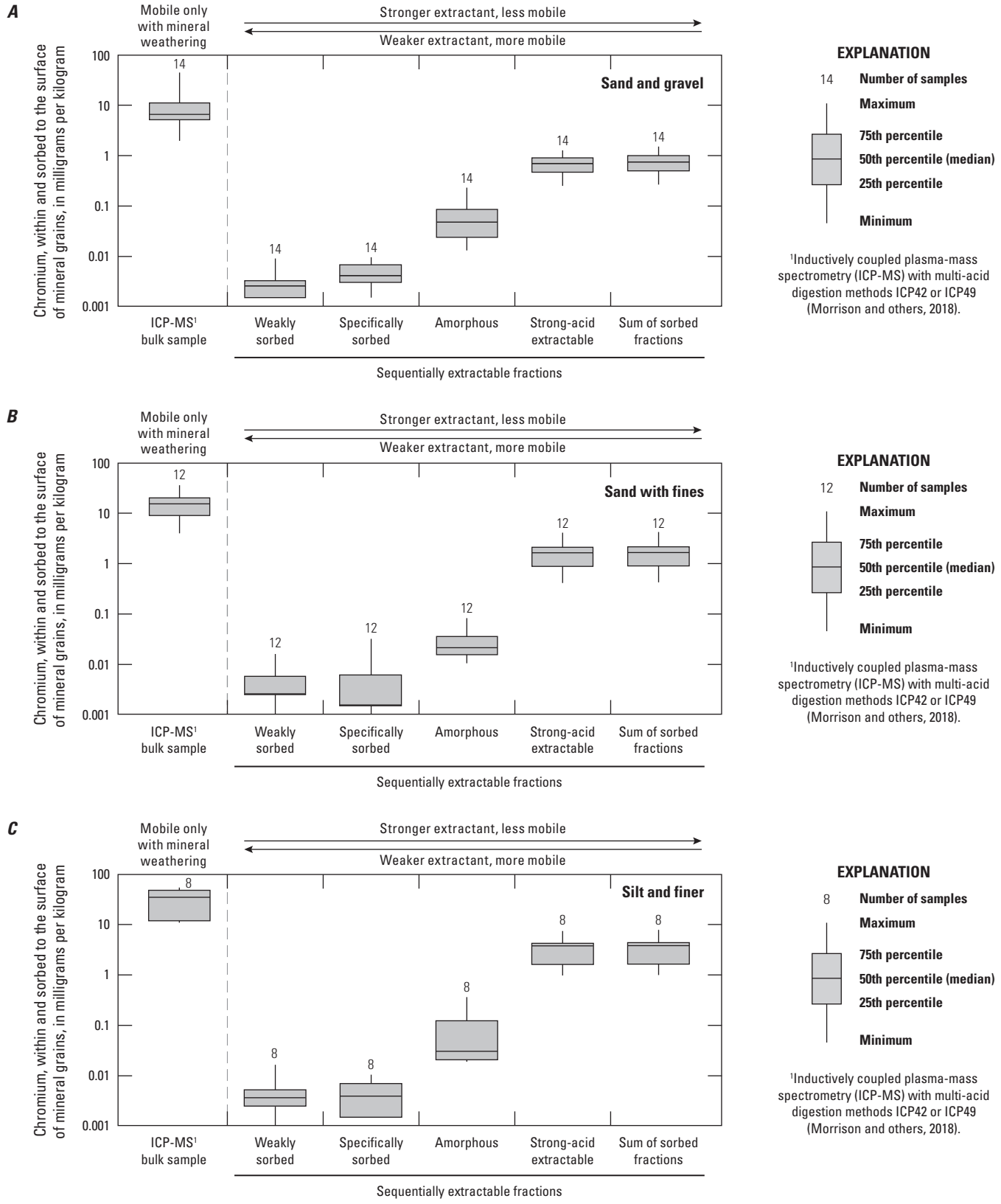

Figure C.15. Chromium concentrations in multi-acid digestions and within sequentially extracted fractions from surficial alluvium and core material in *A*, sand and gravel, *B*, sand with fines, and *C*, silt and finer textures, from Hinkley and Water Valleys, western Mojave Desert, California. Data are from U.S. Geological Survey (2021).

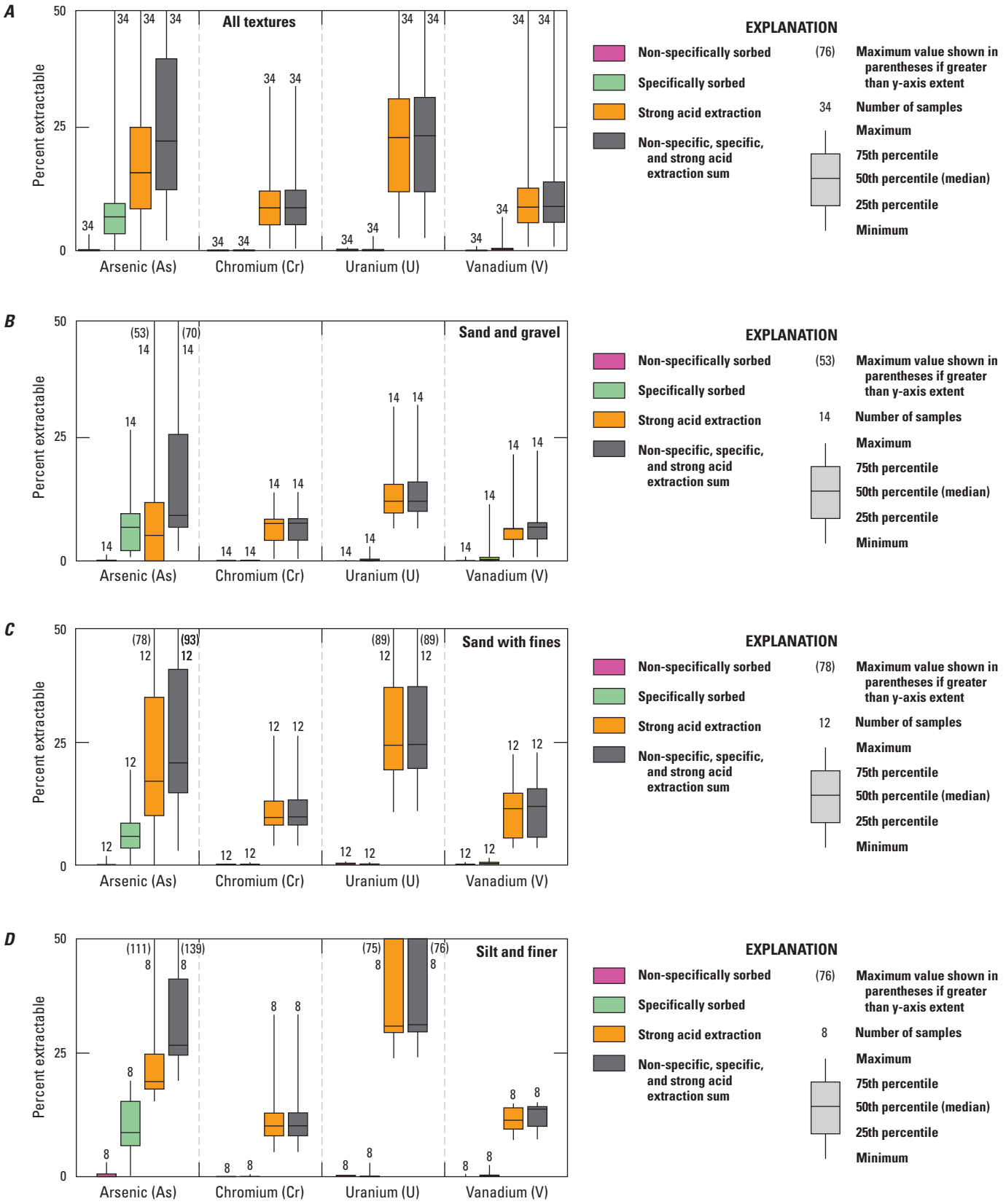

Figure C.16. Percent arsenic, chromium, uranium, and vanadium extractable from mineral grains in *A*, all samples and selected samples of *B*, sand and gravel, *C*, sand with fines, and *D*, silt and finer-textured surficial alluvium and core material, Hinkley and Water Valleys, western Mojave Desert, California. Data are from Morrison and others (2018) and U.S. Geological Survey (2021).

Differences in the extractable concentrations of arsenic, uranium, and vanadium are shown for comparison with chromium (fig. C.16). Although commonly present at lower concentrations in rock and core material than chromium, higher percentages of arsenic and uranium are extractable from the surfaces of mineral grains, and these elements are potentially more available to groundwater than chromium (fig. C.16). The percentage of arsenic and uranium extractable from surface exchange sites was greater in fine-textured materials than in coarse textured materials; median extractable arsenic and uranium concentrations ranged from 9 to 12 percent in sand and gravel and from 28 to 32 percent in silt and finer-textured material. In one sample, all of the arsenic was extractable, and in another sample, as much as 76 percent of the uranium was extractable. Unlike other elements measured, 6 to 10 percent of arsenic was within the specifically sorbed (pH-dependent) fraction, and in some samples, almost 20 percent of the arsenic was present within the specifically sorbed fraction and potentially mobile into groundwater with increases in pH. Vanadium is distributed within extractable fractions similarly to chromium with little variation by texture. Rather than having weathered directly from mineral grains, some arsenic, uranium, and chromium were likely weathered from mineral grains elsewhere, transported by groundwater, and incorporated into surface coatings measured as part of this study.

Although less abundant than chromium in geologic materials, arsenic and uranium are more available to groundwater than chromium or vanadium as a result of differences in mineral weathering and sorption. As a consequence, in 2016, arsenic and uranium exceeded their respective maximum contaminant levels (MCLs) of 10 and 30 µg/L in almost 40 and 8 percent of sampled domestic wells in Hinkley and Water Valleys, respectively (Izbicki and Groover, 2018).

C.4. Distribution of Chromium in Selected Geologic Materials

Chromium abundance in geologic materials and its potential mobility into water from wells are of concern to local stakeholders from a regulatory and public health standpoint. Wells yielding water having high Cr(VI) concentrations of interest include wells completed in (1) weathered bedrock, (2) Miocene deposits and deposits containing weathered Miocene minerals, (3) secondary-oxidized alluvium, (4) mudflat/playa deposits, and (5) older Mojave River alluvium downgradient from the western excavation site in the western subarea (Lahontan Regional Water Quality Control Board, 2014). Chemical and mineralogic data presented previously for core material adjacent to the screened interval of wells in these areas were examined to determine the concentration of chromium, the distribution of chromium within mineral grains, the extent of weathering of mineral grains, the concentration, including the distribution of extractable chromium on the surfaces of mineral grains, and the potential for oxidation of Cr(III) weathered from mineral grains to Cr(VI) in the presence of manganese oxides. Chemical and mineralogic data were used to evaluate potential occurrence of naturally occurring Cr(VI) in water from these wells.

Aqueous geochemistry, including redox and pH, can influence Cr(VI) concentrations in groundwater. Most groundwater in Hinkley and Water Valleys is oxic (contains dissolved oxygen), and the redox status of groundwater does not vary greatly in the study area. In contrast, the pH of groundwater differs across Hinkley and Water Valleys, and the effect of pH-dependent sorption, with higher aqueous Cr(VI) concentrations at higher strongly alkaline pH values, differs across Hinkley and Water Valleys. Groundwater age is a measure of groundwater contact with aquifer materials; older groundwater ages reflect greater contact time, greater potential for aquifer materials to have reacted with groundwater, and in general, more alkaline pH values. Chromium concentrations, aqueous geochemistry, and isotopic data in water from wells are discussed in greater detail in chapters D, E, and F, respectively, within this professional paper. Mineralogic data are compared to groundwater Cr(VI) concentrations, pH, and groundwater age (time since recharge) data in chapter G within this professional paper.

C.4.1. Weathered Bedrock

As a result of groundwater pumping and subsequent water-level declines, unconsolidated deposits in parts of Hinkley and Water Valley were dry during conditions at the time of this study (2015–18), and some monitoring wells were completed partly or entirely in weathered bedrock. These wells include (1) MW-96S in weathered quartz diorite underlying the eastern subarea, (2) MW-164D and MW-159C in weathered quartz diorite underlying the western subarea, and (3) MW-119D and MW-153S in weathered hornblende diorite underlying the western subarea (Groover and Izbicki, 2018). Chromium concentrations measured by pXRF in quartz diorite that crops out within the study area were low (table B.2) and are not discussed further in this section. However, hornblende diorite that crops out in the study area has chromium concentrations measured by pXRF as high as 530 mg/kg (table B.3).

Well MW-153S in the western subarea, screened from 93.5 to 108.5 ft bls, is completed in weathered hornblende diorite. The total chromium concentration (multi-acid digestion, Method ICP42 or ICP49; Morrison and others, 2018) in core material (composited between 100.5 and 108.5 ft bls) was 105 mg/kg (Morrison and others, 2018). Chromium concentrations in weathered hornblende diorite in core material, measured by pXRF at depths adjacent to the screened interval of well MW-153S, were as high as 405 mg/kg (Groover and Izbicki, 2018) and are among the highest chromium concentrations measured in core material as part of this study. Manganese concentrations in core material adjacent to the screened interval of the well, measured by ICP-MS and pXRF, were as high as 815 and 4,940 mg/kg, respectively. Chromium and manganese concentrations measured by pXRF exceeded thresholds for scoring within the SSA of 85 and 970 mg/kg, respectively (chapter B, fig. B.11).

Examination of core material from MW-153 (100.5 to 108.5 ft bls; fig. C.10) shows hornblende to be the most abundant mineral; XRD data show the mineral assemblage includes clay minerals (fig. C.10). However, chromium within core material was distributed throughout a wide range of particle sizes and was not solely associated with silt and finer-grained material (less than 38 µm size; fig. C.17). This distribution reflects the weathered bedrock nature of these materials and lack of sorting by alluvial processes. Almost no heavy minerals were extracted by density separation from core material at MW-153 (fig. C.17). Although small amounts of heavy minerals, including magnetite (fig. C.12), were identified within this sample by SEM (Morrison and others, 2018), chromium was not identified in these heavy minerals by EDS.

Total extractable chromium (the sum of the weakly sorbed, specifically sorbed, and strong-acid extractable fractions) comprised about 14 percent of the total chromium within core material from MW-153. This percentage value is higher than chromium concentrations in core material from most other wells in Hinkley and Water Valleys (Groover and Izbicki, 2019) and elsewhere in the Mojave Desert (Izbicki and others, 2008). The total extractable chromium concentration of almost 15 mg/kg was the highest measured in Hinkley and Water Valleys, including total extractable concentrations from core material within the mapped plume, and exceeds the total extractable concentrations measured on mafic alluvium within the Sheep Creek fan, west of the study area. High total extractable manganese concentrations of 550 mg/kg within core material from MW-153S indicates potential for oxidation of Cr(III) to Cr(VI), although the mineralogy and oxidation state of manganese oxides in core material were not measured at this site.

The Cr(VI) concentration in water from well MW-153S sampled in March 2015 as part of the USGS Cr(VI) background study was 3.3 µg/L (chapter E) and exceeded the interim regulatory Cr(VI) background concentration of 3.1 µg/L established on the basis of the 2007 Cr(VI) background study (CH2M Hill, 2007). Hexavalent chromium

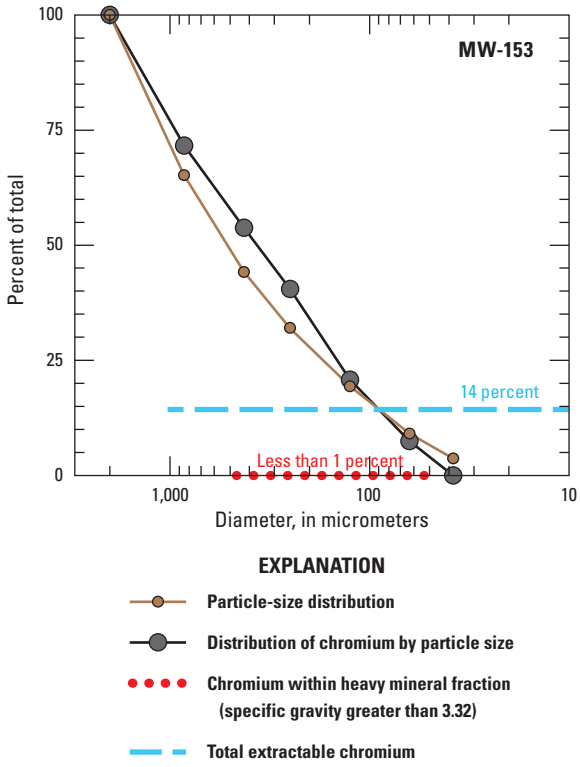

Line indicates range of particle sizes measured.

Size not differentiated for heavy-mineral or sorbed fractions.

Core material from site MW-153 from 100.5 to 108.5 feet below land surface (ft bls); Cr_{solid}=105 milligrams per kilogram; well MW-153S screened 93.5 to 108.5 ft bls; hexavalent chromium, Cr(VI)=3.3 micrograms per liter (March 2015).

Figure C.17. Distribution of chromium within aquifer material adjacent to the screen of well MW-153S by particle size, mineral density, and sum of extractable fractions, Hinkley Valley, western Mojave Desert, California. Data are from Morrison and others (2018) and U.S. Geological Survey (2021).

data collected quarterly for regulatory purposes between March 2012 and July 2017 ranged from 2.2 to 7.6 µg/L with a median concentration of 4.1 µg/L. Although greater than the interim regulatory Cr(VI) background concentration of 3.1 µg/L, these concentrations are not high given the mineralogy and extractable chromium and manganese concentrations in core material adjacent to the screened interval well MW-153S.

C.4.2. Miocene Deposits

Miocene deposits (5.3 to 23 million years old) underlie alluvium in parts of the western subarea, and alluvium in parts of Water Valley was partially eroded from Miocene deposits east of the study area. Minerals within these Miocene materials have weathered to a greater extent than minerals within Mojave-type deposits and most locally derived alluvium. Core material adjacent to the screened intervals of wells MW-203D in the western subarea and well MW-193S1 are representative of these materials.

C.4.2.1. Well MW-203D

Well MW-203D in the western subarea, screened from 108 to 118 ft bls (fig. C.18*A*), is completed in Miocene deposits that predate the arrival of the Mojave River in Hinkley Valley (Miller and others, 2018). The total chromium concentration measured by ICP-MS in bulk core material adjacent to the screened interval of well MW-203D (composited from 108 to 118 ft bls) was 15 mg/kg (Morrison and others, 2018). However, chromium concentrations in core material measured by pXRF at individual depths adjacent to the screened interval of the well were as high as 350 mg/kg, indicating considerable variability in chromium concentrations within this material. Similarly, the total manganese concentrations in bulk core material by ICP-MS was 370 mg/kg, with pXRF concentrations as high as 1,150 mg/kg. Total chromium and manganese concentrations in core material measured by ICP-MS did not exceed the thresholds for scoring within the SSA of 85 and 970 mg/kg, respectively (chapter B, fig. B.11), although pXRF data indicate that some high-chromium and manganese concentration materials in excess of the SSA thresholds are present.

Chromium within core material from MW-203 was associated with the coarser-grained, greater than 425 µm fraction (fig. C.18*A*), although the chromium concentration in the silt and finer-grained (less than 38 µm size) fraction of 32 mg/kg was more than twice the bulk concentration. Much of the chromium within the coarser-grained fractions may be associated with thick oxide coatings observed on the surfaces of mineral grains (fig. C.9*D*). Consistent with thick oxide coatings on the surfaces of mineral grains, chromium on sorption sites comprised about 27 percent of the total chromium. As previously discussed, pXRF data (Groover and Izbicki, 2018) show that extractable chromium concentrations in Miocene materials penetrated by well MW-203D could be as high as 94 mg/kg; however, the measured chromium concentration within the extractable fractions of 4 mg/kg was not as high as in MW-153S discussed previously. Manganese was distributed with particle size in a manner similar to chromium and was associated with a thick oxide coating on the surfaces of mineral grains (not shown on fig. C.18*A*).

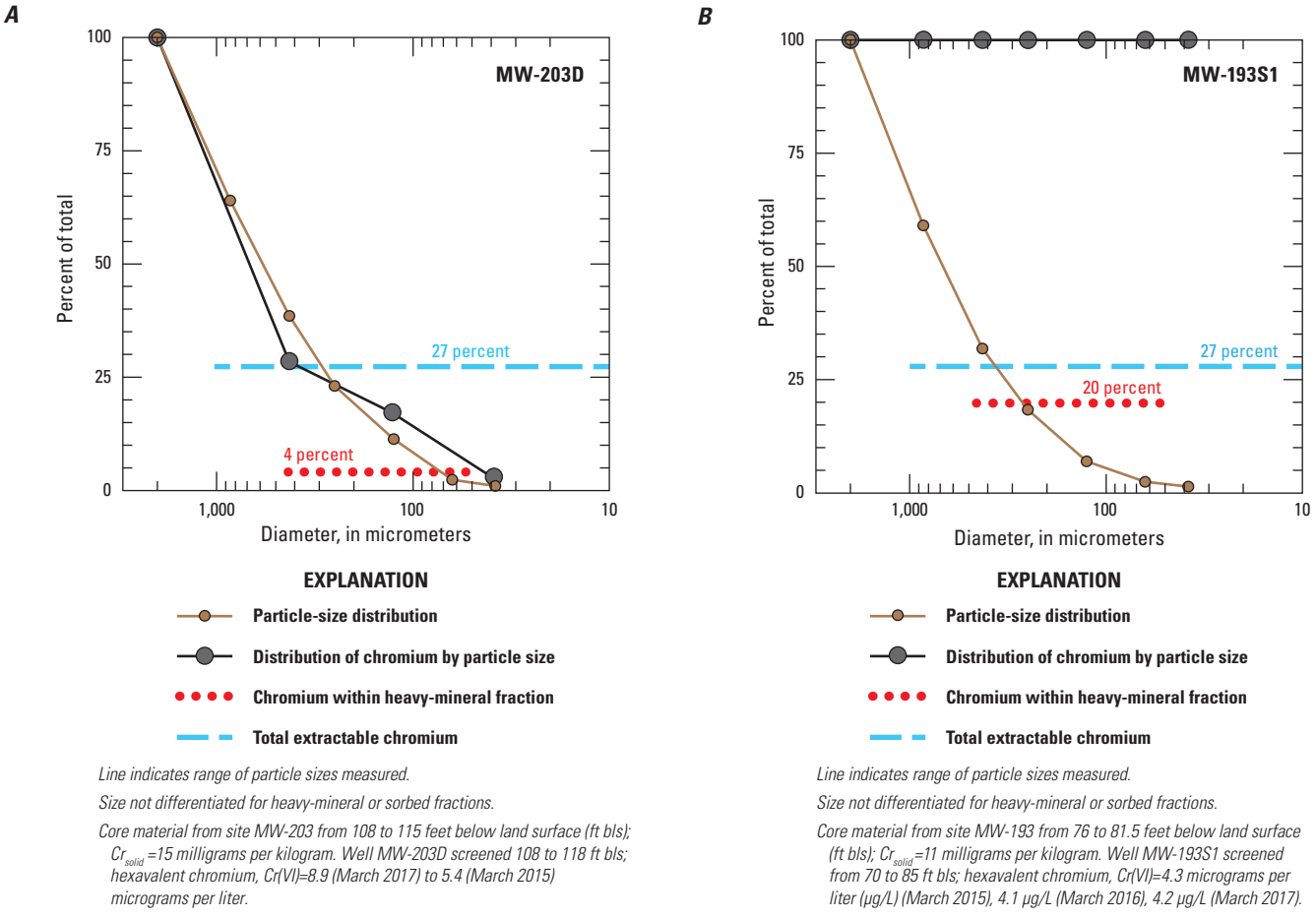

Line indicates range of particle sizes measured.

Size not differentiated for heavy-mineral or sorbed fractions.

Core material from site MW-203 from 108 to 115 feet below land surface (ft bls); Cr_{solid} =15 milligrams per kilogram. Well MW-203D screened 108 to 118 ft bls; hexavalent chromium, Cr(VI)=8.9 (March 2017) to 5.4 (March 2015) micrograms per liter.

Line indicates range of particle sizes measured.

Size not differentiated for heavy-mineral or sorbed fractions.

Core material from site MW-193 from 76 to 81.5 feet below land surface (ft bls); Cr_{solid} =11 milligrams per kilogram. Well MW-193S1 screened from 70 to 85 ft bls; hexavalent chromium, Cr(VI)=4.3 micrograms per liter (µg/L) (March 2015), 4.1 µg/L (March 2016), 4.2 µg/L (March 2017).

Figure C.18. Distribution of chromium in aquifer material adjacent to the screens of wells *A*, MW-203D and *B*, MW-193S1 by particle size, mineral density, and the sum of extractable fractions, Hinkley and Water Valleys, western Mojave Desert, California. Data are from Morrison and others (2018) and U.S. Geological Survey (2021).

Optical (fig. C.9*D*) and X-ray diffraction data (fig. C.10) from MW-203 show a mineral assemblage that differs from Mojave-type alluvium. Optical examination of mineral grains from MW-203 shows evidence of weathering, including dissolution pits (fig. C.9*D*). Heavy minerals present in MW-203, including magnetite, account for only 4 percent of the total chromium (fig. C.18*A*). Other chromium-containing minerals, such as amphiboles (including actinolite associated with older Mojave River deposits and hornblende associated with material eroded or weathered from Iron Mountain), were not identified in core material from MW-203 (Morrison and others, 2018). Differences in source areas during Miocene deposition have resulted in different mineralogy in core material MW-203 compared with other material sampled as part of this study.

Hexavalent chromium concentrations in water from well MW-203D sampled as part of the USGS Cr(VI) background study were 8.9 µg/L in March 2015 and 5.4 µg/L in March 2017 (chapter E) and exceeded the 2007 interim regulatory Cr(VI) background concentration of 3.1 µg/L (CH2M Hill, 2007). Hexavalent chromium concentrations in data collected quarterly for regulatory purposes between October 2013 and July 2017 were highly variable and ranged from less than the reporting level of 0.06 µg/L to as high as 10 µg/L. Higher Cr(VI) concentrations in water from well MW-203D, compared to well MW-153S, may result from aqueous geochemistry (discussed in chapter E within this professional paper).

C.4.2.2. Wells MW-193S1 and MW-193S3

Well MW-193S1 in Water Valley, screened from 71 to 86 ft bls, is completed in alluvium partly eroded from Miocene deposits east of the study area (Miller and others, 2018). The chromium concentration measured by ICP-MS in bulk core material adjacent to the screened interval of well MW-193S1 (composited from 76 to 81.5 ft bls) was 7 mg/kg. Chromium concentrations measured by pXRF ranged from 9 to 27 mg/kg. Manganese concentrations by ICP-MS were 160 mg/kg, with pXRF concentrations ranging from 120 to 590 mg/kg. Chromium and manganese concentrations in core material did not exceed thresholds for scoring within the SSA of 85 and 970 mg/kg, respectively (chapter B, fig. B.11).

Chromium within the heavy-mineral fraction adjacent to the screened interval of well MW-193S1 composed about 20 percent of the total chromium (fig. C.18*B*), although only trace amounts of magnetite were present in the heavy-mineral fraction (Morrison and others, 2018). Other chromium-containing minerals, such as actinolite (associated with older Mojave River deposits), were identified in core material, consistent with a partial Mojave River source. Optical examination of mineral grains from core material adjacent to the screened interval of well MW-193S1 shows evidence of weathering, including weathering rinds, dissolution pits, and thick oxide coatings (fig. C.9*C*); consistent with extensive weathering of mineral grains, extractable chromium in core material from well MW-193S1 was 27 percent of the total chromium and similar to Miocene core material from well MW-203D. Some magnetite mineral grains, normally resistive to weathering, showed optical evidence of weathering to hematite (figs. C.9*B,C*), which also is consistent with a Miocene source for these weathered minerals.

Hexavalent chromium concentrations in water from well MW-193S1 ranged from 4.0 to 4.3 µg/L in three samples collected in March 2015, 2016, and 2017 as part of this study (chapter E). On the basis of data submitted by PG&E for regulatory purposes, hexavalent chromium concentrations in quarterly data collected for regulatory purposes from well MW-193S1 between August 2013 and July 2016 ranged from 4.2 to 4.7 µg/L (https://www.waterboards.ca.gov/lahontan/water_issues/projects/pge/, accessed January 12, 2018).

Core material at MW-193 from 136 to 141 ft bls, adjacent to the screened interval of well MW-193S3 (not shown on fig. C.18), is partly composed of Miocene material within local alluvium (Miller and others, 2020). Chromium and manganese at this depth were detected only in the silt and finer-grained (less than 38 µm) particle-size fraction. Consistent with extensive weathering of mineral grains, total extractable chromium comprised 14 percent of the total chromium within the sample (Morrison and others, 2018). Portable (handheld) X-ray fluorescence data (Groover and Izbicki, 2018) show that chromium concentrations in core material adjacent to the screened interval of well MW-193S3 are as high as 31 mg/kg, and extractable chromium concentrations in materials penetrated by well MW-193S3 could be as high as 8.4 mg/kg.

Hexavalent chromium concentrations in water from well MW-193S3, screened in unconsolidated alluvium eroded from Miocene deposits east of the study area from 125 to 145 ft bls, were less than 0.5 µg/L in March 2015 and 2016 as a result of suboxic conditions (dissolved-oxygen concentrations of 0.3 mg/L) in water from the well (chapter E). However, Cr(VI) concentrations in regulatory data collected after the well was installed were as high as 275 µg/L in January 2014. In contrast to chromium, core material adjacent to the screened interval of well MW-193S3 from 135 to 141 ft bls had total extractable manganese concentrations of 460 mg/kg, the highest measured as part of this study; comparison with pXRF data indicate that more than 70 percent of manganese had weathered from primary minerals and was present as oxides on the surfaces of mineral grains. Although the redox status of Mn oxides in these materials was not measured, it is possible that abundant manganese oxides on the surfaces of mineral grains may have oxidized Cr(III) to Cr(VI) in the presence of dissolved-oxygen concentrations as high as 5 mg/L introduced to the aquifer as a result of drilling and well development.

C.4.3. Secondary-Oxidized Deposits

Aluminum-, iron-, and manganese-oxide coatings are ubiquitous on mineral grains that compose materials in unconsolidated aquifers. These coatings are typically less than 5 µm thick but play an important role in the storage of chromium and other trace elements weathered from mineral grains prior to release into groundwater (Izbicki and others, 2008; Ščančar, and Milačič, 2014). Oxide coatings also may provide a manganese-rich matrix that can facilitate oxidation of Cr(III) to Cr(VI) (Schroeder and Lee, 1975). In addition to the oxide coatings associated with weathered Miocene material discussed previously, visually abundant oxide coatings were observed near the water table and in geologic and lithologic contacts within core material from wells throughout Hinkley and Water Valleys. Oxide coatings are natural features, developed in response to mineral weathering and as a consequence of changing redox conditions and redox gradients within aquifer materials.

Chromium concentrations as high as 120 mg/kg were measured in visually abundant oxide coatings within core material adjacent to well MW-121D (fig. C.13*D*; Groover and Izbicki, 2018). Similar coatings were observed in core material collected near the water table and near redox gradients associated with lithologic or geologic contacts (figs. C.13*A,B*). Chromium distribution, aquifer mineralogy, and the mineralogy and chemistry of oxide coatings from core material within site BG-0004 were examined to further understand the role of oxides in the occurrence of Cr(VI) in groundwater. Chromium within oxide coatings also was examined from core material at site SA-RW-48 within the mapped Cr(VI) regulatory plume to see if chromium within the Cr(VI) plume differs from naturally occurring oxide coatings; these visually abundant oxide coatings play a role in the storage of chromium and oxidation of Cr(III) to Cr(VI) on surface coatings of aquifer materials.

C.4.3.1. Well BG-0004A

Well BG-0004A (fig. C.19) in the eastern subarea (screened from 58 to 68 ft bls) is completed in recent Mojave River deposits. The chromium concentration measured by ICP-MS in bulk core material adjacent to the screened interval of well BG-0004A (composited from 57 to 61 ft bls) was 13 mg/kg (Morrison and others, 2018). Chromium concentrations measured by pXRF at other depths adjacent to the screened interval of the well ranged from 6.1 to 39 mg/kg, with the higher concentrations in visually oxidized core material penetrated by the deeper part of the well screen below 61 ft. The manganese concentration in bulk core material by ICP-MS was 160 mg/kg; pXRF concentrations of manganese in core material adjacent to the screened interval of the well ranged from 88 to 1,070 mg/kg, with higher concentrations in visually oxidized core material. Chromium concentrations did not exceed the threshold for scoring within the SSA of 85 mg/kg; however, manganese concentrations within visually oxidized core material exceeded the SSA threshold for manganese of 970 mg/kg (chapter B, fig. B.11).

About 65 percent of chromium within core material from BG-0004A was within the coarse-grained fraction between 450 and 2,000 µm (fig. C.19). Although the chromium concentration in the silt and finer (less than 38 µm) fraction of 47 mg/kg was higher than the bulk concentration, the sample is largely coarse grained, and few silt and finer materials are within this sample. Manganese was distributed similarly to chromium, with concentrations in the silt and finer (less than 38 µm) fraction of 480 mg/kg. Although heavy minerals compose less than 1 percent of the total sample by mass, chromium within the heavy-mineral fraction composed 31 percent of the total chromium. Magnetite was detected by X-ray diffraction at trace amounts, whereas actinolite (associated with mafic Pelona Schist in older Mojave River deposits) was not identified optically.

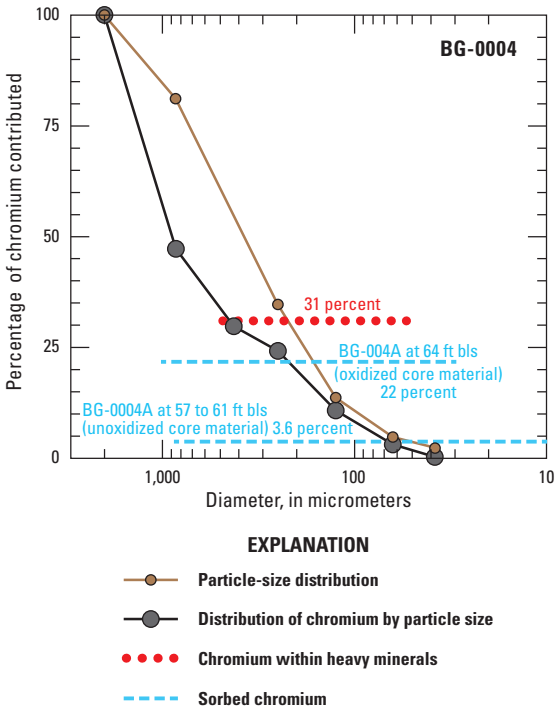

Line indicates range of particle sizes measured.

Size not differentiated for heavy mineral or sorbed fractions.

Core material from site BG-0004 from 57 to 61 feet below land surface (ft bls); Cr_{solid} =13 milligrams per kilogram.

Core material from well BG-0004A screened 58 to 68 ft bls; hexavalent chromium, Cr(VI)=2.3 to 3.1 micrograms per liter (January 2016 to January 2018).

Figure C.19. Distribution of chromium in aquifer material adjacent to the screen of well BG-0004A by particle size, mineral density, and the sum of extractable fractions, Hinkley Valley, western Mojave Desert, California. Data are from Morrison and others (2018) and U.S. Geological Survey (2021).

Raman spectra, collected at the USGS laboratory in Menlo Park, show manganese oxides on quartz mineral grains from BG-0004 at 64 ft bls are hollandite, a mineral within the coronadite mineral group (fig. C.20). The coronadite mineral group consists of various monovalent metals (sodium and potassium) and divalent metals (lead, barium, and strontium) associated with manganese-3/manganese-4 [Mn(III/IV)] oxides. Similar Mn(III/IV) oxides within this mineral group were identified elsewhere on the surfaces of mineral grains throughout the study area and are capable of oxidizing Cr(III) to Cr(VI). Total extractable chromium within unoxidized core material penetrated by the upper part of the well composed 3.6 percent of the total chromium. In contrast, total extractable chromium within visibly oxidized core material composed 22 percent of the total chromium, the third highest percentage of extractable chromium measured as part of this study, representing about 2.9 mg/kg of the 13 mg/kg chromium within the sample.

The Cr(VI) concentration in water from well BG-0004A, screened from 57 to 67 ft bls in recent Mojave River deposits, ranged from 2.2 to 2.3 µg/L in quarterly samples collected as part of this study between April 2017 and January 2018 and were as high as 3.1 µg/L in May 2016, after the well was first installed. Regulatory Cr(VI) data were not collected for water from this well. Although reactive chromium and manganese were identified on the surface coatings on mineral grains, water from samples collected from well BG-0004A did not exceed the regulatory interim Cr(VI) background value of 3.1 µg/L.

C.4.3.2. Well SA-RW-48

Visually abundant oxide accumulations were observed in core material at a number of locations within the mapped Cr(VI) regulatory plume. These accumulations ranged from fine-scale features associated with small changes in aquifer lithology to massive accumulations such as those observed in well SA-RW-48, about 0.3 mi downgradient from the Hinkley compressor station (fig. C.21). At the time core material was collected from SA-RW-48, the location was not impacted by in situ reduction of Cr(VI) to Cr(III), which was used to remediate Cr(VI) in groundwater (chapter A), and these oxide accumulations are related to Cr(VI) released from the Hinkley compressor station. Massive iron- and manganese-oxide accumulations, including black coatings on mineral grains identified as chromium-containing hydrocalcite, have been described within Cr(VI) plumes (Sedlazeck and others, 2017). Similar oxide accumulations were observed in core material from other sites within the Q4 2015 regulatory Cr(VI) plume, including SA-SB-01, SA-RW-34, SA-RW-35, MW-208, EX-49, and EX-44 (fig. C.2). Fine-scale oxide accumulations were observed within core material distributed in a spider-web manner at otherwise imperceptible lithologic contacts at a number of other sites within the Q4 2015 regulatory Cr(VI) plume. Similar massive and fine-scale oxide accumulations were not observed at sites outside the mapped Cr(VI) regulatory plume.

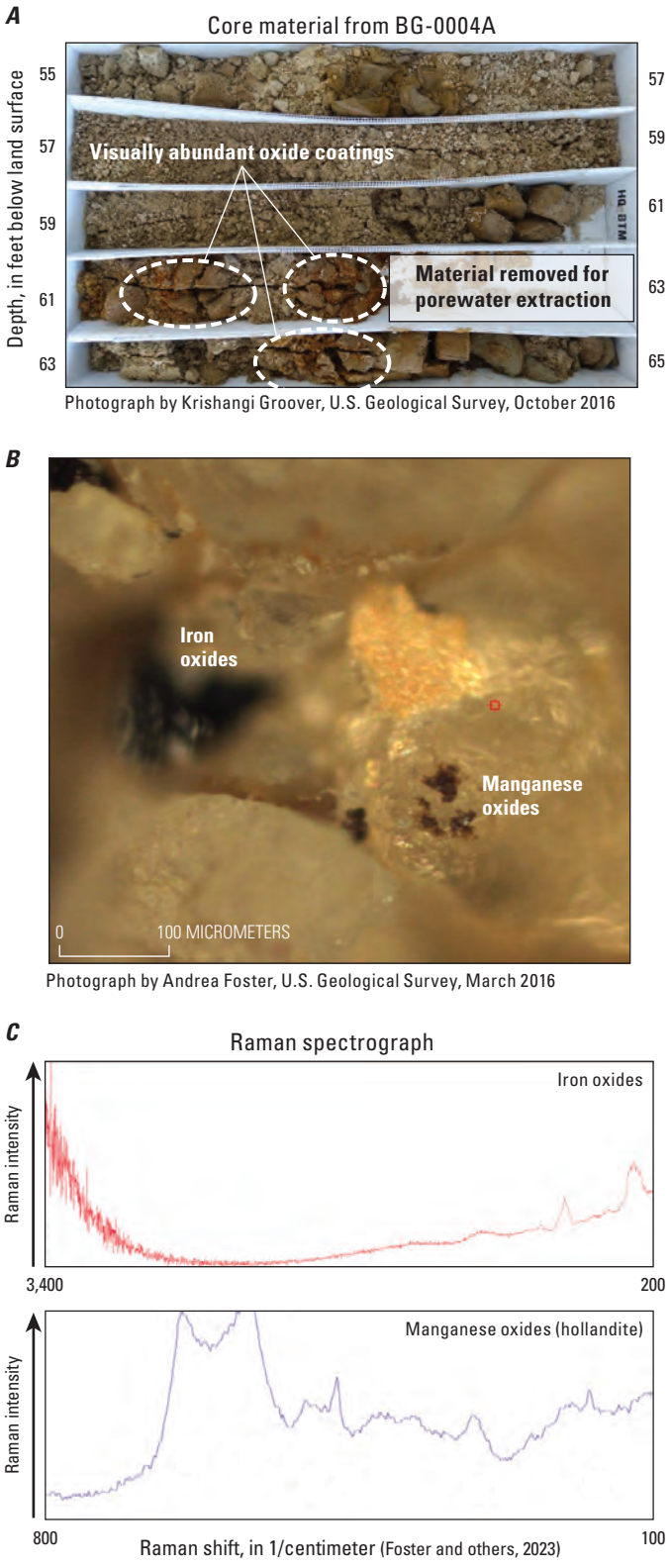

Figure C.20. Oxides within core material at BG-0004A 64 feet below land surface: *A*, photograph of core material, *B*, photograph of quartz mineral grain with iron- and manganese-oxide coatings, and *C*, Raman spectrographs for iron- and manganese-oxide coatings on quartz mineral grain, Hinkley Valley, western Mojave Desert, California.

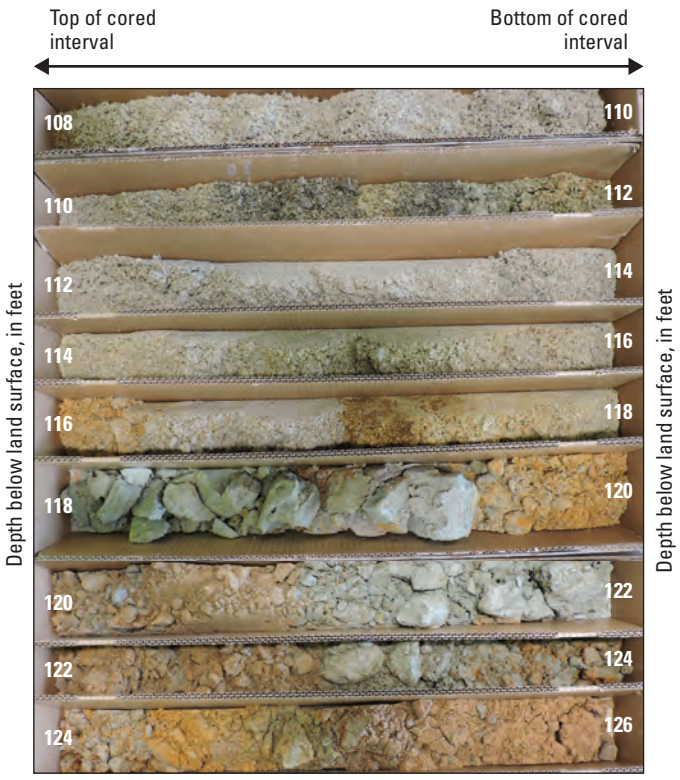

Figure C.21. Oxides on core material from SA-RW-48 within the October–December 2015 (Q4 2015) regulatory hexavalent chromium, Cr(VI), plume downgradient from the Hinkley compressor station, Hinkley Valley, western Mojave Desert, California.

Inductively coupled plasma-mass spectrometry and pXRF data show that median total chromium concentrations within aquifer materials from SA-RW-48 between 104 and 125 ft bls were statistically greater than median chromium concentrations in similar textured Mojave-type materials elsewhere in Hinkley Valley (fig. C.22). However, total extractable chromium and chromium within the strong-acid (HNO_3) extractable fraction at SA-RW-48 were significantly lower than concentrations at other similar sites outside the Cr(VI) plume. Some chromium may be recalcitrant and not extractable using procedures modified from Chao and Sanzolone (1989) and Wenzel and others (2001). In contrast, core materials from SA-RW-48 show almost an order of magnitude higher chromium concentrations within the highly mobile, weakly sorbed (KCl-extractable) fraction than materials outside the regulatory Cr(VI) plume (appendix C.1, table C.1.1). Similar high-chromium concentrations were not extracted within the weakly sorbed fraction from visually abundant oxides on core material from sites MW-121 and BG-0004 outside the mapped Cr(VI) regulatory plume or from mafic alluvium from the Sheep Creek fan. However, high percentages of weakly sorbed extractable chromium were measured for core material adjacent to the screened interval of MW-208S (not shown on fig. C.22), another site within the Q4 2015 regulatory Cr(VI) plume. Highly mobile chromium within the weakly sorbed (KCl-extractable) fraction on aquifer solids may contribute Cr(VI) after Cr(VI) is removed from groundwater.

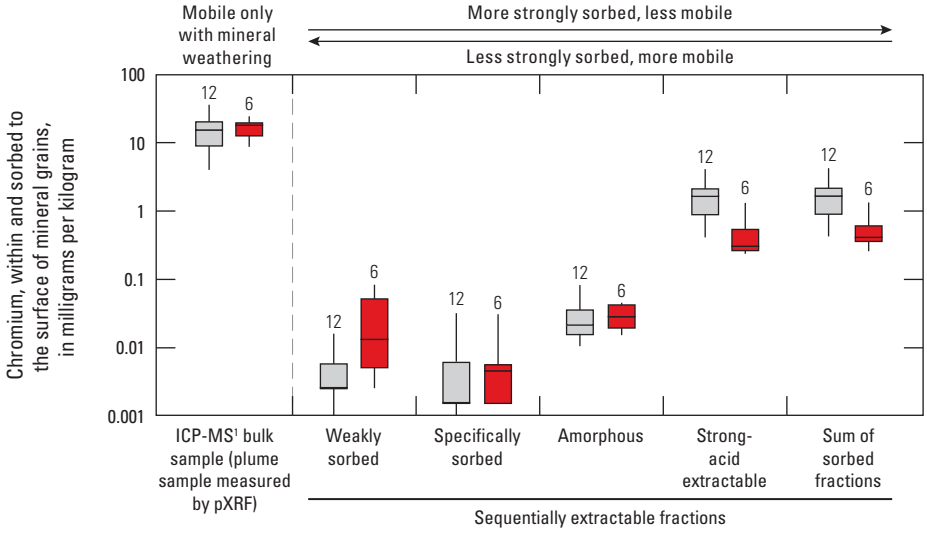

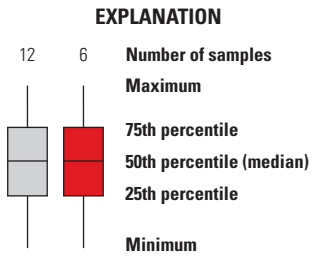

Gray box plots show sequential extraction data from surficial alluvium and core material in Hinkley and Water Valleys. Red box plots show sequential extraction data from visually abundant oxides from core material within October–December 2015 (Q4 2015) regulatory hexavalent chromium, Cr(VI), plume at SA-RW-48.

[1]Chromium from surficial alluvium and core material in Hinkley and Water Valleys measured by inductively coupled plasma-mass spectrometry (ICP-MS) with multi-acid digestion (Methods ICP42 or ICP49; Morrison and others, 2018). Chromium from core material within October–December 2015 (Q4 2015) regulatory hexavalent chromium, Cr(VI), plume measured by handheld (portable) X-ray fluoresence (pXRF).

Figure C.22. Comparison of sequential extraction data from SA-RW-48, within the regulatory hexavalent chromium, Cr(VI), plume downgradient from the Hinkley compressor station, with data from similar texture material outside the plume, Hinkley and Water Valleys, western Mojave Desert, California. Data are from U.S. Geological Survey (2021).

C.4.4. Brown Clay and Mudflat/Playa Deposits

Brown clay and mudflat/playa deposits are interspersed within Mojave-type deposits throughout Hinkley Valley. In some places, especially within the eastern subarea, these materials are hydrologically important and separate permeable, coarse deposits within the upper aquifer into shallow and deep zones (ARCADIS and CH2M Hill, 2011; Jacobs Engineering Group, Inc., 2019). Mudflat/playa deposits are present at the surface in the eastern subarea near Mount General. Mudflat/playa deposits are especially abundant in the northern subarea, where under conditions at the time of this study (2015–18), these deposits composed much of the saturated aquifer. Detailed chemistry and mineralogic data are presented for core materials collected from 60 to 62 and 70 to 72 ft bls adjacent to the screened interval of well MW-192 in the eastern subarea and for sites MRP3 and HEP1 (land surface) within the playa near Mount General. For comparison, detailed mineralogic data also are presented for core material from 72 to 77 ft bls within mudflat/playa deposits in the northern subarea adjacent to the screened interval of well MW-154S1 in the northern subarea. The oxidation state of Mn oxides was measured for mudflat/playa deposits.

C.4.4.1. Eastern Subarea

Well MW-192S in the eastern subarea of Hinkley Valley (screened from 63 to 78 ft bls) is completed in Mojave River stream deposits. Typical of coarse-textured Mojave River stream deposits, material adjacent to the well screen from 62 to 67 ft bls had a chromium concentration of 6 mg/kg (fig. C.23*A*). X-ray diffraction data show the material to be felsic (fig. C.10), with most chromium within the less than 63 mm particle-size fraction and the heavy-mineral fraction (fig. C.23*A*). Only 6 percent of the chromium is extractable from the surfaces of mineral grains and readily available to groundwater (fig. C.23*A*). Finer-textured material typical of the brown clay was consolidated from overlying clay layers and clay within the well screen (60 to 62 ft bls and 70 to 72 ft bls). The brown clay also had a felsic mineralogy and a chromium concentration of only 11 mg/kg with 12 percent of the chromium extractable from the surfaces of mineral grains (not shown on fig. C.23*A*; Morrison and others, 2018; appendix C.1, table C.1.1).

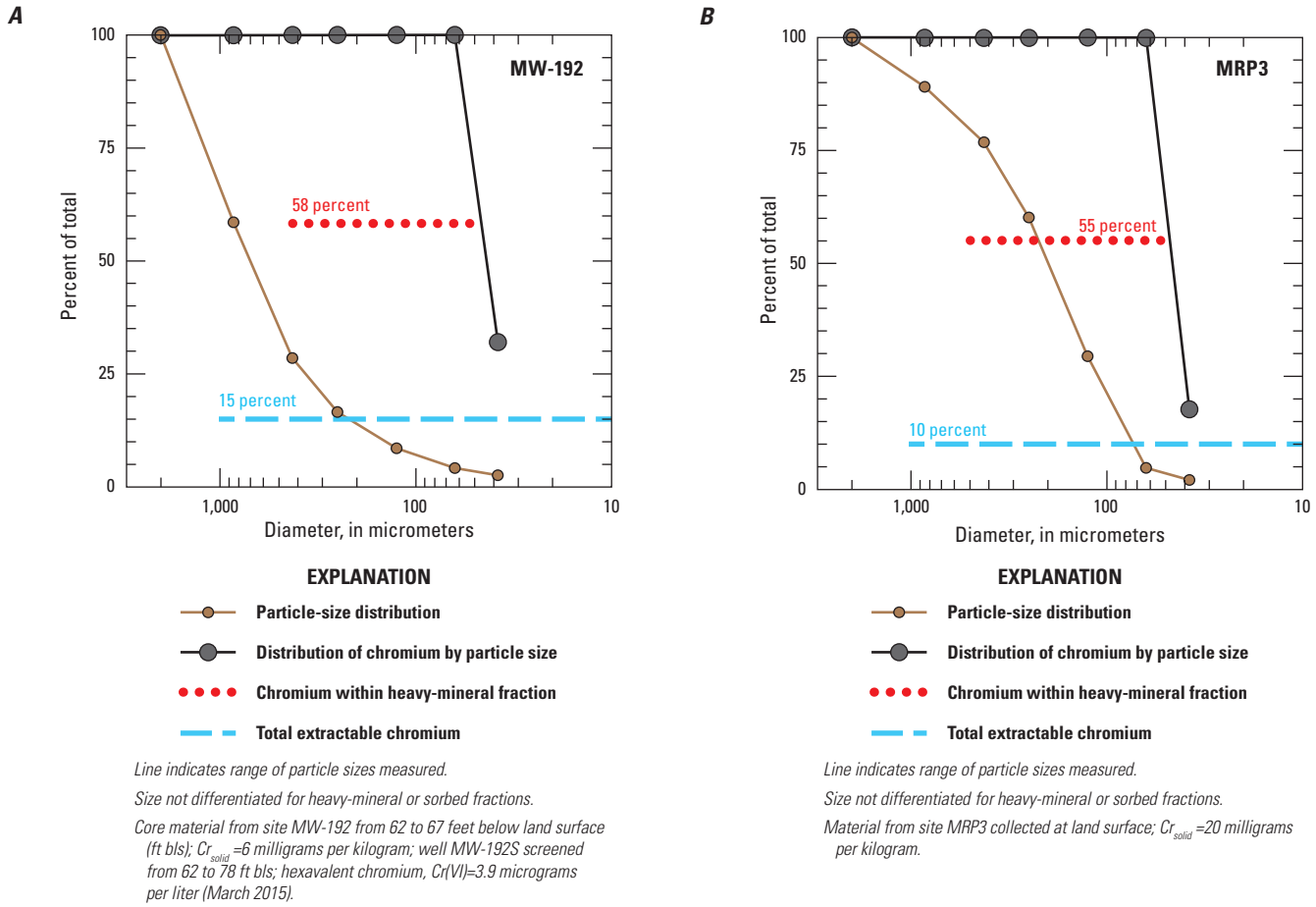

Figure C.23. Distribution of chromium in aquifer material *A*, adjacent to the screen of well MW-192S and *B*, mudflat/playa deposits MRP-3 by particle size, mineral density, and the sum of extractable fractions, eastern subarea of Hinkley Valley, western Mojave Desert, California. Data are from Groover and Izbicki (2018) and Morrison and others (2018).

Despite low chromium concentrations within the Mojave River stream and brown clay deposits penetrated by well MW-192S, the Cr(VI) concentration in water from well MW-192S sampled as part of this study in March 2015 was 3.9 µg/L (chapter E) and exceeded the interim regulatory Cr(VI) background concentration of 3.1 µg/L. Hexavalent chromium data collected quarterly for regulatory purposes between August 2013 and July 2015 were similar and ranged from 3.4 to 4.4 µg/L, with a median concentration of 3.9 µg/L.

Chromium concentrations in fine-textured mudflat/playa deposits were examined as a possible source of Cr(VI) in water from well MW-192S and other wells in this part of the eastern subarea. Site MRP3 (fig. C.23*A*), collected at land surface, is within the clay-3 mineral cluster (fig. C.10). Mudflat/playa deposits at MRP3 have a chromium concentration of 20 mg/kg, similar to other clay-3 materials (fig. C.11). Chromium was distributed by particle-size and heavy-mineral fraction similar to core material from MW-192, with only 10 percent of the chromium extractable from the surfaces of mineral grains and readily available to groundwater. Mudflat/playa deposits from HEPL1 (not shown on fig. C.23), also collected at land surface, had a chromium concentration of 19 mg/kg (Groover and Izbicki, 2018). Within the felsic mineral cluster (fig. C.10), chromium within HEPL1 was distributed in a manner similar to chromium within MRP3, with most of the chromium in the less than 38-mm-size fraction and 5 percent of the chromium extractable from the surfaces of mineral grains; however, in contrast to MRP3, only 9 percent of the chromium in HEPL1 was within the heavy-mineral fraction.

On the basis of data collected from core material at MW-192 and mudflat/playa deposits at MRP3 and HEPL1, brown clay and mudflat/playa deposits in the eastern subarea do not have high concentrations of chromium that can be readily mobilized into groundwater. However, these materials are known to contain visible manganese staining (dragon's breath) and manganese nodules (fig. C.13*C*). Manganese can oxidize Cr(III) to Cr(VI) (Schroeder and Lee, 1975). Manganese oxides on the surfaces of mineral grains from selected Mojave-type materials and manganese nodules within brown clay from site PZ-07 were examined using X-ray absorption near-edge structure (XANES) to determine the oxidation state of manganese within materials in Hinkley Valley (fig. C.24). On the basis of XANES data, most manganese oxides on the surfaces of mineral grains within older Mojave-type deposits (BG-0005) appear to be manganese-2/manganese-3 [Mn(II/III)] oxides, and they appear slightly less oxidative than the Mn(III/IV) oxides within recent Mojave-type deposits (BG-0004) observed using Raman spectroscopy at BG-0004 (fig. C.20; Foster and others, 2023). Manganese oxides on materials within the regulatory Cr(VI) plume (SA-SB-01) are similar to material in recent Mojave-type deposits and do not appear to be altered by Cr(VI) within the plume. In contrast, manganese nodules from PZ-07 do not show manganese-2 [Mn(II)] or manganese-3 [Mn(III)] peaks present in other samples, but rather show a manganese-4 [Mn(IV)] peak consistent with strongly oxidative material. The potential influence of Mn(IV) oxides on the oxidation of Cr(III) to Cr(IV) and the potential mobility of Cr(VI) into groundwater is discussed in greater detail in chapter E within this professional paper.

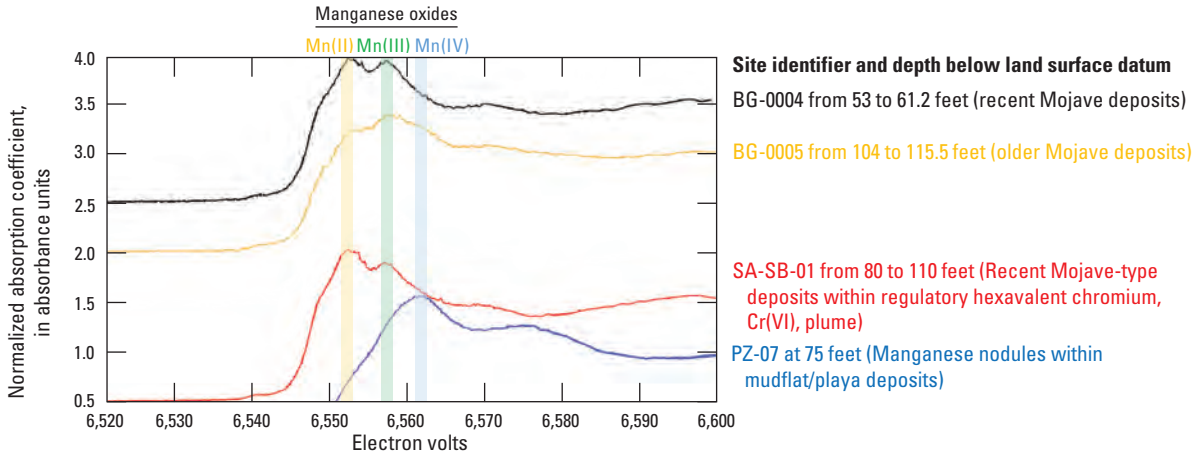

Figure C.24. X-ray absorption near-edge structure (XANES) spectra and redox status of manganese oxides on the surfaces of mineral grains from selected sites, Hinkley Valley, western Mojave Desert, California. Data are from Foster and others (2023).

C.4.4.2. Northern Subarea

Well MW-154S1 in the northern subarea (screened from 70 to 85 ft bls) is completed in mudflat/playa deposits. The total chromium concentrations (multi-acid digestion Method ICP42 or ICP49; Morrison and others, 2018) within fine-textured core material adjacent to the well screen from 72 to 77 ft bls were 55 mg/kg (fig. C.25), with chromium concentrations measured by pXRF as high as 75 mg/kg. The total manganese concentration (multi-acid digestion Method ICP42 or ICP49) was 980 mg/kg, with manganese concentrations measured by pXRF as high as 1,340 mg/kg. Manganese by pXRF exceeded the threshold for scoring within the SSA of 970 mg/kg (chapter B, fig. B.11). Chromium concentrations in similar mudflat/playa materials from well site MW-133 in the northern subarea exceeded the threshold of 85 mg/kg for chromium.

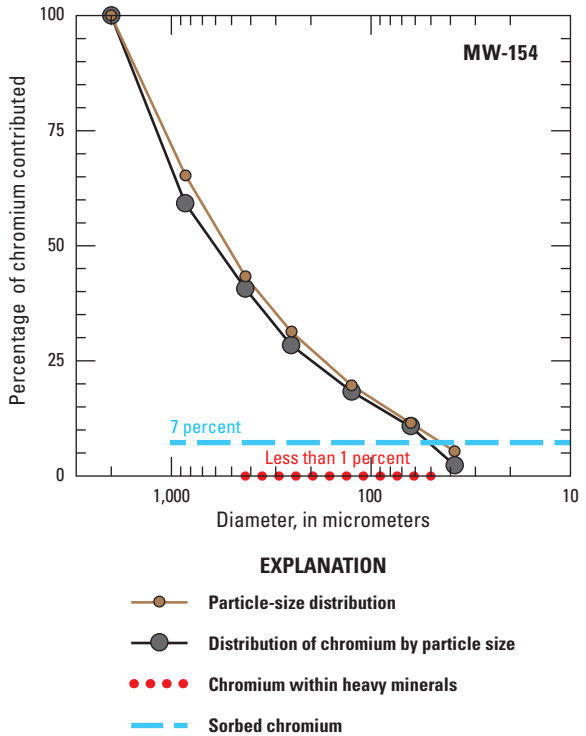

Line indicates range of particle sizes measured.

Size not differentiated for heavy mineral or sorbed fractions.

Core material from site MW-154 from 62 to 67 feet below land surface (ft bls); Cr_{solid} =55 milligrams per kilogram; well MW-154S1 screened from 70 to 86 ft bls; hexavalent chromium, Cr(VI) =11 micrograms per liter (March 2015).

Figure C.25. Distribution of chromium in aquifer material adjacent to the screen of well MW-154S1 by particle size, mineral density, and sum of extractable fractions, northern subarea of Hinkley Valley, western Mojave Desert, California. Data are from Groover and Izbicki (2018) and Morrison and others (2018).

On the basis of X-ray diffraction data, mudflat/playa deposits in MW-154 are within the clay-2 mineral group (fig. C.10) and contain chlorite. Although chromium can substitute within the chlorite mineral structure, the chromium concentration within the light-mineral fraction was only 24 mg/kg, indicating little substitution of chromium. Particle-size data from MW-154 range from coarse to fine-grained particles (indicating incomplete disaggregation of clay material that composed the fine-textured sample), and chromium concentrations decreased with particle-size fraction. Heavy minerals were less than 1 percent of the sample mass by weight, and magnetite was not identified. Optical data indicate that magnetite within core material from MW-154 may have oxidized to hematite (fig. C.9*C*). Manganese substituted with magnetite commonly forms pyrolusite ($Mn^{IV}O_2$) during weathering of magnetite (Dixon and Weed, 1989; Anthony and others, 2001). Similar to Mn(VI) identified in nodules within mudflat/playa deposits within the eastern subarea, Mn(IV) oxides would be highly oxidative and may facilitate oxidation of Cr(III) to Cr(VI).

The Cr(VI) concentration in water from well MW-154S1 sampled as part of this study in March 2015 was 11 µg/L, the highest concentration outside the Q4 2015 regulatory Cr(VI) plume. Hexavalent chromium data collected quarterly for regulatory purposes between March 2012 and July 2017 ranged from 7 to 22 mg/L, with a median concentration of 12 µg/L. Hexavalent chromium concentrations in water from well MW-154S1 are consistent with high chromium concentrations in aquifer material and the presence of strongly oxidative Mn(IV) oxides on aquifer solids. Chromium concentrations and the distribution of chromium within sample particle-size and density fractions differs within clay-rich, fine-textured mudflat/playa deposits in the northern subarea and within fine-textured mudflat/playa deposits in the eastern subarea.

C.4.5. Downgradient from the "Western Excavation Site"

The western excavation site (fig. C.2), on property owned by PG&E upgradient of the Lockhart fault, has been investigated as an area possibly containing anthropogenic Cr(VI) (Lahontan Regional Water Quality Control Board, 2014). If anthropogenic Cr(VI) is present in water from wells downgradient from the western excavation site, it would represent a Cr(VI) release separate from releases at the Hinkley compressor station.

Total chromium concentrations measured by (multi-acid digestion Method ICP42 or ICP49; Morrison and others, 2018) ICP-MS in core material from MW-163 (90 to 96 ft bls) and MW-159 (93–96 ft bls) were 8 and 5 mg/kg (fig. C.26), with total manganese concentrations of 237 and 163 mg/kg, respectively (Morrison and others, 2018). Maximum chromium concentrations in core material adjacent to the screened intervals of wells MW-163S and MW-159S measured by pXRF were 30 and 17 mg/kg, respectively; maximum manganese concentrations were 464 and 335 mg/kg, respectively (Groover and Izbicki, 2018). Measured values are lower than the SSA thresholds of 85 mg/kg and 970 mg/kg for chromium and manganese, respectively (figs. B.11*A,B*). Chromium is associated with finer-grained material 125 µm or smaller within the coarser-grained matrix, with a chromium concentration in the silt and finer (less than 38 µm size) fraction of 85 mg/kg (Morrison and others, 2018).

Optical and X-ray diffraction data show a felsic mineral assemblage consistent with Mojave-type deposits in core material adjacent to the screened interval of MW-163S and MW-159S. In contrast, deeper lacustrine deposits at these sites have a more clay-rich mineralogy (fig. C.10). Boreholes at MW-163 and MW-159 penetrated weathered granitic bedrock with chromium concentrations less than 22 mg/kg (Groover and Izbicki, 2018). Bedrock outcrops near the western excavation site also have low chromium concentrations (chapter B, table B.3). Hornblende diorite and trace amounts of unidentified metamorphic minerals that were not observed elsewhere in the Hinkley Valley (possibly associated with metamorphosed volcanic rock that crops out on the south end of Iron Mountain) were present within older Mojave River alluvium from MW-163S and MW-159S (fig. C.9*B*). Optical examination of these minerals showed angular grains with no evidence of weathering, consistent with a local source area and limited transport (fig. C.9*B*). Forty percent of the chromium in core material from well MW-163S (fig. C.26*A*) and 68 percent of the chromium in core material from well MW-159S (fig. C.26*B*) were within the heavy-mineral fraction and presumably substituted within resistive magnetite mineral grains.

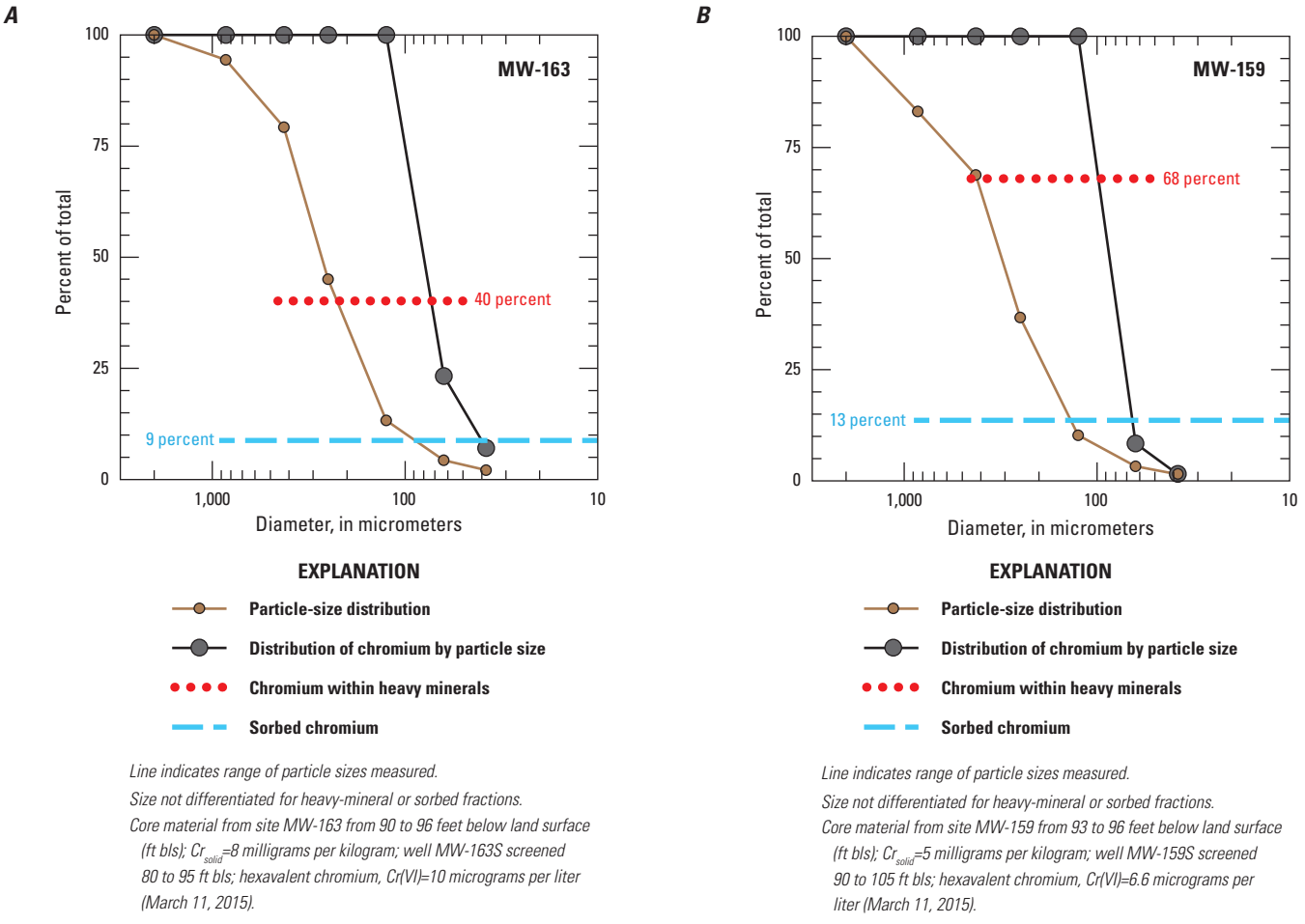

Figure C.26. Distribution of chromium in aquifer material adjacent to the screens of wells MW-163S and MW-159S by particle size, mineral density, and sum of extractable fractions, downgradient from the "western excavation site," Hinkley Valley, western Mojave Desert, California. Data are from Groover and Izbicki (2018) and Morrison and others (2018).

Examination by SEM shows much of the magnetite to be in the less than 100 µm fraction, with no evidence of weathering. Actinolite was identified on the basis of optical analyses (figs. C.9*A,B*). In contrast to hornblende, actinolite is fractured and weathered (fig. C.9*B*). Chromium extracted from the surfaces of mineral grains measured by sequential extractions accounted for 9 to 13 percent of the chromium present in core material adjacent to the screens of wells MW-163S and MW-159S, or about 0.7 and 0.6 mg/kg chromium on sorption sites, respectively.

In March 2015, water from wells MW-163S and MW-159S in older Mojave River alluvium downgradient from the western excavation site had Cr(VI) concentrations of 6.6 to 10 µg/L, respectively. Hexavalent chromium concentrations in water from MW-163S collected for regulatory purposes between November 2012 and July 2016 ranged from 5.4 to 10 µg/L; during the same period, regulatory data from well MW-159S ranged from 5.8 to 6.7 µg/L. In contrast, hexavalent chromium concentrations in wells completed in older Mojave River alluvium within the Mojave River drainage upstream from Barstow, Calif., do not exceed 4 µg/L (Metzger and others, 2015). Total chromium, mineralogy, and chromium concentrations extracted from the surfaces of mineral grains do not appear sufficiently large to explain Cr(VI) concentrations in groundwater from wells MW-163S and MW-159S downgradient from the western excavation site.

C.5. Conclusions

Between 1952 and 1964, hexavalent chromium, Cr(VI), was released into groundwater from a Pacific Gas and Electric Company (PG&E) compressor station in Hinkley, California, in the western Mojave Desert 80 miles northeast of Los Angeles, California. In 2015, the extent of anthropogenic Cr(VI) in groundwater in Hinkley and Water Valleys was uncertain, but some Cr(VI) in groundwater may be from rock and aquifer material. The U.S. Geological Survey was requested by the Lahontan Regional Water Quality Control Board to complete an updated background study of Cr(VI) concentrations in Hinkley and Water Valleys.

Chromium concentrations measured by inductively coupled plasma-mass spectrometry (ICP-MS; with multi-acid digestion) in 34 samples of surficial alluvium and core material from Hinkley and Water Valleys ranged from 2 to 110 milligrams per kilogram (mg/kg), with a median concentration of 14 mg/kg. Chromium concentrations were lowest in Mojave-type deposits (Mojave River stream and lake margin deposits), with a median of 6 mg/kg. For comparison, chromium concentrations in two samples of mafic alluvium eroded from the Pelona Schist in the San Gabriel Mountains to the southwest were 97 and 170 mg/kg. Chromium concentrations within Hinkley Valley were higher in hornblende diorite associated with Iron Mountain and material eroded from that source, with the highest concentrations in weathered hornblende diorite bedrock underlying the western subarea. Chromium concentrations measured by ICP-MS compare favorably, with a coefficient of determination (R^2) of 0.97, with portable (handheld) X-ray fluorescence (pXRF) data (chapter B). Inductively coupled plasma-mass spectrometry and particle-size data show chromium and other selected trace-element concentrations are higher within fine-textured materials. Chromium concentrations were as high as 1,250 mg/kg in heavy minerals having specific gravity greater than 3.32. Although most samples consist of less than 1 percent heavy minerals by weight, chromium within the heavy-mineral fraction accounts for most of the chromium in Mojave-type deposits transported to Hinkley and Water Valleys by the Mojave River. Most chromium within the heavy-mineral fraction was substituted within magnetite, which is resistant to weathering. Magnetite in Mojave-type deposits was primarily within mineral grains less than 100 micrometers (µm) in size and would contribute to chromium within fine-textured materials. Almost no chromite, the most abundant chromium-containing mineral globally, was present.

Quartz and feldspar were the most abundant minerals in unconsolidated deposits that compose aquifers in Hinkley and Water Valleys, especially within recent and older Mojave River deposits. Higher chromium concentrations were measured in samples from the Sheep Creek fan and three clay-rich mineral clusters associated with (1) weathered rock from Iron Mountain, (2) lacustrine deposits in the western subarea and mudflat/playa deposits in the northern subarea, and (3) granitic source material. Lower chromium concentrations were measured in samples having a felsic mineral composition eroded from locally derived alluvium or transported to Hinkley Valley by the Mojave River. Mudflat/playa deposits and brown clay in the eastern subarea contained few clay minerals and were composed of fine-textured felsic minerals transported to Hinkley Valley by the Mojave River. One sample (MW-137 from 158 to 161 feet below land surface; ft bls), containing mineral admixtures from Mount General with a low chromium concentration of 9.7 mg/kg, did not cluster with other samples.

Admixtures of material eroded from various source terrains were identified within Mojave-type deposits sourced from the Mojave River on the basis of optical, X-ray diffraction, and scanning electron microscopy data. Within the northern subarea, these admixtures included basaltic minerals identified within mudflat/playa deposits penetrated by well MW-154S1 and metamorphic minerals within fine-textured materials at site MW-137. Within the eastern subarea, admixtures included metamorphic minerals eroded from Mount General and identified within fine-textured materials at site MW-192 and within surficial mudflat/playa deposits near Mount General. Within the western subarea, admixtures included metamorphic minerals eroded from Iron Mountain and identified within core material from site MW-159 downgradient from the western excavation site. Admixtures within Mojave-type deposits were not readily identified on the basis of elemental analyses from pXRF data (chapter B), and admixtures do not appear to greatly alter the elemental composition of unconsolidated material composing aquifers in Hinkley and Water Valleys. However, admixtures of metamorphic rock eroded from Iron Mountain and basalt in Water Valley may contribute chromium to aquifer material. In contrast, dacitic rocks eroded from Mount General are commonly low in chromium and are not likely to contribute chromium to aquifer material.

Most chromium is contained within heavy minerals having specific gravity greater than 3.32. Most chromium within heavy minerals was substituted within magnetite mineral grains, and chromite was not identified in the study area. Chromium also was substituted within the mineral structure of less-dense, more easily weathered chromium-containing amphiboles, such as actinolite in older Mojave River deposits, hornblende diorite in local alluvium eroded from Iron Mountain, and weathered hornblende diorite bedrock underlying the western subarea. Actinolite and hornblende are within the light-heavy-mineral fraction having a specific gravity between 2.85 and 3.32. Chromium was not commonly detected in the light-mineral fraction having a specific gravity of less than 2.85. More than 90 percent of chromium (median of all samples) remains within unweathered mineral grains, with only about 9 percent of chromium extractable from surface coatings on mineral grains and potentially available to groundwater from surface sorption sites. The fraction of chromium extractable from mineral grains commonly ranged from 5 percent in sand and gravel to 11 percent in clay-texture material. However, the fraction of chromium extractable from mineral grains was as high as 27 percent in Miocene material and as high as 22 percent in material containing visually abundant iron- and manganese-oxide surface coatings on mineral grains. Although extractable percentages were only 14 percent, the highest concentrations of chromium extractable from the surfaces of mineral grains, 105 mg/kg, and potentially mobile into groundwater were in weathered hornblende diorite. Most chromium weathered from mineral grains is within the strong acid (4-normal nitric acid, 4N HNO_3) extractable fraction, which is comparatively less available to oxic groundwater through desorption than chromium within the weakly sorbed, specifically sorbed, or amorphous extractable fractions. Although generally resistant to weathering, magnetite weathered to hematite in (1) Miocene materials underlying unconsolidated deposits in the western subarea of Hinkley Valley and (2) in alluvium within Water Valley partly eroded from Miocene rock east of the study area, thereby contributing to the high percentage of extractable chromium in these materials.

In contrast to chromium, a median of 22 percent of arsenic and 24 percent of uranium was extractable from mineral grains, with 28 and 32 percent of arsenic and uranium extractable from the surfaces of silt and finer-textured material, respectively. In some materials, 100 percent of the arsenic was extractable from mineral grains and potentially mobile into groundwater. Compared to chromium, the percentages of arsenic and uranium were higher in the highly mobile, non-specifically sorbed and specifically (pH dependent) sorbed fractions. Arsenic and uranium in these fractions are more available to groundwater than chromium. Arsenic and uranium are less abundant than chromium in geologic materials, but as a result of differences in mineral weathering and sorption, in 2016, arsenic and uranium exceeded their respective maximum contaminant levels (MCLs) of 10 and 30 micrograms per liter in almost 40 and 8 percent of sampled domestic wells in Hinkley and Water Valleys, respectively.

Hinkley Valley is naturally low in chromium compared to the average bulk continental abundance of 185 mg/kg. However, on the basis of chemical and mineralogic data, natural geologic sources of chromium were identified that may account for some Cr(VI) concentrations in water from wells that exceed the interim Cr(VI) background concentration of 3.1 µg/L. Chromium concentrations are high in aquifer material weathered from hornblende diorite bedrock. Mineral weathering in Miocene deposits may contribute to Cr(VI) concentrations in water from wells completed in Miocene deposits. Independent of the texture of the material, secondary oxides may contain high concentrations of chromium and other trace elements extractable from the surface coatings on mineral grains that are potentially mobile into groundwater. The manganese-3/manganese-4 (Mn-III/Mn-IV) oxides within these surface coatings can convert trivalent chromium, Cr(III), weathered from mineral grains to Cr(VI). Visually abundant oxide coatings are a natural feature within unconsolidated deposits in Hinkley and Water Valleys and were observed in core material near redox boundaries at the water table and near geologic and lithologic contacts. Brown clay and mudflat/playa deposits in the eastern subarea commonly have a felsic mineral composition consistent with a Mojave River source and are low in chromium, although mudflat/playa deposits may contain manganese nodules composed of Mn(IV) that may facilitate the conversion of Cr(III) to Cr(VI). Mudflat/playa deposits in the northern subarea contain clay minerals and have higher chromium concentrations. The highest Cr(VI) concentration in water from wells outside the October–December 2015 (Q4 2015) regulatory Cr(VI) plume was 11 µg/L in water from well MW-154S1 that was completed in mudflat/playa deposits in the northern subarea. Unusual natural abundance, mineralogy, or sorptive properties for chromium on the surfaces of mineral grains were not identified in aquifer materials downgradient from the western excavation site in the western subarea.

Chemical and mineralogic data show that chromium availability to groundwater is a function of geologic abundance of chromium and the availability of chromium as a result of weathering and sorption to mineral grains. The influence of aqueous geochemistry, including groundwater age (and contact time) on Cr(VI) concentrations in water from wells, is discussed in chapters E and F within this professional paper.

Sequential-extraction data from SA-RW-48 show highly mobile chromium within the weakly sorbed fraction on aquifer materials within the Q4 2015 regulatory Cr(VI) plume. Similar materials were observed at other sites within the regulatory Cr(VI) plume. Highly mobile chromium on aquifer materials is likely a consequence of high concentrations of anthropogenic Cr(VI), a strong oxidant, reacting with aquifer materials as Cr(VI) moved with groundwater downgradient through the aquifer release locations within the Hinkley compressor station. Anthropogenic chromium extractable from these oxides may be highly mobile and may enter groundwater with changes in the ionic strength or pH of groundwater. The extent of anthropogenic Cr(VI) affected materials and total mass of chromium associated with these materials within the aquifer is not known.

C.6. References Cited

Anthony, J.W., Bideaux, R.A., Bladh, K.W., and Nichols, M.C., eds., 2001, Handbook of mineralogy: Chantilly, Va., Mineralogical Society of America, accessed December 17, 2020, at http://www.handbookofmineralogy.org/.

ARCADIS, 2016, Annual cleanup status and effectiveness report (January to December 2015) Pacific Gas and Electric Company, Hinkley Compressor Station, Hinkley, California: San Francisco, Calif., Pacific Gas and Electric Company, prepared by ARCADIS, Oakland, Calif., RC000699, [variously paged], accessed February 2016, at https://documents.geotracker.waterboards.ca.gov/esi/uploads/geo_report/9395357131/SL0607111288.PDF.

ARCADIS and CH2M Hill, 2011, Development of a groundwater flow and solute transport model, appendix G *of* Pacific Gas and Electric Company, Addendum #3 to the Hinkley Compressor Station site feasibility study: San Francisco, Calif., Pacific Gas and Electric Company, [variously paged], accessed September 4, 2019, at https://geotracker.waterboards.ca.gov/esi/uploads/geo_report/2112934887/SL0607111288.pdf.

Ball, J.W., and Nordstrom, D.K., 1998, Critical evaluation and selection of standard state thermodynamic properties for chromium metal and its aqueous ions, hydrolysis species, oxides, and hydroxides: Journal of Chemical & Engineering Data, v. 43, no. 6, p. 895–918, https://doi.org/10.1021/je980080a.

Bezore, S.P., and Shumway, D.O., 1994, Mineral lands classification of a part of southwestern San Bernardino County, California: California Division of Mines and Geology, Open-File Report 94–04, 62 p.

Boettcher, S.S., and Walker, J.D., 1993, Geologic evolution of Iron Mountain, central Mojave Desert, California: Tectonics, v. 12, no. 2, p. 372–386, https://doi.org/10.1029/92TC02423.

CH2M Hill, 2007, Groundwater background study report—Hinkley compressor station, Hinkley, California: Oakland, Calif., CH2M Hill, [variously paged], accessed January 12, 2018, at https://www.waterboards.ca.gov/lahontan/water_issues/projects/pge/docs/2007_background_study_report.pdf.

CH2M Hill, 2013, Conceptual site model for groundwater flow and the occurrence of chromium in groundwater of the western area, Pacific Gas and Electric Company, Hinkley Compressor Station, Hinkley, California: Oakland, Calif., CH2M Hill, [variously paged], accessed December 10, 2019, at https://geotracker.waterboards.ca.gov/esi/uploads/geo_report/7274906218/SL0607111288.pdf.

Chao, T.T., and Sanzolone, R.F., 1989, Fractionation of soil selenium by sequential partial dissolution: Soil Science Society of America Journal, v. 53, no. 2, p. 385–392, https://doi.org/10.2136/sssaj1989.03615995005300020012x.

Cox, B.F., Hillhouse, J.W., and Owen, L.A., 2003, Pliocene and Pleistocene evolution of the Mojave River, and associated tectonic development of the Transverse Ranges and Mojave Desert, based on borehole stratigraphy studies and mapping of landforms and sediments near Victorville, California, *in*Enzel, Y., Wells, S.G., and Lancaster, N., eds., Paleoenvironments and paleohydrology of the Mojave and southern Great Basin Deserts—Boulder, Colorado: Geological Society of America Special Paper 368, p. 1–42, https://doi.org/10.1130/0-8137-2368-X.1.

Cyr, A.J., Miller, D.M., and Mahan, S.A., 2015, Paleodischarge of the Mojave River, southwestern United States, investigated with single-pebble measurements of ^{10}Be: Geosphere, v. 11, no. 4, p. 1158–1171, https://doi.org/10.1130/GES01134.1.

Deer, W.A., Howie, R.A., and Zussman, J., 1992, An introduction to the rock forming minerals (2d ed.): Harlow, England, Pearson Education Limited, 696 p.

Degen, T., Sadki, M., Bron, E., König, U., and Nénert, G., 2014, The HighScore suite: Powder Diffraction, v. 29, Supplement S2, p. S13–S18, https://doi.org/10.1017/S0885715614000840.

Dibblee, T.W., Jr., 1967, Areal geology of the western Mojave Desert, California: U.S. Geological Survey Professional Paper 522, 153 p., https://doi.org/10.3133/pp522.

Dixon, J.B., and Weed, S.B., eds., 1989, Minerals in soil environments: Madison, Wis., Soil Science Society of America, 1244 p., https://doi.org/10.2136/sssabookser1.2ed.

Ehlig, P.L., 1958, The geology of the Mount Baldy region of the San Gabriel Mountains, California: Los Angeles, University of California, Ph.D. dissertation, 195 p.

Evans, J.G., 1982, The Vincent thrust, eastern San Gabriel Mountains, California: U.S. Geological Survey Bulletin 1507, 15 p., https://doi.org/10.3133/b1507.

Fletcher, J.M., and Martin, M.W., 1998, Geologic map of the Hinkley Hills: Geological Society of America Digital Map and Chart Series, scale 1:12,000, https://doi.org/10.1130/1998-fletcher-hinkleyhills.

Folk, R.L., 1954, The distinction between grain size and mineral composition in sedimentary-rock nomenclature: The Journal of Geology, v. 62, no. 4, p. 344–359, https://doi.org/10.1086/626171.

Foster, A.L., Wright, E.G., Bobb, C., Choy, D., and Miller, L.G., , 2023, Optical petrography, bulk chemistry, micro-scale mineralogy/chemistry, and bulk/micron-scale solid-phase speciation of natural and synthetic solid phases used in chromium sequestration and re-oxidation experiments with sand and sediment from Hinkley, CA: U.S. Geological Survey data release, https://doi.org/10.5066/P9ENBLGY.

Garbarino, J.R., Kanagy, L.K., and Cree, M.E., 2006, Chapter 1. Determination of elements in natural-water, biota, sediment, and soil samples using collision/reaction cell inductively coupled plasma-mass spectrometry: U.S. Geological Survey Techniques and Methods, book 5, chap. B1, 88 p., https://doi.org/10.3133/tm5B1.

Garcia, A.L., Knott, J.R., Mahan, S.A., and Bright, J., 2014, Geochronology and paleoenvironment of pluvial Harper Lake, Mojave Desert, California: Quaternary Research, v. 81, no. 2, p. 305–317, https://doi.org/10.1016/j.yqres.2013.10.008.

Groover, K.D., and Izbicki, J.A., 2018, Field portable X-ray fluorescence and associated quality control data for the western Mojave Desert, San Bernardino County, California: U.S. Geological Survey data release, https://doi.org/10.5066/P9CU0EH3.

Groover, K.D., and Izbicki, J.A., 2019, Selected trace-elements in alluvium and rocks, western Mojave Desert, southern California: Journal of Geochemical Exploration, v. 200, p. 234–248, https://doi.org/10.1016/j.gexplo.2018.09.005.

Haley and Aldrich, Inc., 2010, Feasibility study, Pacific Gas and Electric Company Hinkley compressor station, Hinkley, California: San Francisco, Calif., Pacific Gas and Electric Company, [variously paged], 3 addendums, accessed November 27, 2018, at https://www.waterboards.ca.gov/lahontan/water_issues/projects/pge/fsr083010.html.

Housley, R.M., and Reynolds, R.E., 2002, Mineralogical survey of the Mount General area, *in* Reynolds, R.E., ed., 2002, Between the basins—Exploring the western Mojave and southern Basin and Range Province: California State University, Desert Studies Consortium.

Izbicki, J.A., and Groover, K., 2018, Natural and man-made hexavalent chromium, Cr(VI), in groundwater near a mapped plume, Hinkley, California—Study progress as of May 2017, and a summative-scale approach to estimate background Cr(VI) concentrations: U.S. Geological Survey Open-File Report 2018–1045, 28 p., accessed April 19, 2018, at https://doi.org/10.3133/ofr20181045.

Izbicki, J.A., Ball, J.W., Bullen, T.D., and Sutley, S.J., 2008, Chromium, chromium isotopes and selected trace elements, western Mojave Desert, USA: Applied Geochemistry, v. 23, no. 5, p. 1325-1352, https://doi.org/10.1016/j.apgeochem.2007.11.015.

Izbicki, J.A., Wright, M.T., Seymour, W.A., McCleskey, R.B., Fram, M.S., Belitz, K., and Esser, B.K., 2015a, Cr(VI) occurrence and geochemistry in water from public-supply wells in California: Applied Geochemistry, v. 63, p. 203–217, https://doi.org/10.1016/j.apgeochem.2015.08.007.

Izbicki, J.A., O'Leary, D.R., Burgess, M.K., Kulp, T.R., Suarez, D.L., Barnes, T., Ajwani, C., Kim, T.J., and Tseng, I., 2015b, In-situ arsenic removal during groundwater recharge through unsaturated alluvium: Denver, Colo., Water Research Foundation, 59 p., accessed December 21, 2018, at https://pubs.er.usgs.gov/publication/70176457.

Jacobs Engineering Group, Inc., 2019, Ground water flow modeling to support the Hinkley chromium background study, San Bernardino County, California, Project no. 706888CH, for Pacific Gas and Electric Company: Redding, Calif., Jacobs Engineering Group, Inc., [variously paged], accessed March 24, 2020, at https://geotracker.waterboards.ca.gov/view_documents?global_id=T10000010367&enforcement_id=6411598, with Appendixes A through H https://geotracker.waterboards.ca.gov/view_documents?global_id=T10000010367&enforcement_id=6411607.

Jennings, C.W., with modifications by Gutierrez, C., Bryant, W., Saucedo, G., and Wills, C., 2010, Geologic map of California: California Geological Survey, Geologic Data Map No. 2, scale 1:750,000.

Keon, N.E., Swartz, C.H., Brabander, D.J., Harvey, C., and Hemond, H.F., 2001, Validation of an arsenic sequential extraction method for evaluating mobility in sediments: Environmental Science & Technology, v. 35, no. 13, p. 2778–2784, https://doi.org/10.1021/es001511o.

Lahontan Regional Water Quality Control Board, 2014, Comments on report for cleanup of waste pit (western excavation site), Pacific Gas and Electric Company (PG&E), San Bernardino County (Assessor Parcel no. 0488-074-03), WDID no., 6B361403001: California Water Boards Investigative Order no. R6V-2014-0019, 6 p., accessed August 21, 2018, at https://www.waterboards.ca.gov/lahontan/board_decisions/adopted_orders/2014/docs/19.pdf.

Lane, E.W., 1947, Report of the subcommittee on sediment terminology: Eos, Transactions American Geophysical Union, v. 28, no. 6, p. 936–938, https://doi.org/10.1029/TR028i006p00936.

Lumpkin, G.R., 2001, Crystal chemistry and durability of the spinel structure type in natural systems: Progress in Nuclear Energy, v. 38, no. 3–4, p. 447–454, https://doi.org/10.1016/S0149-1970(00)00156-6.

Metzger, L.F., Landon, M.K., House, S.F., and Olsen, L.D., 2015, Mapping selected trace elements and major ions, 2000–2012, Mojave River and Morongo groundwater basins, southwestern Mojave Desert, San Bernardino County, California: U.S. Geological Survey data release, accessed September 10, 2018, at https://doi.org/10.5066/F7Q23X95.

Miller, D.M., Haddon, E.K., Langenheim, V.E., Cyr, A.J., Wan, E., Walkup, L.C., and Starratt, S.W., 2018, Middle Pleistocene infill of Hinkley Valley by Mojave River sediment and associated lake sediment—Depositional architecture and deformation by strike-slip faults *in* Miller, D.M., ed., Against the current—The Mojave River from sink to source: 2018 Desert Symposium Field Guide and Proceedings, April 20–24, 2018.

Miller, D.M., Langenheim, V.E., and Haddon, E.K., 2020, Geologic map and borehole stratigraphy of Hinkley Valley and vicinity, San Bernardino County, California: U.S. Geological Survey Scientific Investigations Map 3458, pamphlet 23 p., 2 sheets, scale 1:24,000, https://doi.org/10.3133/sim3458.

Mojave Water Agency, 2014, Geospatial library: Mojave Water Agency web page, accessed May 22, 2014, at https://www.mojavewater.org/data-maps/geospatial-library.

Morrison, J.M., Goldhaber, M.B., Lee, L., Holloway, J.M., Wanty, R.B., Wolf, R.E., and Ranville, J., 2009, A regional-scale study of chromium and nickel in soils of northern California, USA: Applied Geochemistry, v. 24, no. 8, p. 1500–1511, https://doi.org/10.1016/j.apgeochem.2009.04.027.

Morrison, J.M., Goldhaber, M.B., Mills, C.T., Breit, G.N., Hooper, R.L., Holloway, J.M., Diehl, S.F., and Ranville, J., 2015, Weathering and transport of chromium and nickel from serpentine in the Coast Range ophiolite to the Sacramento Valley, California, USA:Applied Geochemistry, v. 61, p. 72–86, https://pubs.er.usgs.gov/publication/70148593. [Also available at https://doi.org/10.1016/j.apgeochem.2015.05.018.]

Morrison, J.M., Benzel, W.M., Holm-Denoma, C.S., and Bala, S., 2018, Grain size, mineralogic, and trace-element data from field samples near Hinkley, California: U.S. Geological Survey data release, https://doi.org/10.5066/P9HUPMG0.

Munsell Color, 1975, Munsell soil color charts: Baltimore, Md., Munsell Color, Inc.

Munsell Color, 1994, Munsell soil color charts: Baltimore, Md., Munsell Color, Inc.

Neaman, A., Mouélé, F., Trolard, F., and Bourrié, G., 2004, Improved methods for selective dissolution of Mn oxides—Applications for studying trace element associations: Applied Geochemistry, v. 19, no. 6, p. 973–979, https://doi.org/10.1016/j.apgeochem.2003.12.002.

Neter, J., and Wasserman, W., 1974, Applied linear statistical models: Homewood, Ill., Richard D. Irwin, Inc., 842 p.

Nesse, W.D., 2000, Introduction to mineralogy: New York, N.Y., Oxford University Press, 442 p.

Oze, C., Bird, D.K., and Fendorf, S., 2007, Genesis of hexavalent chromium from natural sources in soil and groundwater: Proceedings of the National Academy of Sciences of the United States of America, v. 104, no. 16, p. 6544–6549, https://doi.org/10.1073/pnas.0701085104.

Pacific Gas and Electric Company, 2011, Addendum #2 to the feasibility study: San Francisco, Calif., Pacific Gas and Electric Company, [variously] paged, accessed May 7, 2020, at https://www.waterboards.ca.gov/lahontan/water_issues/projects/pge/docs/addndm2.pdf.

Potter, R.M., and Rossman, G.R., 1979, Mineralogy of manganese dendrites and coatings: The American Mineralogist, v. 64, nos. 11–12, p. 1219–1226.

Rai, D., and Zachara, J.M., 1984, Chemical attenuation rates, coefficients, and constants in leachate migration, v. 1—A critical overview: Palo Alto, Calif., Electric Power Research Institute, EA-3356, NTIS no. 198417, 318 p.

Reimann, C., and de Caritat, P., 1998, Chemical elements in the environment: Berlin, Germany, Springer Verlag, 398 p., https://doi.org/10.1007/978-3-642-72016-1.

Ščančar, J., and Milačič, R., 2014, A critical overview of Cr speciation analysis based on high performance liquid chromatography and spectrometric techniques: Journal of Analytical Atomic Spectrometry, v. 29, no. 3, p. 427–443, https://doi.org/10.1039/C3JA50198A.

Schroeder, D.C., and Lee, G.F., 1975, Potential transformations of chromium in natural waters: Water, Air, and Soil Pollution, v. 4, no. 3–4, p. 355–365, https://doi.org/10.1007/BF00280721.

Sedlazeck, P., Höllen, D., Müller, P., Mischitz, R., and Gieré, R., 2017, Mineralogical and geochemical characterization of a chromium contamination in an aquifer—A combined analytical and modeling approach: Applied Geochemistry, v. 87, p. 44–56, https://doi.org/10.1016/j.apgeochem.2017.10.011.

Smith, D.B., Cannon, W.F., Woodruff, L.G., Solano, F., and Ellefsen, K.J., 2014, Geochemical and mineralogical maps for soils of the conterminous United States: U.S. Geological Survey Open-File Report 2014–1082, 386 p., https://doi.org/10.3133/ofr20141082.

Stamos, C.L., Martin, P., Nishikawa, T., and Cox, B., 2001, Simulation of groundwater flow in the Mojave River basin, California: U.S. Geological Survey Water-Resources Investigations Report 2001–4002, 129 p., https://doi.org/10.3133/wri014002.

Stantec, 2013, Compliance with provision 1.C. of cleanup and abatement order R6V-2008-0002-A4 and requirements of investigation order R6V-2013-0029: Lafayette, Calif., Stantec, [variously paged], https://geotracker.waterboards.ca.gov/esi/uploads/geo_report/8126426041/SL0607111288.pdf

Stover, R.C., Sommers, L.E., and Silviera, D.J., 1976, Evaluation of metals in wastewater sludge: Journal of the Water Pollution Control Federation, v. 48, no. 9, Annual Conference Issue, September 1976, p. 2165–2175.

Strong, T.R., and Driscoll, R.L., 2016, A process for reducing rocks and concentrating heavy minerals: U.S. Geological Survey Open-File Report 2016–1022, 16 p., https://doi.org/10.3133/ofr20161022.

Taggart, J.E., Jr., ed., 2002, Analytical methods for chemical analysis of geologic and other materials, U.S. Geological Survey: U.S. Geological Survey Open-File Report 2002–223, 20 p., accessed July 27, 2020, at https://doi.org/10.3133/ofr02223.

U.S. Department of Agriculture, 1996, Soil survey laboratory methods manual: U.S. Department of Agriculture, Soil Survey Investigations Report no. 42, version 3.0, 716 p.

U.S. Environmental Protection Agency, 2007, Method 7010—Graphite furnace atomic absorption spectrometry, Revision 0: U.S. Environmental Protection Agency, accessed November 1, 2018, at https://www.epa.gov/sites/production/files/2015-12/documents/7010.pdf.

U.S. Geological Survey, 2005, Mineral resources data system: U.S. Geological Survey data release, ver. 20160315, accessed August 2, 2018, at https://mrdata.usgs.gov/mrds/.

U.S. Geological Survey, 2021, USGS water data for the Nation: U.S. Geological Survey National Water Information System database, accessed July 12, 2021, at https://doi.org/10.5066/F7P55KJN.

Wenzel, W.W., Kirchbaumer, N., Prohaska, T., Stingeder, G., Lombi, E., and Adriano, D.C., 2001, Arsenic fractionation in soils using an improved sequential extraction procedure: Analytica Chimica Acta, v. 436, no. 2, p. 309–323, https://doi.org/10.1016/S0003-2670(01)00924-2.

White, A.F., Peterson, M.L., and Hochella, M.F., Jr., 1994, Electrochemistry and dissolution kinetics of magnetite and ilmenite: Geochimica et Cosmochimica Acta, v. 58, no. 8, p. 1859–1875, https://doi.org/10.1016/0016-7037(94)90420-0.

Appendix C.1. Sequential Extraction Data for Selected Surficial Materials and Core Materials, Hinkley and Water Valleys, California

This appendix contains tables of sequential extraction data and quality assurance data (table C.1.1, available for download at https://doi.org/pp1885) for selected surficial material and core materials analyzed as part of the U.S. Geological Survey hexavalent chromium background study. The extraction procedures, modified from Chao and Sanzolone (1989) and Wenzel and others (2001), included (1) weakly sorbed [0.5 molar potassium chloride, KCl]; (2) specifically sorbed [0.5 molar ammonium dihydrogen phosphate, $(NH_4)H_2PO_4$]; (3) amorphous aluminum, iron, and manganese hydroxides [0.2 molar ammonium oxalate, $(NH_4)_2C_2O_4 \cdot H_2O$]; (4) well-crystallized aluminum, iron, and manganese hydroxides [0.2 molar ammonium oxalate and 0.1 molar ascorbic acid, $(NH_4)_2C_2O_4 \cdot .H_2O$ and $C_6H_8O_6$]; and (5) strong acid [4 normal nitric acid, HNO_3] extractions (table C.2). Most extractions were done at the U.S. Geological Survey San Diego office laboratory prior to shipment to the U.S. Geological Survey National Water Quality Laboratory in Denver, Colorado, for analysis. Each extract was analyzed for aluminum, iron, manganese, and for the oxyanion-forming elements arsenic, chromium, uranium, and vanadium by inductively coupled plasma-mass spectrometry (Garbarino and others, 2006). Samples required dilution prior to analysis to prevent damage to instruments. Chromium also was analyzed, without dilution, prior to analysis at the U.S. Geological Survey trace element laboratory in Boulder, Colorado, by graphite furnace atomic absorption spectrometry using U.S. Environmental Protection Agency (EPA) Method 7010 (U.S. Environmental Protection Agency, 2007) to obtain a laboratory reporting level of 0.02 micrograms per liter. Data are available in U.S. Geological Survey (2021), and additional description of site materials is provided in Groover and Izbicki (2018).

References Cited

Chao, T.T., and Sanzolone, R.F., 1989, Fractionation of soil selenium by sequential partial dissolution: Soil Science Society of America Journal, v. 53, no. 2, p. 385–392, https://doi.org/10.2136/sssaj1989.03615995005300020012x.

Garbarino, J.R., Kanagy, L.K., and Cree, M.E., 2006, Determination of elements in natural-water, biota, sediment and soil samples using collision/reaction cell inductively coupled plasma-mass spectrometry: U.S. Geological Survey Techniques and Methods, book 5, chap. B1, 88 p., https://doi.org/10.3133/tm5B1.

Groover, K.D., and Izbicki, J.A., 2018, Field portable X-ray fluorescence and associated quality control data for the western Mojave Desert, San Bernardino County, California: U.S. Geological Survey data release, https://doi.org/10.5066/P9CU0EH3.

U.S. Environmental Protection Agency, 2007, Method 7010—Graphite furnace atomic absorption spectrometry, Revision 0: U.S. Environmental Protection Agency, accessed November 1, 2018, at https://www.epa.gov/sites/production/files/2015-12/documents/7010.pdf.

U.S. Geological Survey, 2021, USGS water data for the Nation: U.S. Geological Survey National Water Information System database, accessed July 12, 2021, at https://doi.org/10.5066/F7P55KJN.

Wenzel, W.W., Kirchbaumer, N., Prohaska, T., Stingeder, G., Lombi, E., and Adriano, D.C., 2001, Arsenic fractionation in soils using an improved sequential extraction procedure: Analytica Chimica Acta, v. 436, no. 2, p. 309–323, https://doi.org/10.1016/S0003-2670(01)00924-2.

For more information concerning the research in this report, contact the

Director, California Water Science Center
U.S. Geological Survey
6000 J Street, Placer Hall
Sacramento, California 95819
https://www.usgs.gov/centers/ca-water/

Publishing support provided by the U.S. Geological Survey
Science Publishing Network, Sacramento Publishing Service Center

USGS

Groover and others—**Chapter C: Chromium in Minerals and Selected Aquifer Materials**—PP 1885-C

ISSN 2330-7102 (online)
https://doi.org/10.3133/pp1885C